IMPROVEMENTS IN MOVING SPRINKLER IRRIGATION SYSTEMS FOR CONSERVATION OF WATER

by

Donald L. Miles

Colorado Water
Resources Research Institute

Completion Report No. 49

Colorado State University

IMPROVEMENTS IN MOVING SPRINKLER IRRIGATION
SYSTEMS FOR CONSERVATION OF WATER

Completion Report

OWRR Project No. B-039-COLO

by

Donald L. Miles
Department of Agricultural Engineering
Colorado State University

submitted to

Office of Water Resources Research

U. S. Department of Interior
Washington, D. C.   20240

June 1973

ENVIRONMENTAL RESOURCES CENTER
Colorado State University
Fort Collins, Colorado

Norman A. Evans, Director

ABSTRACT

IMPROVEMENTS IN MOVING SPRINKLER IRRIGATION SYSTEMS FOR CONSERVATION OF WATER

Self-propelled center-pivot sprinkler systems have become very popular because of their low labor requirements and ability to economically irrigate rolling sandhills. This equipment applies water uniformly to the soil surface, but the water application rates greatly exceed the infiltration capability of most soils causing water to move on the soil surface from local high areas and slopes to nearby low spots. The resulting nonuniformity of irrigation results in reduced crop yields, waste of water, and fertilizer leaching. This problem was investigated using a laboratory infiltrometer, a mathematical model, a field sprinkler infiltrometer, and field investigations under operating systems. Recommendations were developed to reduce or eliminate the problem through improved system design, special field preparation and farming techniques, and improved operating procedures.

TABLE OF CONTENTS

LIST OF TABLES

LIST OF FIGURES

LIST OF SYMBOLS

Symbol	Description	Dimension
A	A symmetrical application rate pattern with a 60-minute time length	-
A'	Packing factor	-
A_t	Area of tube	L^2
a_i	Off-diagonal element in matrix J	-
B	A non-symmetrical front-humped application rate pattern with a 52-minute time length	-
B'	Particle shape factor	-
B_m	A modified non-symmetrical, front-humped application rate pattern with a 60-minute time length	-
b_i	Diagonal element in matrix J	-
C	A non-symmetrical front-humped application rate pattern with a 40-minute time length	-
C_m	A modified symmetrical front-humped application rate pattern with a 60-minute time length	-
c_i	Off-diagonal element in matrix J	-
D	A symmetrical application rate pattern with a 40-minute time length	-
D'	Distance from the soil surface to the wetted front	L
D_a	Actual water depth applied over time 0 to t	L

Symbol	Description	Dimension
D_p	Potential depth of infiltration at time t, obtained by integrating the flooded infiltration rate, I', over time 0 to t	-
d_m	Geometric mean of rated size of adjacent sieves	L
E	A symmetrical application rate pattern with a 90-minute time length	-
E'	Constant specified by soil type and surface and cropping conditions	-
e	Base of Naperin logarithms	-
F	Constant which Philip called soil sorptivity	$LT^{-\frac{1}{2}}$
F_p	Storage potential of the soil above the impeding strata; equals total porosity minus antecedent water	L
G	Constant specified by soil type and surface and cropping conditions	-
H	Hydraulic head	L
h	Ponded water depth on the soil surface	L
I	Rate of infiltration	LT^{-1}
I'	Infiltration rate at t = 0	LT^{-1}
I_m	Modified potential infiltration rate	LT^{-1}
I_o	Infiltration rate at unit time	LT^{-1}
ID	Intake depth	L
i	Subscript, refers to node number for finite difference grid in length dimension	-
J	Nonlinear operator matrix	-

Symbol	Description	Dimension
j	Superscript, refers to node number for finite difference grid in time dimension	-
K	Saturated hydraulic conductivity	LT^{-1}
K_m	Modified saturated hydraulic conductivity	LT^{-1}
k	Intrinsic permeability, or permeability, a function of the geometry of the media for porous media that are stable in the presence of the fluid occupying them	L^2
k_f	Constant	-
k_r	Relative permeability or relative conductivity	-
k_s	Pore shape factor	-
L	Length of tube	L
M_j	Total number of time steps	-
N	Number of grid points used to divide the soil column for a finite difference approximation	-
n	Exponent, refers to slope of ponded infiltration curve	-
n1	Soil layer at saturated and unsaturated nodes	-
n2	First soil layer in front of wetting front	-
$P_{v+\frac{1}{2}}$	Percentage of sand held between adjacent sieves v and v + 1	-
P_b	Air entry pressure, or bubbling pressure	$ML^{-1}T^{-2}$
P_c	Capillary pressure	$ML^{-1}T^{-2}$
Q	Flow velocity	LT^{-1}
Q_p	Input to node from outside	LT^{-1}

Symbol	Description	Dimension
q_t	Total flow through a tube	$L^3 T^{-1}$
R	Application rate	LT^{-1}
RHS, rhs	Abbreviation of right hand side of Equation 4.8	-
r	Exponent in Equation 5.1	-
r_t	Tube radius	L
S	Saturation	-
S_o	Subscript which refers to Soltrol fluid	-
SL	Represents $\partial S/\partial \psi$	L^{-1}
STOR	Abbreviation for part of Equation 4.3	LT^{-1}
s	Specific surface of porous media	L^{-1}
T	Tortuosity of flow path	-
t	Time	T
t_k	Time of ponding (Kincaid)	T
t_s	Time of ponding (El Shafei)	T
$\bar{u}$	Average velocity in tube	LT^{-1}
V_b	Bulk volume, volume per unit area	L
w	Subscript refers to water	-
Y	A parameter related to soil hydraulic properties	LT^{-1}
Z, z	Depth, measured downward from the surface	L

Symbol	Description	Dimension
γ	Unit weight	$ML^{-2}T^{-2}$
ϵ	Error value	-
θ_d	Water content at depth d	-
μ	Dynamic viscosity	$ML^{-1}T^{-1}$
ρ	Density of soil	ML^{-3}
ϕ	Porosity	-
ψ	Soil water pressure potential	L

CHAPTER I

INTRODUCTION

Background

Self-propelled center-pivot sprinkler systems have become very popular. Low labor requirements and the ability to irrigate rolling sandhills which were previously considered to be uneconomical to irrigate are the reasons most frequently given by irrigators for use of this equipment.

The center-pivot designation results from the principle of operation in which one end of a sprinkler lateral rotates around the pivot point irrigating a circular area with a radius equal to or slightly greater than the length of the lateral. Most laterals are approximately one-quarter mile long and irrigate about 130 acres of a 160 acre field. Water under pressure is supplied to the lateral at the pivot point.

Numerous manufacturers have developed and marketed center-pivot systems. There are many variations of the different components, but the most apparent differences are in means of supporting and propelling the lateral. Most center-pivot laterals consist of a water pipe supported 8 to 13 feet above the ground by trusses or cables on towers spaced 90 to 160 feet apart. Sprinkler heads are mounted on the upper side of the pipe. The towers are mounted on wheels which are propelled by mechanisms driven by electricity, water, oil or air. The problems

associated with the drive systems, controls and supports have received
the greatest attention from manufacturers and marketing firms because
of their immediate effect on sales. However, the quality of irrigation
and its results in terms of crop yields, net returns and water conserva-
tion are ultimately more important to the user and the public. There-
fore, this study was focused on irrigation performance.

Center-pivot sprinkler systems and other continuously-moving
sprinklers have an inherent advantage over stationary sprinklers in
uniformity of water application. Stationary sprinkler systems produce
a grid of overlapping individual sprinkler patterns which often results
in some of the area receiving considerably more or less water than the
average. A continuously-moving sprinkler head produces a continuous
water application pattern which is essentially uniform along its length.
In addition, the sprinkler spacing on center-pivot laterals usually pro-
vides overlap of water application from four or more sprinklers result-
ing in potential for very uniform aerial distribution of water applica-
tion.

The most commonly used index for evaluating uniformity of sprinkler
irrigation is the coefficient of uniformity. The procedure for obtain-
ing this coefficient is to install a grid of cans to catch applied water
for measuring the variability of application depth. Field measurements
under actual systems indicate that very high coefficients of uniformity
are usually obtained throughout center-pivot irrigated fields except for
that area served by the sprinklers at the extreme outer end of the lateral.

The Problem

Center-pivot sprinklers pass the traditional test for irrigation uniformity with flying colors. However, the coefficient of uniformity is not really a measure of irrigation uniformity but of potential uniformity. It is based on the assumption that the system is designed so that the intake rate of the soil always exceeds the water application rate. This is standard design practice for stationary sprinkler systems.

However, the actual uniformity of refilling the soil profile can be considerably different from the measured application uniformity if the water does not infiltrate into the soil at the point of application, but instead moves on the surface. As it moves around the field, much of the center-pivot lateral applies water at cloudburst rates. Most soils cannot absorb the water this rapidly. Much of it runs from high spots and slopes to nearby low areas causing waste of water and yield reductions.

These high application rates are inherent in the principles of operation of a center-pivot system. For a system to have a uniform depth of application, the application rates must increase as the distance from the pivot increases.

Sprinkler heads on a stationary sprinkler lateral are all the same size. Therefore, the amount of water applied per unit of lateral length is essentially constant. This is appropriate because the land area irrigated per unit length of lateral is the same regardless of location on the lateral.

On the other hand, the area irrigated by each portion of a center-pivot lateral is a ring with a radius equal to the distance from the pivot. The area within each ring is proportional to the distance from the pivot and therefore requires an amount of water based on this area. If the sprinklers are equally spaced, the water can be applied uniformly only if the discharge of each sprinkler is proportional to its distance from the pivot. Because the pattern radius for individual sprinklers does not increase greatly with increasing discharge, the application rates must increase with distance from the pivot.

Another important difference between continuously-moving sprinklers and stationary sprinklers is the relationship between application rate and time. The average application rate for a stationary sprinkler remains constant throughout its period of operation. Application rates vary with time for continuously-moving sprinklers as the sprinkler pattern moves across any given point on the surface. As shown in Figure 1.1, the application rate for a center-pivot sprinkler begins at 0 as the sprinkler line approaches a given point and increases to a maximum as the sprinkler lateral is directly above this point. The application rate then decreases to 0 again as the sprinkler lateral passes. Pattern a represents the more common wide sprinkler spacing as compared with Pattern b which represents the application rate pattern for sprinklers which are spaced closer on the lateral. Peak application rates range from 1.0 to 2.6 inches per hour for most center-pivot systems currently in use.

As shown in Figure 1.2, the application rate exceeds the ponded infiltration rate curves for most soils, and the peak application rates occur after the infiltration rate has declined. The actual infiltration
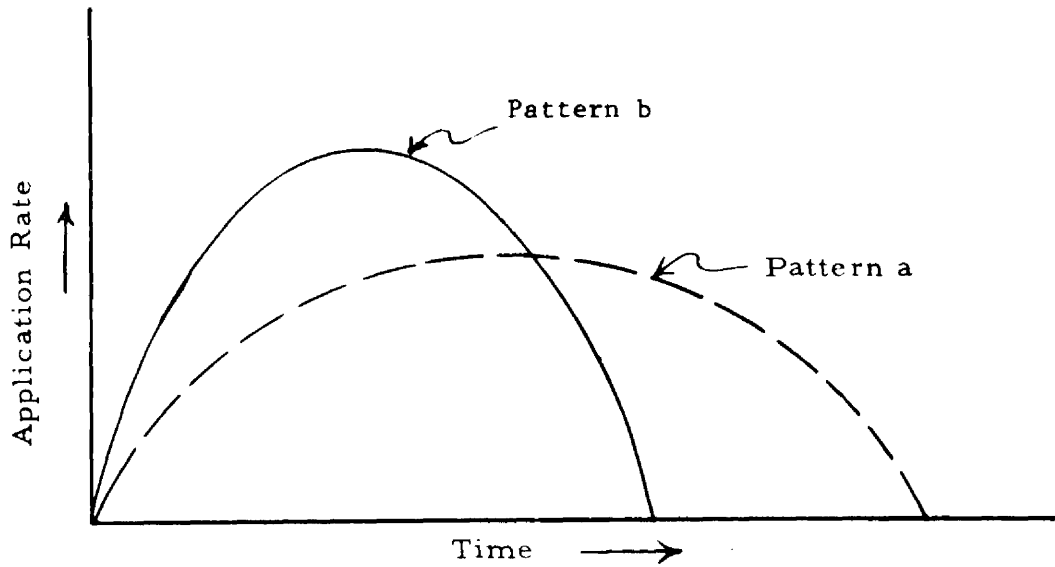
Figure 1.1 Center-pivot application rate patterns
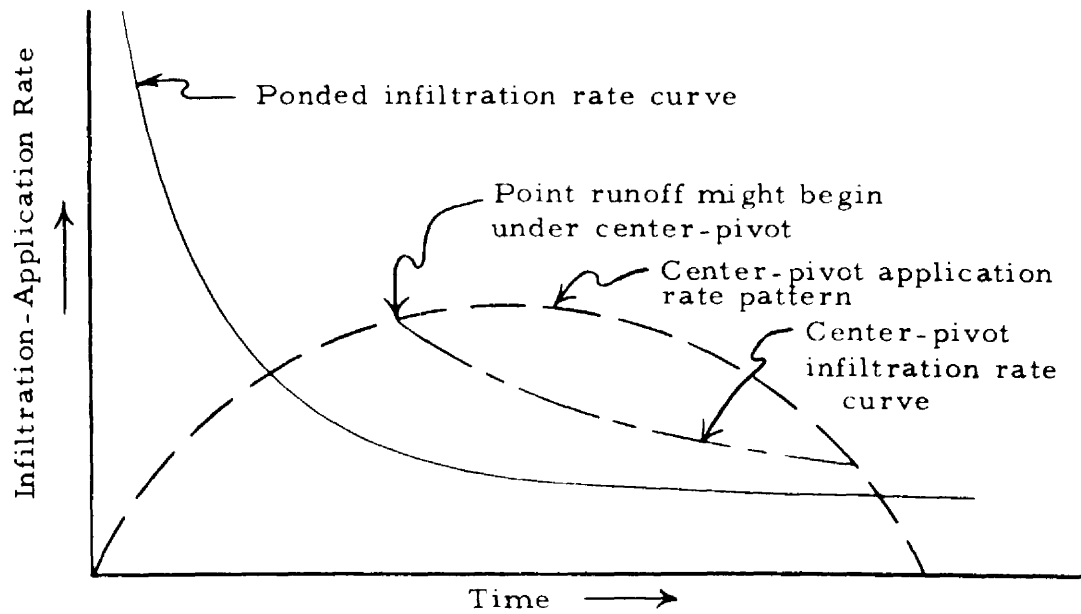
Figure 1.2   Ponded infiltration rate curve and infiltration
rate curve for a center-pivot pattern

rate curve can be expected to shift somewhat to the right as shown in Figure 1.2. This is a result of less water being in the soil than would have been present if the water had been applied at a rate equal to the infiltration rate from the time application began. The water applied in excess of the infiltration rate is potential runoff.

Project Objectives

Because center-pivot sprinklers apply water uniformly, the application of water in such a manner that it can infiltrate without surface movement would result in great improvements in irrigation uniformity A desirable goal is to match water application with soil infiltration characteristics. Therefore, the original objectives of this study were:

A. To investigate the effect of time-varying water application rates on infiltration rates under moving sprinkler systems.

B. To incorporate the findings of Objective A into mathematical models of moving sprinkler irrigation systems to modify design and operation for improved performance.

The study revealed that less could be done with Objective B than originally hoped. However, it became apparent that several variables were more important than expected, and that other approaches would be productive. Therefore, the following objectives were added:

C. To study other potential modifications of water application characteristics of moving sprinkler systems to increase irrigation uniformity and conserve water.

D. To find methods of increasing soil infiltration rates under moving sprinkler systems.

Chapter II

LITERATURE REVIEW

Considerable literature has been written on water infiltration

under rainfall, surface irrigation, and sprinkler irrigation. The

effects of many variables on infiltration have been studied. Equations

have been proposed which attempt to simplify the study of infiltration.

Numerical models to study infiltration and water movement in the

soil have become popular in the last ten years. Each of these areas

will be examined in this literature review.

Infiltration Variables

Water infiltration into soil is a complex process. Small

changes in physical and chemical actions cause large changes in in-

filtration rates. The first section of the literature review will ex-

amine some of the infiltration variables as studied by other re-

searchers.

Soil Physical Properties

Soil can be considered to consist of three phases: the solid,

solution, and gas phases. The solid phase consists of the soil parti-

cles. The solution and gas phase occupy the space between the soil

particles. This space is called pore space and consists of irregularly-shaped interconnected capillaries or small tubes.

During vertical infiltration, water enters the soil at the surface and flows through the pore space because of two main forces acting on the water; namely, gravity and capillarity.

The ratio of the volume of pore space to the bulk volume of the soil is called porosity. Primary porosity is the pore space between individual soil grains, while secondary porosity is between aggregates of soil grains. A soil having a relatively high value of secondary porosity is called a structured soil.

Total porosity and pore space distribution have a significant effect on the hydraulic behavior of a soil. Porosity and pore size are affected by mean particle size and distribution, the degree of structuring, and the shape of the particles. Some of the empirical and semi-theoretical equations which related permeability or conductivity to some of these physical properties of soils will now be presented.

The Fair-Hatch equation (18), which is listed below, gives the permeability of a sand as a function of porosity, packing, particle shape, and particle size.

$$k = \frac{1}{A' \left[\frac{(1-\phi)^2}{\phi^3} \left(\frac{B'}{100} \sum_{v=0}^{N} \frac{P_{v+\frac{1}{2}}}{d_{m_{v+\frac{1}{2}}}} \right)^2 \right]} \tag{2.1}$$

in which

k = intrinsic permeability, a function of the geometry of the media for porous media that are stable in the presence of the fluid occupying them.

A' = a packing factor

ϕ = porosity

B' = a shape factor

$P_{v+\frac{1}{2}}$ = percentage of sand held between adjacent sieves v and v + 1

N = number of sieves used

d_m = geometric mean of rated size of adjacent sieves v and v + 1.

According to Equation 2.1, increasing the porosity from 0.4 to 0.5 will triple the permeability, and increasing the average particle diameter by 20 percent increases the permeability 44 percent.

The Carmen-Kozeny equation (6) is somewhat similar to the Fair-Hatch equation.

$$k = \frac{\phi^3}{s^2 k_s T} \qquad (2.2)$$

in which

k and ϕ = defined in Equation 2.1

s = specific surface of porous medium

k_s = a pore shape factor

T = tortuosity of the flow path.

Both the Fair-Hatch and Carmen-Kozeny equations (Equations 2.1 and 2.2) are more accurate in determining the intrinsic permeability of sand than of other soils. These equations do give an indication of the importance of certain factors, particularly porosity, for describing infiltration into soils.

Moisture Content

Moisture weakens the bonds between soil particles and lubricates the soil particles. An increase in moisture content causes an increase in settlement for most loosely packed soils (27). Since moisture tension forces depend on moisture content, Keller (27) theorized that the total strength of aggregates of some moistened soils is almost wholly dependent on moisture tension forces.

Day and Holmgren (11) used micro-photography to study compression in soils. They found that aggregates lose strength and deform particularly in the area of contact between aggregates. As shown in Equations 2.1 and 2.2, a small percentage decrease in porosity causes a much larger percentage decrease in permeability. Therefore, deformation of aggregates caused by moisture can decrease permeability considerably.

Surface puddling results in considerable disruption of the surface soil aggregates (3). On a disturbed soil, the bulk density increases during wetting, particularly at the surface, thereby reducing the infiltration rate.

The degree of saturation has a very significant effect on the infiltration rate of a soil. An increase in saturation decreases the capillary pressure, thereby decreasing the potential gradient of the capillary force which reduces the moisture movement. An increase in saturation increases the relative permeability, thereby partially offsetting the decrease in gradient; however, normally the gradient decreases faster than the relative permeability increases.

An increase in saturation also provides less available water storage which causes the wetting front to advance faster. As the wetting front advances faster, the gradient of the capillary pressure at the surface decreases faster, which reduces the infiltration rate. Other effects of moisture content will be discussed under swelling and shrinking.

Water Drop Energy

Surface puddling caused by a saturated condition is only one factor causing a crust to be formed at the soil surface. Another factor which may be much more important is the water drop energy as the energy is dissipated in the surface layer of the soil. Many researchers have studied the decrease in infiltration rate caused by increased drop energy.

Bityukov (3) applied water on a loam soil at the rate of 0.5 mm per minute using various drop sizes. He examined the relationship

between percent of disruption of aggregates and diameter of drops. The percentage disruption of aggregates was checked by observation of individual soil particles before and after irrigation. A 1.0 mm drop size caused a 5.4 percent disruption of aggregates, a 2.3 mm drop size caused a 11.2 percent disruption of aggregates, and a 5.2 mm drop size caused a 14.0 percent disruption in aggregates.

Levine (32) studied the effect of sprinkler drop size on infiltration into six soils (Figure 2.1). Approximately 5 to 60 percent decrease in infiltration rate was observed by Levine as the apparent drop diameter increased from a range of 0-5 mm to a range of 15-25 mm.

Levine did not measure actual drop size but measured the wetted diameter a drop caused when falling on a paper towel. The wetted diameter was termed apparent drop size. Frost and Schwalen (21) actually measured drop sizes using a sprinkler with the same nozzle sizes Levine used. Correlating Levine's and Frost and Schwalen's data gives the following approximate relationships: 2.5 mm apparent drop diameter ≈ 0.4 mm actual drop diameter, 10 mm apparent drop diameter = 1.2 mm actual drop diameter and 20 mm apparent drop diameter = 3.0 mm actual drop diameter.

Many center pivots have much larger sprinklers than Levine used. Larger drops would result from the larger sprinkler causing greater decreases in soil infiltration rates.
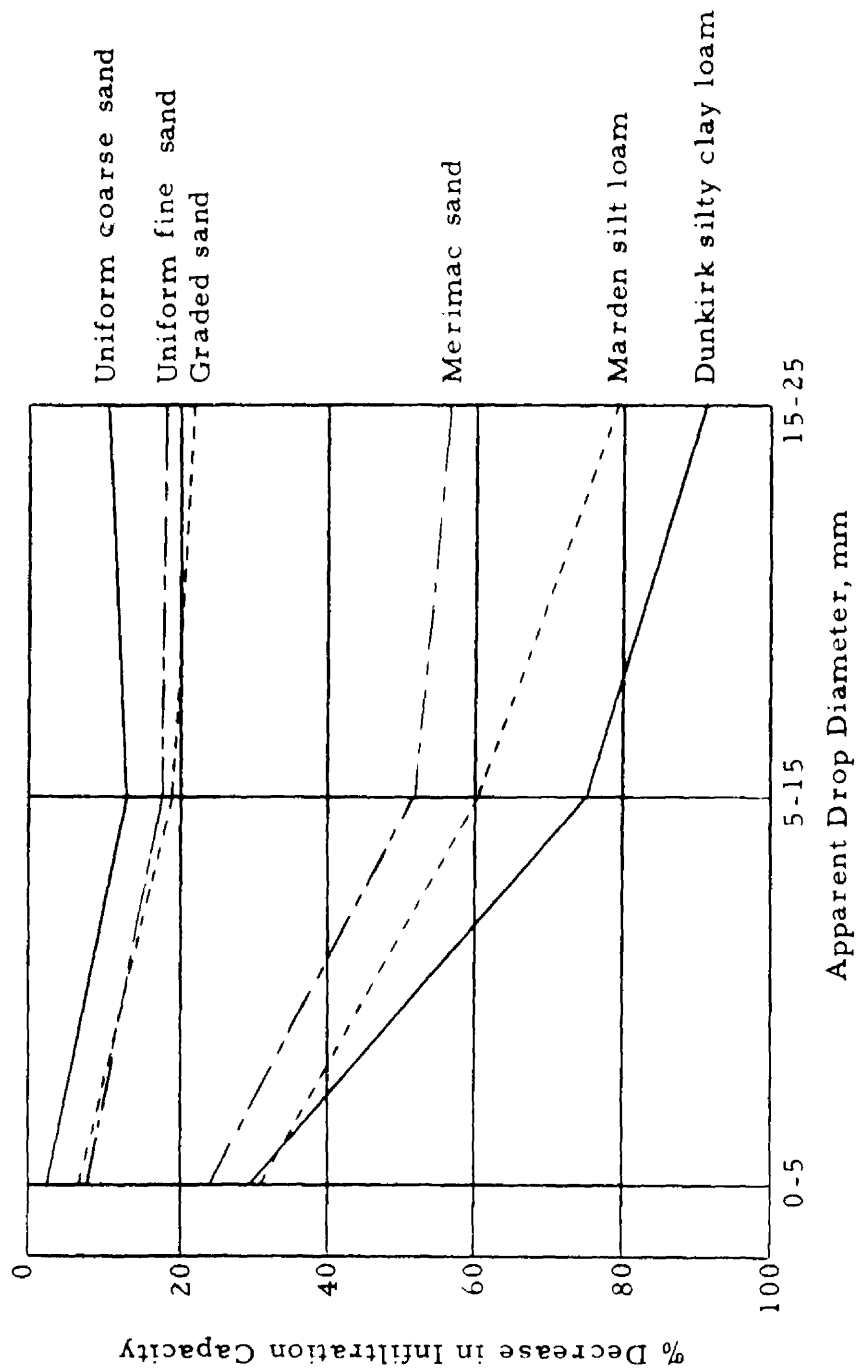
Figure 2.1 Effect of impact of various size drops on
infiltration (32)

Ellison and Slater (17) studied the relationship between drop velocity and infiltration on four soils composed primarily of silt and fine sand. As the drop velocity increased from 0 to 20 feet per second, the infiltration rate at the end of one hour decreased from a range of 2.0 to 6.7 inches per hour to nearly zero. The infiltration rates at five minutes were greatly reduced as the drop velocity increased. The average rainfall intensity on these tests was very high, being approximately seven inches per hour.

Laws (31) compared infiltration into soil using different drop sizes. The infiltration rate decreased approximately 70 percent as the drop size increased from 1.0 to 2.2 mm.

Infiltration tests were undertaken by Bisal (2) using drop heights of 6.55 m and 0.46 m. The infiltration rate of a loam soil under the 6.55 m drop height was approximately one-half the rate under the 0.46 m drop height. The infiltration rate of a clay soil under the 6.55 m drop height was approximately 1/6 the rate under the 0.46 m drop height. The velocity at impact produced by the rainfall simulator at 6.55 m would be approximately three times the velocity for the 0.46 m drop height.

Surface Protection

Many tests have been conducted using rainfall simulators to compare infiltration of a bare soil with infiltration of the same soil

having a burlap, straw, or fiberglass protection. The protective
cover is suspended a few inches above the soil surface. Duley (14)
performed infiltration tests on a sandy loam soil and initially pro-
tected the surface with straw. The infiltration rate with the straw
cover was 1.2 inches per hour. When the straw was removed, the
infiltration rate was reduced almost immediately to 0.3 inches per
hour. The crust was then removed and burlap placed over the soil.
The infiltration rate with the burlap cover was 1.5 inches per hour.
When the burlap was removed, the infiltration rate dropped rapidly
to 0.25 inches per hour.

Two silt loams, a silty clay loam, and a clay loam with the
surface protected by straw or other materials maintained a high in-
filtration rate for a considerable period of time (14). Once the pro-
tective cover was removed, the intake rate was quickly and severely
reduced.

Swartzendruber, et al., (48) compared infiltration into several
soils with and without fiberglass protection. Total infiltration
amounts for a silt loam and a loam soil were three to four times
higher into the fiberglass-protected surface as compared with the un-
protected surface. Sprinkling tests on a sandy loam soil showed
little difference in intake rate with and without a fiberglass cover.

Laboratory measurements of rain and no-rain permeability
on fifty-seven different wet soils are given by Mannering (33). The

rain treatment consisted of applying simulated rainfall to soil samples from above. The no-rain treatment consisted of saturating soil samples from below. The mean ratio of permeabilities of rain over no-rain was 0.41. In only two of the fifty-seven soils was the permeability after thirty minutes higher for the rain treatment than for the no-rain treatment. These two soils were a silt loam and a fine, sandy loam. A gravelly, sandy loam and a sandy loam had thirty-minute rain/no-rain permeability ratios between 0.75 and 1.0. Three loams, one silty clay, one silty-clay loam, and one clay loam had thirty-minute rain/no-rain permeability ratios less than 0.29. The other forty-seven soils had rain/no-rain permeability ratios between 0.30 and 0.75. Surprisingly, one sand with only 4 percent silt and 2 percent clay content had a permeability ratio of rain over no-rain of 0.25; however, the permeability was quite high even after the rain treatment.

Mannering also compared infiltration in the field between seven protected and unprotected soils. Two one-hour 7.0 cm applications were made twenty-four hours apart. A sand showed no difference in intake rate between protected and unprotected applications the first day. During the second day, the unprotected/protected intake rate ratio was 0.70. On two sandy loams the unprotected/protected intake rate ratio was approximately 0.5 during the first day. The second day the ratio was approximately 0.3. With three silty loams the

ratio was between 0.2 and 0.5. A silty clay had an 0.7 ratio during the first day and a 1.0 ratio during the second day. All of these comparisons are final intake rate ratios.

Peale and Beale (39) compared infiltration into a sandy clay loam between straw incorporated into the soil and straw spread on the soil surface. Infiltration rates for the incorporated straw was twice the rate of the untreated bare soil, but only 1/10 the rate of the soil whose surface was protected from raindrop action by placing straw on the soil surface.

A protected surface can also result from a 20 mm water layer developing on the soil surface (38). Palmer's (38) tests showed that the drop impact stress increased as the water layer depth increased from 0 to approximately 5 mm. The water layer had to be deeper than 20 mm before the stress became less than the stress at the zero water depth.

McIntyre (35) divided impact of raindrops at the soil surface into four successive processes. These processes are: (1) a rapid wetting at the surface causing low cohesion and high splash rates; (2) formation of a crust on the surface, a decrease in splash and accumulation of water; (3) removal of the crust by water turbulence and an increase in permeability; and (4) percolation of sufficient water to cause dissipation of drop energy on the soil once more, and an increase in splash rate.

Application Rate

As the application rate increases, the drop energy per unit area also increases (assuming drop size does not change). Mantell and Goldberg (34) conducted a study to examine the effect of water application rate on the structure of a clay soil with high aggregate stability. Application amounts of 5.6 mm with a drop size of 2.59 mm and with a two meter height of fall were used. After water application, the air permeability of the wet crust was determined. Increasing the application rate from 1.7 to 3.4 mm per hour decreased air permeability 50 percent. Increasing the application rate from 3.4 to 20.7 mm per hour decreased the air permeability 50 percent further.

Moldenhauer and Long (36) used a rainfall simulator to apply water at rates from 3.4 to 7.0 cm per hour on a fine sand, a loam, a silt, a silty clay loam, and a silty clay. Total infiltration in 90 minutes was the same regardless of intensity rate except on the fine sand. On the fine sand, total infiltration increased from 5 to 7 cm as the intensity was increased from 3.4 to 7.0 cm per hour. Runoff on all soils with an intensity of 6.78 cm per hour began in one-half the time that runoff began with a 3.43 cm per hour intensity.

Infiltration decreased 50 percent on a silt loam soil used by Sor and Bertrand (45) when the simulated rainfall intensity was increased from 1.6 to 2.8 inches per hour. On a sandy loam soil, the

infiltration only decreased 20 percent as the intensity was increased from 1.6 to 2.8 inches per hour.

Crust Breakup

Tillage operations will break up a crust, thereby producing a disturbed soil with an increased infiltration rate. Sixty-five percent of the applied water occurred as runoff on an uncultivated crusted silt loam soil, but only 1.7 percent runoff occurred on the same soil with a broken surface on tests performed by Borst and Woodburn (4). Borst and Woodburn applied artificial rainfall at an intensity of 2.2 inches per hour for one hour. A straw mulch of two tons per acre was applied on the surface.

Swelling and Shrinking

As a soil shrinks, the pores increase in size and cracks begin to form. When moisture is added, the soil swells, closing the cracks and reducing the pore size.

The size of the pores has a very significant effect on the infiltration capacity of a soil. Corey (9) discusses Poiseulle's equation which shows the effect that the radius of a tube has on the fluid velocity in the tube.

$$\bar{u} = -\frac{r_t^2 \, \Delta H}{8\mu \, L} \tag{2.3}$$

in which

$\bar{u}$ = average velocity in the tube

r_t = tube radius

μ = dynamic viscosity

H = hydraulic head

L = length of tube

The total flow through a tube is given below and shows that the flow is proportional to the fourth power of the tube radius.

$$q_t = A_t \bar{u} = - \frac{\pi r_t^4 \triangle H}{4\mu L} \tag{2.4}$$

in which

q_t = total flow through a tube

A_t = cross sectional area of tube.

Reasons for Swelling

Schmehl[1] states that the interlayer bond is related to the amount of swelling. If the interlayer bond is relatively strong, polar molecules such as water cannot enter the basal plane and the clay or other mineral is essentially non-expanding. If the bond is weaker, the clay will swell in a polar solvent. Swelling is inversely proportional to bonding energy, and bonding energy is directly proportional to the amount of clay surface.

---

[1]Class Notes, Soil Chemistry, Ag 560, Colorado State University, Spring, 1971.

The first few layers of water molecules absorbed on the clay surface may be considered part of the clay surface and will affect some properties of the clay. The bonding energy holding the water molecules to the clay surface become progressively weaker with each successive water layer.

Each layer's surface has an electrical double layer resulting from ionic concentration in the free water. Both layers contain ions of the same charge causing the double layer on one clay surface to repulse or push away the double layer on the other clay surface. The adjacent clay surfaces are repulsed, causing soil swelling.

The amount of swell varies considerably with clay type (Table 2.1) (50). Free swelling is defined as the increase in volume of the substrata upon the addition of a certain volume of water. The decreasing order of swell is montmorillonite > illite > halloysite > kaolinite.

Table 2.1   Free swelling data for various clay minerals (in percent)
(50)

Ca--montmorillonite	45-145
Na--montmorillonite	1,400-1,600
Na--hectorite	1,600-2,000
Illite	15-60
Kaolinite	5-60

The nature of the ion adsorbed on the surface affects swelling as shown in comparing the Ca and Na montmorillonite. Baver and Winterkorn (1) found that, for Wyoming bentonite, swelling decreased in the following order: sodium > lithium > potassium > calcium > magnesium > hydrogen.

The magnitude of swelling also varies with variation in particle size distribution, electrolyte content of the solution phase, void size, and distribution of void sizes.

Time Dependence of Swelling

When water infiltrates into a soil, the least resistance to flow occurs in the larger inter-granular spaces. More resistance, or slower flow, occurs in the inter-crystal spaces and smaller inter-granular spaces. The slowest flow occurs into the interlayer regions which must expand to accept water molecules. The interlayer region is the area where most of the swelling occurs. Baver and Winterkorn (1) reported on rate of water intake with various colloids and ions adsorbed on the clay surface. As shown in Figure 2.2, time has considerable effect on swelling. The rate of water intake also varies considerably with what ion is adsorbed on the surface. The rate of water intake was the slowest percentage-wise with the colloids of highest ultimate swells: e.g., Li and Na Putnam colloids. Many researchers-- e.g., Winterkorn and Baver (53), Tressler and Williamson (49), Dubose (13), --show soils continue to swell for hours or days.
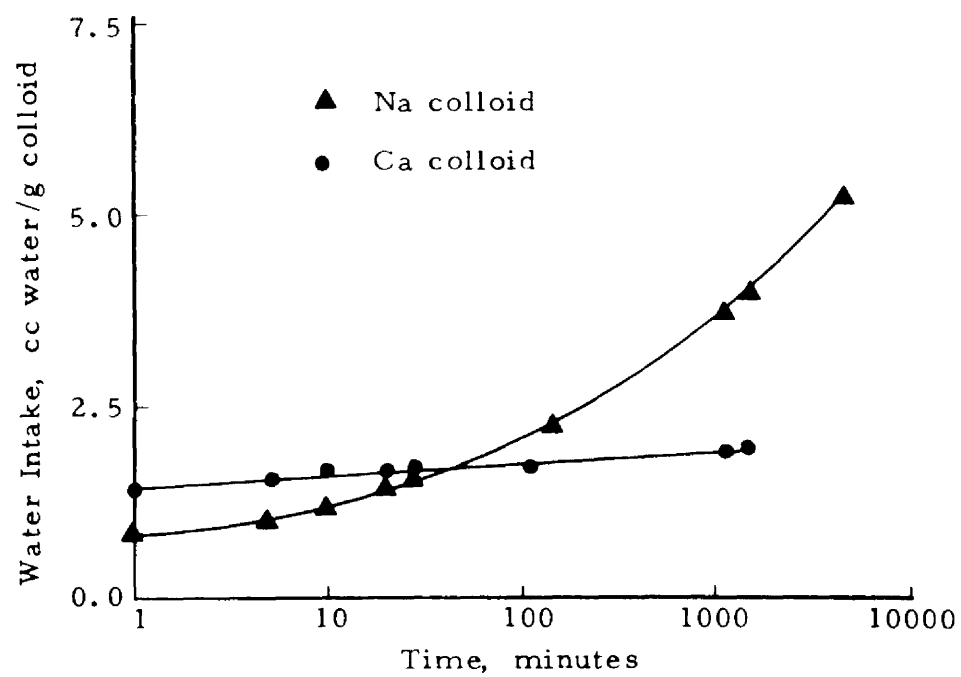
Figure 2.2 Cumulative water intake by Putnam colloid
saturated with different cations (1)

Infiltrating Fluid

The most common infiltrating fluid--water--usually contains impurities. The capillary potential is directly proportional to the surface tension, which is reduced by impurities.

Hydraulic conductivity is indirectly proportional to the solution viscosity as shown in Equation 2.3. The fluid viscosity is changed by adding impurities and by the interaction of the water with the soil. Water near the soil particles has an increase in viscosity because of an electrical potential between the water and the soil. This potential can have an important effect on hydraulic conductivity in very fine-textured soils.

Infiltration Equations

Measuring the variables affecting infiltration is difficult. The effect some variables have on infiltration is impossible to define at present. Some empirical and semi-theoretical equations have been proposed to simplify the study of infiltration. Some of these equations will now be reviewed.

Green-Ampt (22) proposed an infiltration law:

$$I = K (h + D' - P_{b/\gamma})/D' \qquad (2.5)$$

in which

I = rate of infiltration

h = ponded water depth on the surface

P_b = air entry pressure or bubbling pressure

γ = specific weight of water

D' = distance from the soil surface to the wetted front

K = saturated hydraulic conductivity of the soil.

The advancing water front is assumed to be a precisely-defined surface. This front separates saturated soil behind it, of uniform hydraulic conductivity K, from unsaturated and as yet uninfluenced soil beyond it.

Kostiakov (30) developed an empirical equation stating

$$I = I_o t^n \tag{2.6}$$

in which

I = infiltration rate at time t

I_o = infiltration rate at unit time

t = time elapsed from start of infiltration

n = constant, $-1 < n < 0$

In this equation, I goes to zero as t become infinite, which is not true under vertical infiltration.

Horton (26) proposed an intuitive equation

$$I = I_c + (I_o - I_c) e^{-k_f t} \tag{2.7}$$

in which

I_c = final or steady state infiltration rate

t, I, I_o = defined for Equation 2.6

I' = infiltration rate at $t = 0$

e = base of Naperian logarithms

k_f = constant.

Horton assumed that the process involved in the reduction of I as rain continued is of a similar nature to exhaustion processes. Included were the processes of rainpacking, in-washing, breaking down of the crumb-structure of the soil, the swelling of colloids and in cases where they occur, the closing of cracks. Horton attributed most changes in I to occur at or close to the surface, except for pure sands and clayey soils with deep and numerous cracks.

For soils with a restricting strata, Holton (24) proposed an infiltration equation

$$I = E' F_p^G + I_c \qquad (2.8)$$

in which

I and I_c = defined in previous equations

F_p = storage potential of the soil above an impeding strata; equals total porosity minus antecedent water expressed in units of L

E' and G = constants specified by soil type and surface and cropping conditions.

Equation 2.8 allows for the effect of initial soil moisture content. The equation also allows the infiltration rate to become a constant value. The problem is determining the control depth to be used in computing the storage potential, F_p. Holton, et al., (25) further divided F_p into gravitational water and plant-available water capacity.

Philip (41) derived an equation from an analysis of the partial differential form of the moisture flow equation applied to water movement in vertical columns.

$$I = 0.5 F t^{-0.5} + Y \qquad (2.9)$$

in which

F = constant which Philip called soil sorptivity

Y = a parameter related to soil hydraulic properties

I and t = previously defined.

The infiltration equations described above have several limitations. Most parameters cannot be determined from physical properties of the soil. Infiltration from a ponded surface is the only upper boundary condition considered. For sprinkler irrigation or rainfall, a ponded condition is usually not the initial upper boundary condition.

Infiltration Studies Involving Non-Ponded Conditions

This section contains published analytical and numerical solutions to infiltration problems which do not necessarily involve ponded conditions at the surface.

Analytical Solutions

El-Shafei (16) hypothesized that "the time at which surface ponding occurs, t_s, is the time at which the cumulative rain (sprinkler) infiltration is equal to the cumulative flooded (ponded) infiltration." The surface ponding time, t_s, is the time runoff begins under rainfall or sprinkling.

In equation form:

$$Rt_s = \int_0^{t_s} I_o t^n \, dt \tag{2.10}$$

in which

R = application rate

n = a constant

I_o = flooded infiltration rate at unit time.

Integrating the right side of Equation 2.10 results in:

$$Rt_s = I_o \frac{t_s^{1+n}}{1+n} \tag{2.11}$$

Solving for time of surface ponding, t_s, under sprinkler irrigation results in:

$$t_s = \left[\frac{I_o}{(1+n) R} \right]^{\frac{-1}{n}} \tag{2.12}$$

El-Shafei does not predict what form the infiltration rate curve takes after runoff begins. All of the tests he presents have either a flooded surface condition or a constant application rate.

Kincaid, et al., (28) studied runoff under center pivot sprinkler systems. Their proposed modified potential infiltration rate, I_m, before runoff began was

$$I_m = I \, D_p / D_a ,$$ (2.13)

in which

I = flooded infiltration rate at time t

D_p = potential depth of infiltration at time t, obtained by integrating the flooded infiltration rate, I, over time 0 to t

D_a = actual water depth applied over time 0 to t.

Using a constant application rate, R,

$$I_m = R \text{ at } t = t_k ,$$ (2.14)

in which

t_k = surface ponding time for Kincaid, et al. (28).

The depth applied, D_a, at time of runoff, t_k, is

$$D_a = R \, t_k .$$ (2.15)

The potential infiltrated depth, D_p, at time t_s is

$$D_p = \int_0^{t_k} I \, dt ,$$ (2.16)

and

$$I = I_o t_k^n \text{ at } t = t_k. \qquad (2.17)$$

Substituting for I in Equation 2.16

$$D_p = \frac{I_o t_k^{1+n}}{1+n}. \qquad (2.18)$$

Substituting values from Equations 2.14, 2.15, 2.27 and 2.18 into Equation 2.13 results in

$$R = (I_o t_k^n) \frac{\left(\frac{I_o t_k^{1+n}}{1+n}\right)}{R t_k}. \qquad (2.19)$$

Solving for surface ponding time, t_k

$$t_k = \left[\frac{I_o}{R \sqrt{1+n}}\right]^{-\frac{1}{n}}. \qquad (2.20)$$

The ratio for surface ponding times of Kincaid, et al., (26) (Equation 2.20), to El-Shafei (16) (Equation 2.12), using a constant application rate, is

$$\frac{t_k}{t_s} = \sqrt{1+n}^{-\frac{1}{n}}. \qquad (2.21)$$

For $n = -0.5$, $\frac{t_k}{t_s} = 0.5$.

Kincaid, et al., (28) defines the infiltration rate after runoff begins as

$$I = I_o (t - \Delta t)^n \qquad (2.22)$$

in which

$$\Delta t = t_k - t_o$$

and defining t_o by the equation

$$I (at\ t = t_o) = I_m (at\ t = t_k). \qquad (2.23)$$

Numerical Solutions

Another approach to the solution of vertical infiltration problems is numerical solution of moisture flow equations. Some of the equations which are presently available will be described below.

Darcy (10) formulated a law for saturated flow in soil

$$Q = - K \frac{\Delta H}{\Delta Z} \qquad (2.24)$$

in which

Q = flow velocity

Z = vertical dimension measured positive downward from the

   soil surface

K = saturated conductivity

H = hydraulic head.

Childs and Collis-George (7) (8) verified Darcy's law under unsaturated flow conditions. Darcy's law for unsaturated flow is

$$Q \quad - K \, k_r \frac{\Delta H}{\Delta Z} \qquad\qquad (2.25)$$

in which

k_r = relative permeability or relative conductivity, or ratio of

unsaturated conductivity value to saturated conductivity.

The continuity equation for one dimension is

$$\frac{\partial Q}{\partial Z} = - \frac{\partial(\phi S)}{\partial t} \qquad\qquad (2.26)$$

in which

ϕ = porosity

S = volumetric saturation, $\dfrac{\text{volume of water}}{\text{volume of pores}}$

t = time.

Combining Equations 2.25 and 2.26 results in

$$\frac{\partial}{\partial Z} (K \, k_r \frac{\partial H}{\partial Z}) = \frac{\partial(\phi S)}{\partial t} . \qquad\qquad (2.27)$$

Substituting $- Z + \psi$ for H produces

$$\frac{\partial(\phi S)}{\partial t} = K \frac{\partial}{\partial Z} (k_r \frac{\partial \psi}{\partial Z}) - K \frac{\partial k_r}{\partial Z} \qquad\qquad (2.28)$$

in which ψ is the capillary potential.

This equation (Equation 2.28) is sometimes called the Richards

equation after L. A. Richards (43). To solve this equation at any

point in the soil requires a knowledge of the relationships among ψ,

S, and k_r for the particular soil. Boundary conditions are required,

such as a sprinkler application rate at the surface and a water table at the bottom surface. The initial conditions required usually consist of specifying ψ or S throughout the soil at t = 0.

A solution of Equation 2.28 will provide water content and pressure head curves at a particular time. Thus, the flow of water in the soil can be followed or described.

No analytical solution exists for Equation 2.28. However, many numerical solutions have been published. The techniques continue to become more sophisticated to solve more complex problems.

Klute (29) and Philip (40) numerically solved Equation 2.28 for horizontal and vertical flow from a constant surface saturation. For horizontal flow, the last term $K \frac{\partial k_r}{\partial Z}$ in Equation 2.24 does not appear and Z is a horizontal distance, which considerably simplifies the solution. A constant surface saturation is also a simplified and restricted solution. However, these earlier investigations are very important because they represent the beginning of the numerical solutions for moisture flow problems.

Hanks and Bowers (23) allowed for a two-layered system of soils. Solutions were obtained for vertical upward and vertical downward infiltrations and for horizontal infiltration into two soils. Uniform initial moisture contents were used.

Edwards and Larson (15) modified Hanks and Bowers solution, taking into consideration the surface seal produced under rainfall.

Good agreement was obtained between estimated and field-measured infiltration for a silt loam protected from raindrop impact when water content, capillary pressure, conductivity relations, measured on undisturbed cores, were used as computer input. When the surface was unprotected from raindrop impact, infiltration was overestimated unless the surface seal was taken into consideration. As the surface seal develops, the suction through the seal is shown to increase.

These first solutions of Klute (29), Philip (40), and Hanks and Bowers (23) allow for a constant inlet boundary condition, which is applicable only to a flooded condition. Whisler and Klute (52), Rubin (44), and Freeze (20) presented infiltration solutions for either rainfall or ponding at the upper boundary. Whisler and Klute studied the phenomenon of hysteresis in columns with non-uniform initial moisture contents. Rubin used a uniform initial moisture content.

Smith and Woolhiser (47) allowed for rainfall and ponded conditions and included overland flow resulting from runoff. Good agreement was obtained between measured and predicted hydrographs for a 40-foot laboratory flume and for an experimental watershed.

Use of Equation 2.28 to study moisture flow in soil has increased in recent years for several reasons. Rapid solutions of the equation are obtained using high-speed computers. With a computer model, it is possible to change only one variable at a time to determine its effect upon the solution. With actual experiments using

soil, it is not always possible to change one variable without influencing others.

CHAPTER III

STUDY APPROACH

Many applied problems need to be studied in more than one way in

order to arrive at satisfactory solutions. In the judgment of the in-

vestigators this project was concerned with that type of problem. Use-

ful information was obtained by studying actual problems which existed

under normal field conditions. This approach is very helpful in main-

taining perspective regarding the relative importance of various phases

of the problem. It also is a convenient method for testing some pro-

posed solutions.

Field Tests

Field work under operating systems also has severe limitations.

Accurate control of variables involved ranges from good to economically

impractical. It is also very difficult, and often impossible, to sep-

arate the effects of many of the variables involved. Care must be used

to avoid measuring a "black box" type of situation which has applica-

tion only to one set of conditions. Field work under operating center-

pivot systems played a valuable, but limited, role in this study.

Sprinkler Infiltrometer

Field infiltrometer tests were run with a specially constructed

sprinkler infiltrometer which was capable of producing continually

varying application rates to simulate various sprinkler patterns on

continuously-moving sprinkler systems. Equipment was constructed so that tests could be run using different shapes of time varying application rate patterns and so that measurements could be taken simultaneously of different water application intensities for each of the patterns. The advantages of these tests over field work under actual systems was that much less work was required to run tests under a variety of conditions. Also a greater degree of control was possible and the results could be measured with a high degree of accuracy. Limitations were that the conditions necessarily had to be altered somewhat from what would be found under actual systems. Also, the effect of the different variables could not be separated as is possible in the laboratory.

Laboratory Tests

Laboratory experiments permit much better control in the study of the infiltration process by making it possible to eliminate many of the variables which occur in the field. In this study, laboratory experiments were used for this purpose and also to develop a model to help in the study of infiltration under time varying application rates.

Two different tests of application rate patterns were used in the laboratory experiments and model simulation (Figure 3.1). The first set consisted of one constant and two 2-step application rate patterns. The second set contained three simulated center-pivot application patterns.

The first set of patterns was used to determine how infiltration rates varied in relation to time and depth of intake. These patterns
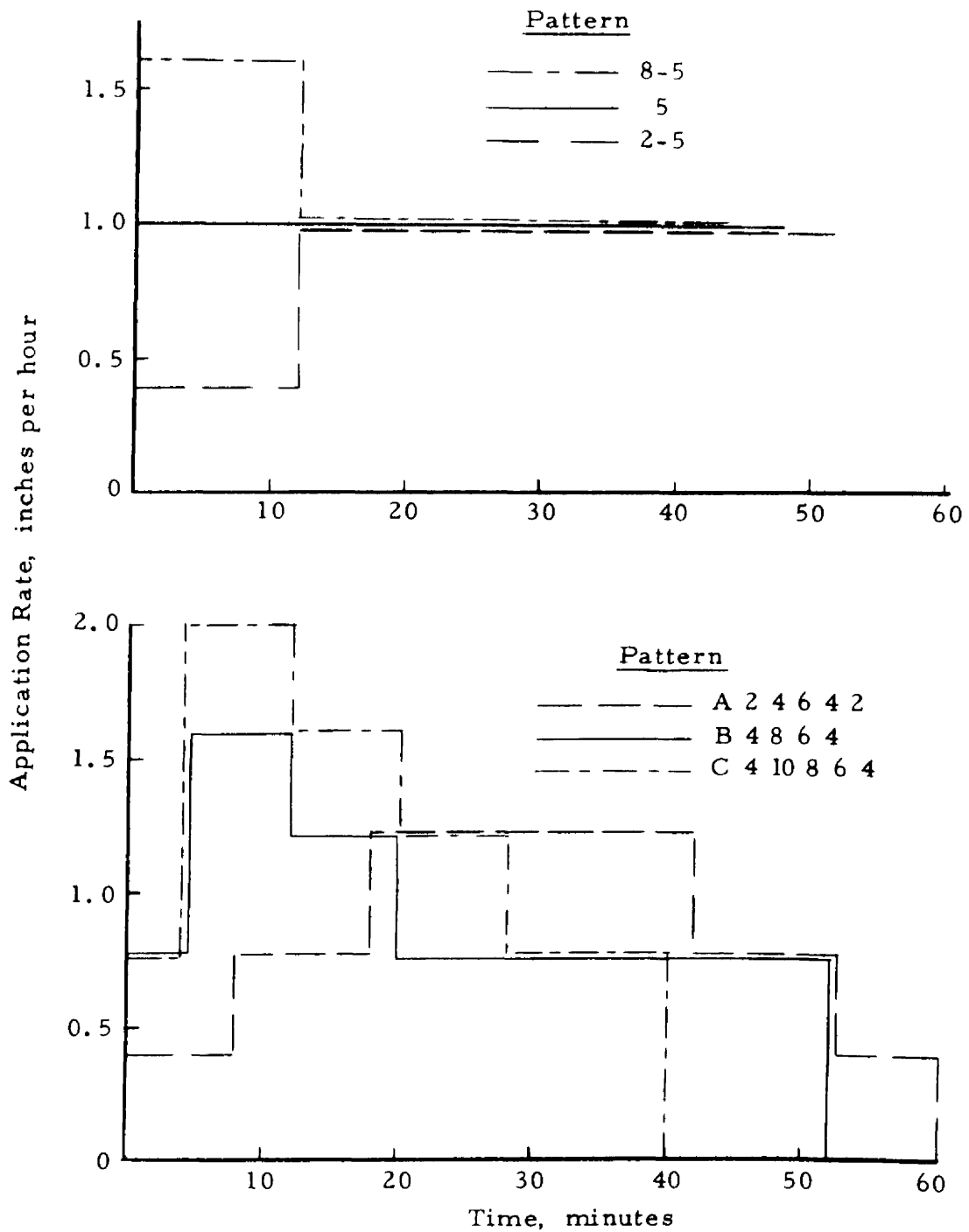
Figure 3.1 Application rate patterns used in the laboratory experiments and model simulation

were used in developing and verifying the model. The second set of patterns was used to study the effect of the application rate pattern on runoff and to compare laboratory results with the model prediction.

In the laboratory experiments, water was applied to the soil which was placed in eight soil compartments. Water which did not infiltrate into the soil ran off the surface and was collected and measured. Between tests, heated air was forced through the soil to dry it (Figure 3.2).

Two types of soil were used to study a wider range of conditions than one soil would have permitted. One soil contained a high percentage of sand and the other a high percentage of silt.

An undisturbed soil managed under field conditions would have been desirable, but there was no practical way of transferring samples from the field to the laboratory. However, once in place, the soil was not disturbed between tests.

Numerical Model

The physical process being modeled involved applying water to the surface of the porous media, water infiltration into the porous media, and water runoff at the surface when the application rate exceeded the infiltration rate (Figure 3.3). The porous media was soil and had to be described in the model in terms of porosities, initial moisture contents, saturated conductivities, and relationships between moisture content, capillary pressure, and relative permeability. Movement of water into and through the soil was described by Equation 2.28.
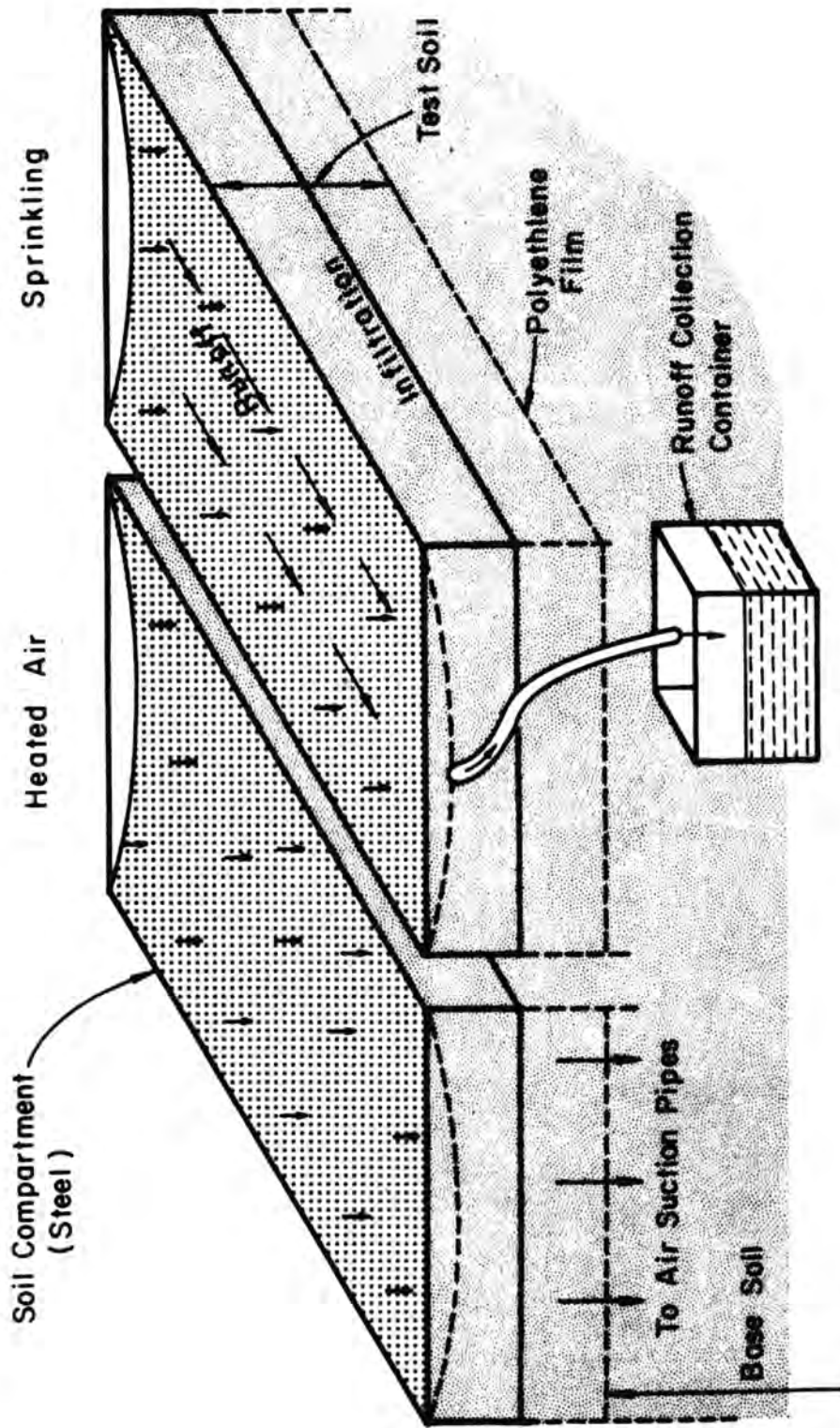
Figure 3.2 Sprinkling and drying of soil
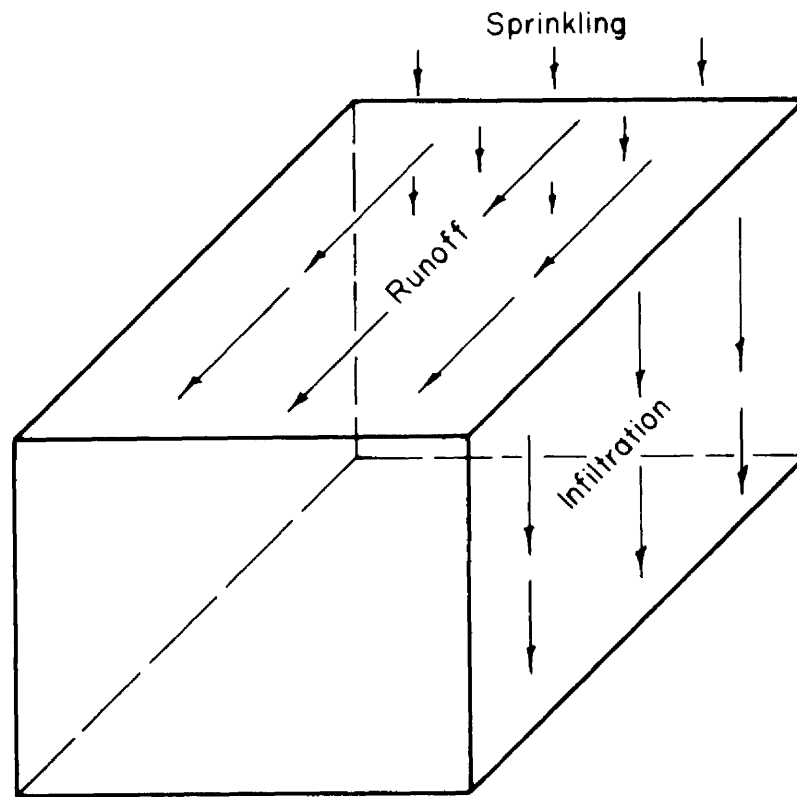
Figure 3.3   Model simulating sprinkling, infiltration,
and runoff

The numerical model was very versatile but had to be calibrated to reasonably fit the laboratory experiments. Because of this versatility the model could handle stratified soils, any initial moisture content, and nearly any boundary condition. However, the model did not allow for change in conductivity caused by swelling.

Tillage and Planting Practices

It became apparent that alterating the manner in which the water was applied could provide only part of the solution on most problem soils. Integrated with this approach needed to be methods of increasing infiltration rates in the field. Replicated tests of water application on six different row crop tillage and planting methods were conducted to determine their relative ability to increase infiltration rates. The results were then transferred to field use.

Chapter IV

PROCEDURE

Laboratory Infiltration Experiments

Equipment

The main components of the equipment are the soil compartments separating the plots, soil drying equipment, traveling spray bar, runoff collection containers, and tensiometers (Figures 4. 1 and 4. 2).

Soil Separation

Soil was placed in eight compartments, each having surface dimensions of 12" x 23. 5". Each compartment had sheet steel sides 5" deep with polyethylene film extending an additional 4" to the bottom of the test soil. These dividers defined the drainage area of each compartment and prevented lateral water movement between samples. The bottom of each compartment was open to permit contact with the base soil.

Soil Drying Equipment

Air pipes were placed in a clay loam soil in the base. The lower soil acted as a sump for the water to drain into from the test soil.

Note: All Pipes Slotted on Bottom For Passage of Air
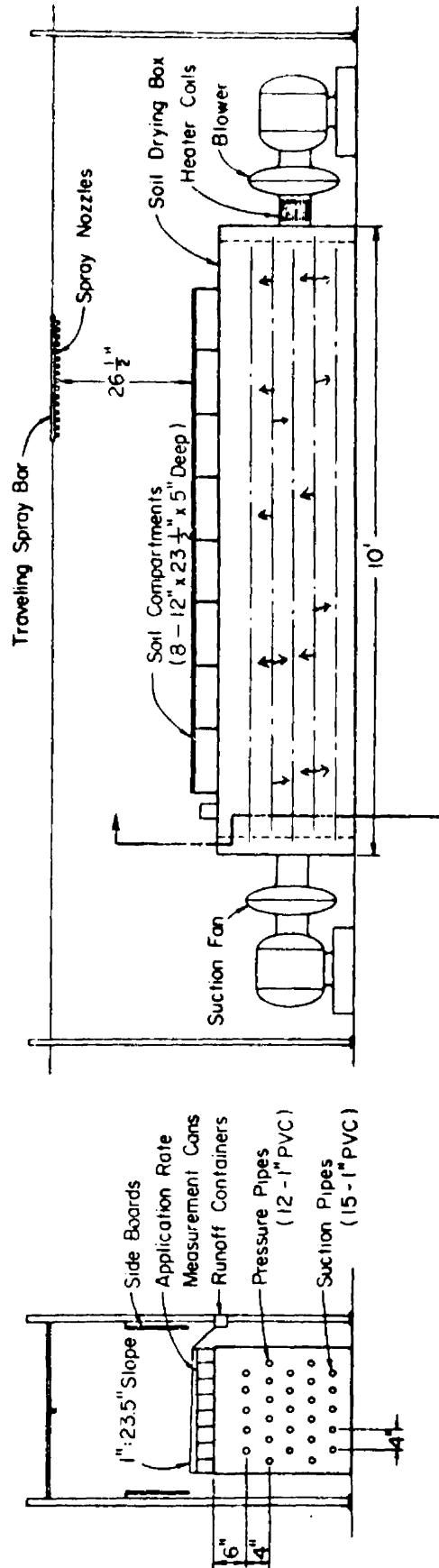
Figure 4.1 Apparatus used for laboratory sprinkler infiltration tests showing air flow between pressure and suction pipes in the soil mass
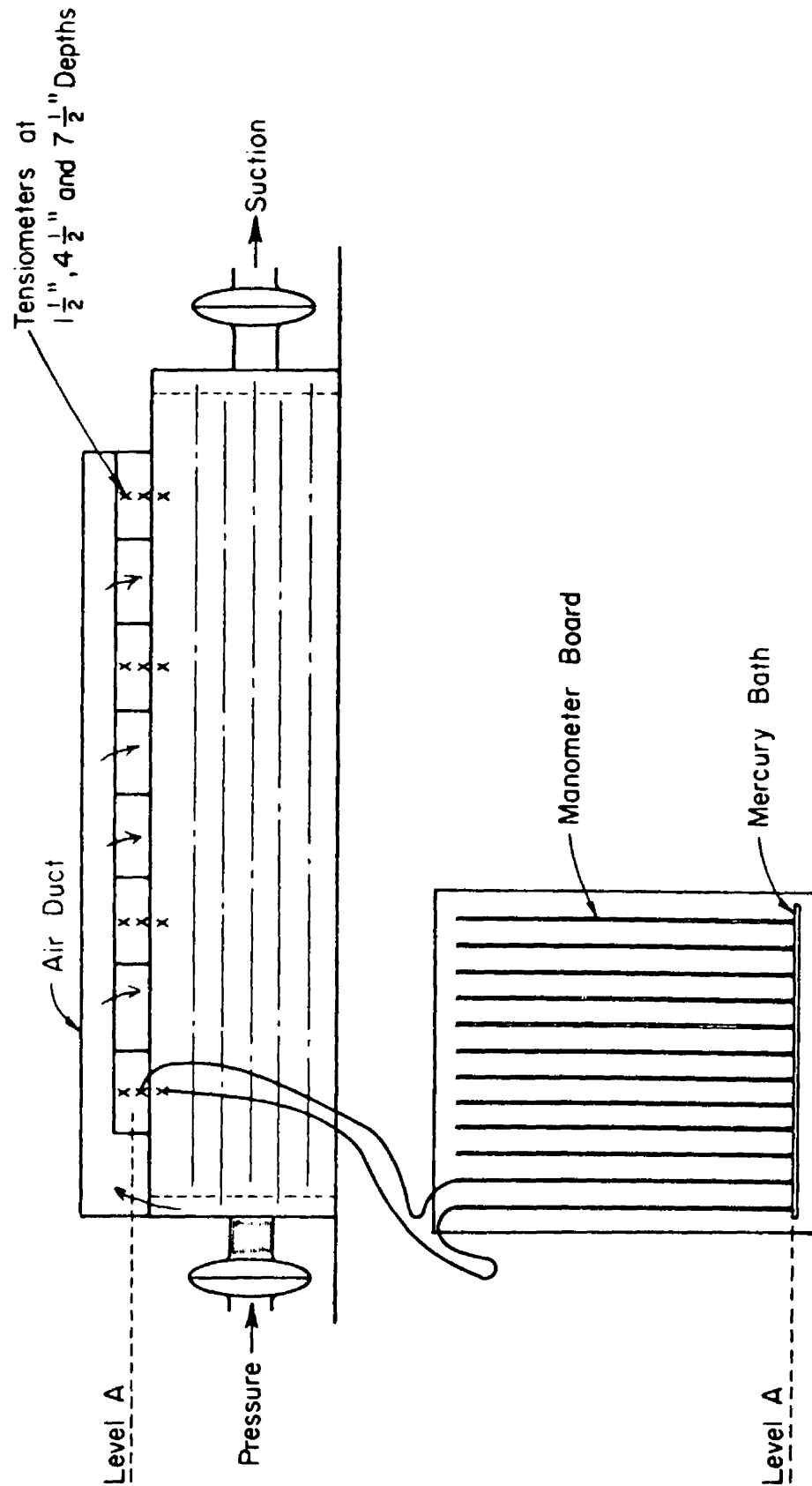
Figure 4.2 Schematic drawing showing location of tensiometers and air duct causing heated air to flow through the soil surface to suction pipes

While a test was being conducted, the wetting front did not extend into the lower soil.

Initially, tests were run and the soil was dried by passing heated air through the soil from the pressure pipes to the suction pipes (Figure 4. 1). However, it was difficult to bring the moisture level of the surface soil much below field capacity.

To obtain drier soil, an air duct was placed over the soil (Figure 4. 2). Most of the pressure pipes were plugged causing the majority of the air to pass through the surface of the soil down to the suction pipes.

Spray Bar

The sprinkler apparatus consisted of a traveling spray bar with valve controlled nozzles which allowed application rates of 0. 2 to 6. 4 inches per hour. Tests were conducted to obtain a nozzle with a uniform application perpendicular to the lines of travel. The nozzle chosen was an 8001E of Spraying Systems Company operated at 50 ± 3 psi. Each nozzle applied approximately 0. 2 inches per hour.

Water was supplied to the traveling spray bar from a tank pressurized with air which was controlled by a regulator.

The depth applied during a test was measured with eight measurement cans which were placed next to the soil compartment at the suction end. The cans were placed perpendicular to the line of travel of the spray bar and were used to determine uniformity of the pattern.

Runoff Collection

The soil surface in the soil compartments had a slope of 2.4 percent towards the runoff outlet and also had a small slope to the center of the compartment to prevent ponding. Runoff was collected in graduated containers. Volume of runoff was read and recorded at two or four minute intervals. The rate of runoff was calculated by dividing the runoff volume by the time interval. The intake rate was the difference between the application rate and the rate of runoff.

Tensiometers

Tensiometers connected to manometers were used to monitor the soil moisture tension (Figure 4.2). Twelve small tensiometers (three per compartment) were installed in soil compartments 1, 3, 6 and 8 as numbered from the suction end. These tensiometers were installed at the end opposite the outlet end (Figure 4.2).

Soils

The topsoil was sieved through a 2.362 mm sieve. Analyses of the two soils used in the experiments are shown in Table 4.1.

After the soil was first placed in the compartment, it was sprinkled a number of times for settlement purposes. The crust was removed and the soil compartments refilled after initial settlement and between each series of tests. Data from the first four runs of a series were not used because of the initial sharp decrease in

Table 4.1 Analyses of soil

Texture	Sand %	Silt %	Clay %	Organic Matter %	Conductivity (Salts) mmhos/cm
Sandy clay loam	59.8	19.0	21.2	1.0	1.9
Loam	34.6	46.0	19.2	1.3	1.0

infiltration rates before the soil stabilized. The continued small decrease in infiltration rates was attributed to formation of a crust and microbiological activity in the soil.

Test Procedure

The tensiometer readings were recorded before beginning a test. After filling the tank with tap water, the tank was pressurized and a selected number of spray nozzles on the traveling spray bar were operated. When the pressure reached 50 psi, the spray bar was started in motion, spraying back and forth across the soil compartments.

Every two or four minutes the runoff volumes in the runoff containers were read and recorded. The runoff volumes in the containers were read in the same sequence from left to right at the end of each time interval. Nozzles were turned on or off at specified times as required to produce the desired application rate pattern.

At the end of the test, tensiometer readings were recorded and the volume of water in each application rate measurement can was recorded.

After the air duct was replaced over the soil compartments, the pressure and suction blowers and the heating coils were turned on to dry the soil 15 hours for two nights - or 30 hours total - prior to the next test run.

Numerical Simulation Model

Equations and Assumptions

Smith (46) describes a combination infiltration and overland flow model. The infiltration component of the model, with modifications, is used in this study.

The soil-moisture movement is described by the following equation.

$$\frac{\partial(\phi S)}{\partial t} = K \frac{\partial}{\partial Z} (k_r \frac{\partial \psi}{\partial Z} - K \frac{\partial k_r}{\partial Z}) \qquad (2.28)$$

The following assumptions are implied by the use of this equation.

1. The gas phase moves under negligible pressure gradients.

2. Darcy's law, Equation 2.25, is valid for unsaturated water movement in soil.

3. Moisture tension, ψ, and relative permeability, k_r, are unique, non-hysteric functions of moisture saturation, S.

4. The soil is a stable non-changing media.

Assumption 1 is reasonable in laboratory studies if the air pressure at the base of a soil sample is atmospheric. Assumption 1 is

also reasonable under most field conditions. Deviations from assumption 2 are small and difficult to prove. Assumption 3 will produce only small errors if an imbibition curve is used and if assumption 4 is correct.

Assumption 4 could be considerably in error for soils containing montmorillonite clay, which are allowed to shrink and develop large cracks. However, the soil was assumed stable because this assumption would considerably simplify the model and because it was initially thought that this assumption would not cause noticeable errors.

Solution of the Equation

To solve Equation 2.28 on a digital computer, the equation is written in finite difference form. The solution of the equation proceeds in time and one dimension of distance. A complete description of the equation and its solution is given by Smith (46), while a general description will be given in this chapter.

An overall view of the solution is shown by the flow chart of the computer program (Figure 4.3). The superscripts j refer to time and the subscripts i refer to distances in the flow chart.

The first step in getting Equation 2.28 into final form for solution is to multiply Equation 2.28 by dz resulting in

$$\frac{\partial}{\partial t} (V_b \phi S) = K \frac{\partial}{\partial Z} (k_r \frac{\partial \psi}{\partial Z}) dz - K \frac{\partial k_r}{\partial z} dz \qquad (4.1)$$

START

READ GENERAL INPUT DATA

SET INITIAL SOIL CONDITIONS - ASSIGN SOIL TYPE TO EACH LAYER

SELECT ΔT^j AND MATRIX SIZE

ESTIMATE COEFFICIENT MATRIX

$\psi_i^{j-1} < 0$?

NO

$RF^j + \dfrac{h(x)}{\Delta t^j} > $ INFIL. CAP.

YES

NO

YES

USE UNSATURATED UPPER BOUNDARY

USE SATURATED UPPER BOUNDARY

CALCULATE $\vec{\psi}$

$\Delta \psi < \epsilon$

NO

YES

CALCULATE INF. RATE

REPEAT FOR ALL RAINFALL INPUT SEGMENTS

WRITE RESULTS

STOP
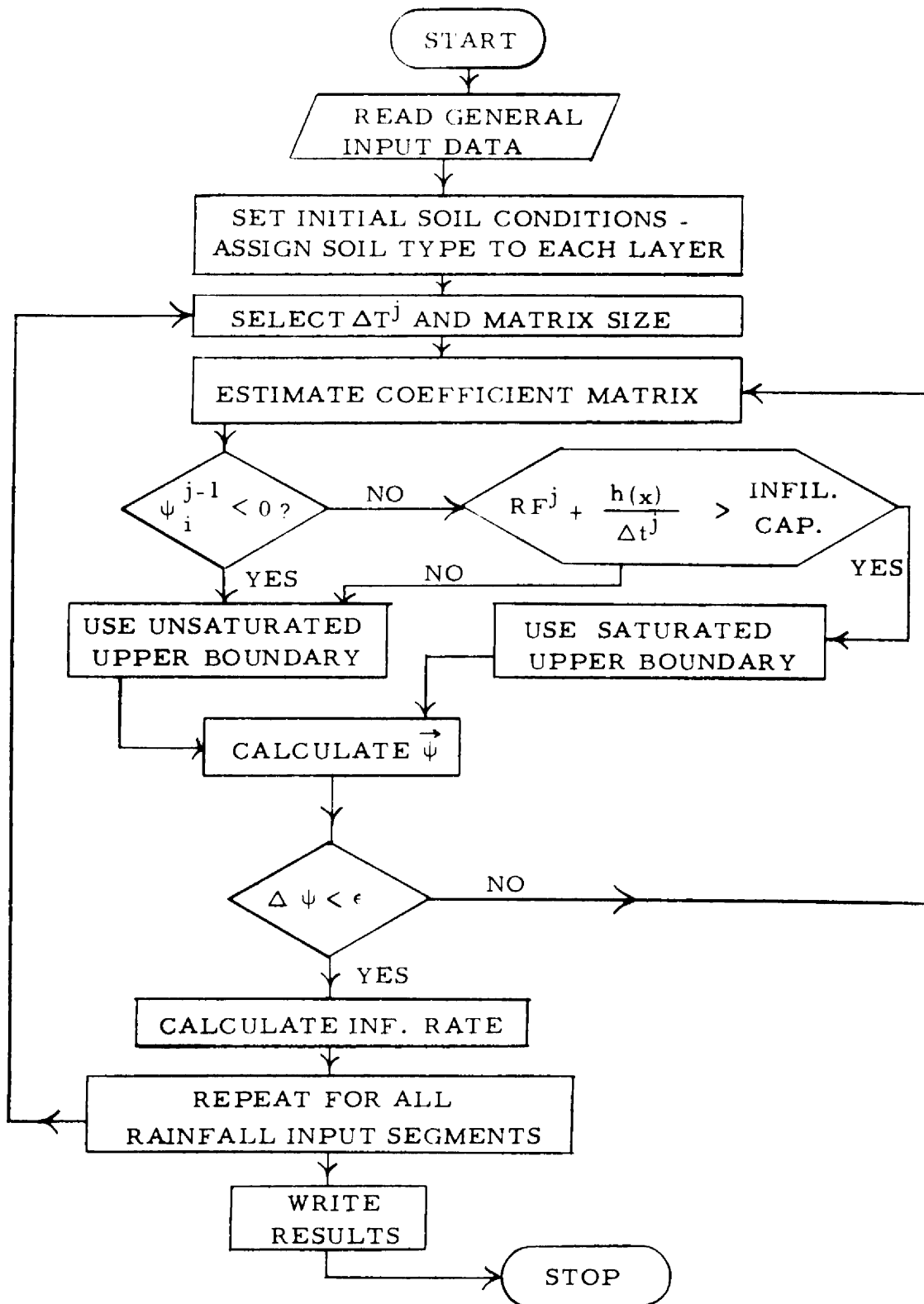
Figure 4.3   Flow chart of computer program

in which V_b is the incremental bulk volume or simply dz for this case of one-dimensional flow.

Swelling Soils

Smith (46) allows for a change in porosity, ϕ, of Equation 4.1. The basic relationship is taken from Philip (42), whereby void volume is expressed as a function of the moisture content. At lower saturation values, ϕ is considered constant in Smith's program. At higher saturation values, ϕ can increase with an increase in moisture content.

Allowing for a change in ϕ changes Equation 4.1 to

$$V_b \frac{\partial}{\partial S} (\phi S) \frac{\partial S}{\partial \psi} \frac{\partial \psi}{\partial t} = K \frac{\partial}{\partial Z} (k_r \frac{\partial \psi}{\partial Z}) dz - K \frac{\partial k_r}{\partial z} dz \quad . \quad (4.2)$$

In this study, ϕ remains constant for a particular soil. The reasoning being that if swelling is to be accounted for, the most important area to consider would be the change in permeability due to change in pore size (e.g., Pouieulle's equation).

Finite Difference Formulations

A finite difference solution grid is shown in Figure 4.4. Equation 4.2 is written in a finite difference form based on time and distance averaged quantities, a form known as the Crank-Nicholsen finite difference form. Equation 4.2 becomes

$$[STOR] \frac{\Delta S}{\Delta \psi} \Delta \psi = \frac{K}{\Delta Z} \Delta \left[k_r \frac{\Delta \psi}{\Delta Z} \right] \Delta Z - K \frac{\Delta k_r}{\Delta Z} \Delta Z \quad (4.3)$$
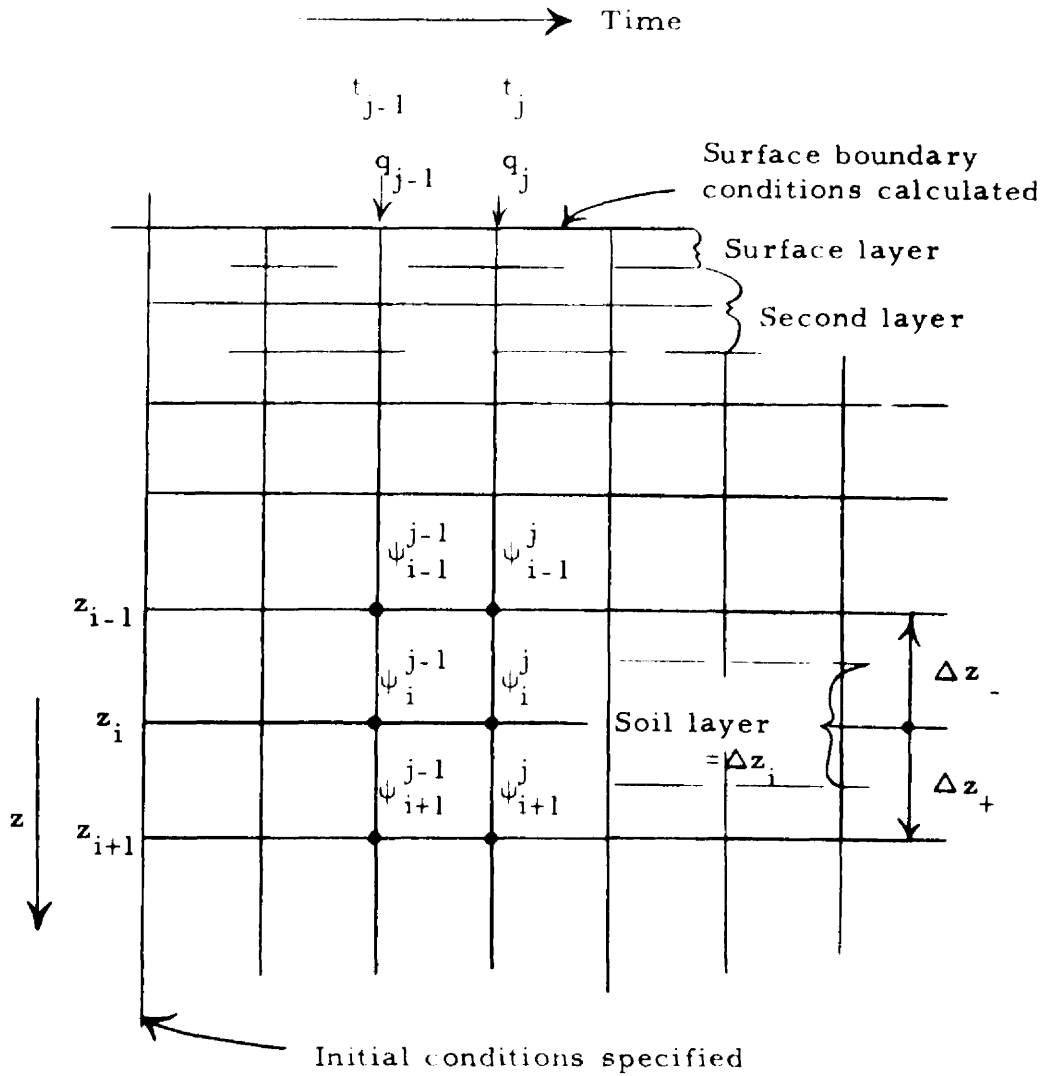
Figure 4.4   Finite difference solution grid and notation
used in solution at Equation 2.28

in which $\text{STOR} = \left[\dfrac{V_b}{\Delta t} \dfrac{\Delta \phi S}{\Delta S} \right]$.

Using the notation shown in Figure 4.4, let

$$\Delta \psi_+^{j-\frac{1}{2}} = \frac{1}{2} \left[\psi_{i+1}^j - \psi_i^j + \psi_{i+1}^{j-1} - \psi_i^{j-1} \right]$$

and

$$\Delta \psi_-^{j-\frac{1}{2}} = \frac{1}{2} \left[\psi_i^j - \psi_{i-1}^j + \psi_i^{j-1} - \psi_{i-1}^{j-1} \right]$$

in which

$i = 1, 2, 3, \cdots, N$ \qquad\qquad $j = 1, 2, 3, \cdots, M_j$

N = total number of soil layers,

M_j = total number of time steps.

The relative permeabilities are defined at the node from which flow

originates and are

$$k_{r_+}^{j-\frac{1}{2}} = \frac{1}{2} \left[k_{r_i}^j + k_{r_i}^{j-1} \right]$$

$$k_{r_-}^{j-\frac{1}{2}} = \frac{1}{2} \left[k_{r_{i-1}}^j + k_{r_{i-1}}^{j-1} \right]$$.

The distance step sizes are

$$\Delta \bar{Z}_+ = Z_{i+1} - Z_i$$

$$\Delta \bar{Z}_- = Z_i - Z_{i-1}$$.

Saturated conductivity between adjacent layers is taken as the harmonic mean:

$$K_+ = K_{i+\frac{1}{2}} = \frac{2\Delta\bar{Z}_+}{\dfrac{\Delta Z_{i+1}}{K_{i+1}} + \dfrac{\Delta Z_i}{K_i}}$$

$$K_- = K_{i-\frac{1}{2}} = \frac{2\Delta\bar{Z}_-}{\dfrac{\Delta Z_i}{K_i} + \dfrac{\Delta Z_{i-1}}{K_{i-1}}}$$

Using these definitions and reversing sides, Equation 4.3 may be expanded to:

$$K_{i+\frac{1}{2}} \, k_{r_+}^{j-\frac{1}{2}} \left[\frac{\psi_{i+1}^j - \psi_i^j + \psi_{i+1}^{j-1} - \psi_i^{j-1}}{2\Delta\bar{Z}_+} \right]$$

$$- K_{i-\frac{1}{2}} \, k_{r_-}^{j-\frac{1}{2}} \left[\frac{\psi_i^j - \psi_{i-1}^j + \psi_i^{j-1} - \psi_{i-1}^{j-1}}{2\Delta\bar{Z}_-} \right]$$

$$- K_{i+\frac{1}{2}} \, k_{r_+}^{j-\frac{1}{2}} + K_{i-\frac{1}{2}} \, k_{r_-}^{j-\frac{1}{2}} = \left[STOR \right]_i^{j-\frac{1}{2}} SL_i^{j-\frac{1}{2}} X$$

$$\left[\psi_i^j - \psi_i^{j-1} \right] - Q_{p_i} \qquad\qquad (4.4)$$

in which

Q_{p_i} = input to node i from the outside, used only at the surface for rainfall input up to ponding: $Q_{p_i} = 0$ for $i > 1$, and

$$SL_i^{j-\frac{1}{2}} = \left[\frac{\Delta S}{\Delta \psi}\right]_i^j \qquad .$$

Separating the ψ terms of Equation 4.4:

$$\left[\frac{K_{i-\frac{1}{2}} k_{r_-}}{2\Delta \overline{Z}_-}\right] \psi_{i-1}^j - \left[\frac{K_{i+\frac{1}{2}} k_{r_+}}{2\Delta \overline{Z}_+} + \frac{K_{i-\frac{1}{2}} k_{r_-}}{2\Delta \overline{Z}_-} + [STOR]_i^{j-\frac{1}{2}} \times\right.$$

$$\left[SL\right]_i^{j-\frac{1}{2}}\right] \psi_i^j + \left[\frac{K_{i+\frac{1}{2}} k_{r_+}}{2\Delta \overline{Z}_+}\right] \psi_{i+1}^j = RHS_i^{j-\frac{1}{2}} \qquad (4.5)$$

in which

$$RHS_i^{j-\frac{1}{2}} = -[STOR]_i^{j-\frac{1}{2}} [SL]_i^{j-\frac{1}{2}} \psi_i^{j-\frac{1}{2}} - Q_{p_i}$$

$$-\frac{K_{i-\frac{1}{2}} k_{r_+}}{2\Delta \overline{Z}_+} \left[\psi_{i+1}^{j-1} - \psi_i^{j-1} - 2\Delta \overline{Z}_+\right]$$

$$+\frac{K_{i-\frac{1}{2}} k_{r_-}}{2\Delta \overline{Z}_-} \left[\psi_i^{j-1} - \psi_{i-1}^{j-1} - 2\Delta \overline{Z}_-\right] \qquad . \qquad (4.6)$$

A set of N linear equations in N variables of the form

$$a_i \psi_{i-1} + b_i \psi_i + c_i \psi_{i+1} = RHS_i \qquad (4.7)$$

is represented by Equation 4.5 or as a matrix equation

$$[J] \vec{\psi} = \overrightarrow{RHS} \qquad . \qquad (4.8)$$

Equation 4.7 will be written in a N x N matrix $[J]$ and an N-dimensional vector $\overrightarrow{RHS}$ after applying the boundary conditions.

Upper Boundary Conditions

For the upper boundary $i-1$ does not exist and Equation 4.7 is

$$b_1 \psi_1 + c_1 \psi_2 = RHS_1 \quad .$$

At the soil surface, for the rainfall and ponded case, $K_{i-\frac{1}{2}}$ does not exist and Equations 4.5 and 4.6 become

$$\left[\frac{K_{1\frac{1}{2}} k_{r_+}}{2\Delta \bar{Z}_+} \right] \left[\psi_2^j - \psi_1^j \right] - \left[STOR \right]_1^{j-\frac{1}{2}} \left[SL \right]_1^{j-\frac{1}{2}} \psi_1^j$$

$$= - \left[STOR \right]_1^{j-\frac{1}{2}} \left[SL \right]_1^{j-\frac{1}{2}} \psi_1^{j-1} - Q_{P_1}$$

$$- \frac{K_{1\frac{1}{2}} k_{r_+}}{2\Delta \bar{Z}_+} \left[\psi_2^{j-1} - \psi_1^{j-1} - 2\Delta \bar{Z}_+ \right] . \qquad (4.9)$$

For the ponded case, $\psi_1^j = h$ which is the depth of water on the surface. The known ψ_1^j terms are placed on the right hand side of Equation 4.7 and the first equation in the set for this case is for the second layer $i = 2$.

As saturation proceeds below the surface to some node nl (Figure 4.5) the ψ_i^j terms are calculated from knowing $Z(nl)$ and h (depth of ponding) for all $i < nl$ and these ψ_i terms are moved to the right side of Equation 4.7. The ψ_n^j term is

$$\psi_n^j = Z(nl) \left[1 - \frac{Q}{K(nl)} \right] + h \qquad (4.10)$$
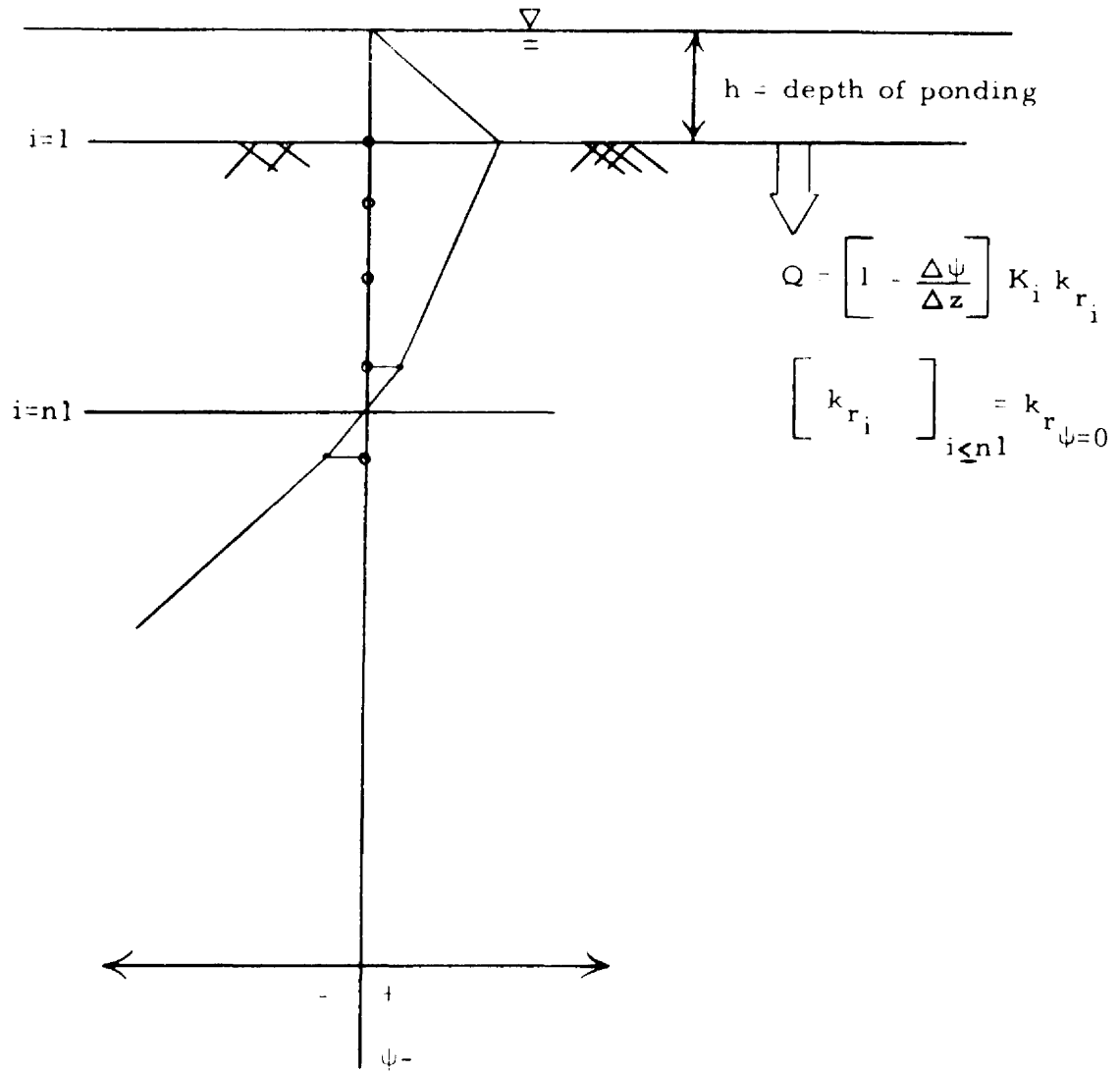
Figure 4. 5   Pressure relations when water is ponded on the soil surface

which is Darcy's law in the form

$$Q = K(n)\left(1 + \frac{h - \psi_n^j}{Z(n)}\right)_i \qquad (4.11)$$

Also, $\frac{\partial S}{\partial \psi} = 0$ for $i < n$.

Lower Boundary Conditions

The lower boundary condition is a sufficient soil depth (semi-infinite) so that no significant water movement occurs below the soil depth under study.

When soil water movement has progressed to a point $n2$ in a column, all terms in $n2 + 1$ are known from initial conditions and are set on the right side of Equation 4.7. Point $n2$ is chosen such that $i \leq n2$, $|\psi_i^{j-1} - \psi_i^0| \leq \epsilon$, where ϵ is a very small error value.

Matrix Solution

Using the upper and lower boundary conditions just described, Equation 4.8 is written as follows

$$\begin{bmatrix} b_1 c_1 & & & & \bigcirc \\ a_2 b_2 c_2 & & & & \\ & a_3 b_3 b_3 & & & \\ & & & a_{n2-1} b_{n2-1} c_{n2-1} & \\ \bigcirc & & & & a_{n2} b_{n2} \end{bmatrix} \begin{bmatrix} \psi_1 \\ \psi_2 \\ \psi_3 \\ \\ \psi_{n2-1} \\ \psi_{n2} \end{bmatrix} = \begin{bmatrix} rhs_1 \\ rhs_2 \\ rhs_3 \\ \\ rhs_{n2-1} \\ rhs_{n2} \end{bmatrix} \qquad (4.12)$$

The column vector ψ can be solved by a recursion algorithm for Gauss elimination as given by Varga (51).

Solution of Equation for a Given Time Step

Soil Data Input

A table of soil hydraulic relations ψ vs. S vs. k_r values are experimentally obtained in the laboratory and used as input to the computer program. Intermediate points are found by linear interpolation. Any one of the three variables may be used to find corresponding values of the other two.

Equipment used (Figure 4.6) to obtain ψ vs. S vs. k_r relationships (for lower tensions) is located in the Porous Media Laboratory at Colorado State University. A pressure plate was used to obtain ψ vs. S relationships at higher tensions. A log k vs. log ψ relationship discussed by Brooks and Corey (5) is used to calculate ψ vs. k_r relationships at higher tensions.

The main items of equipment required (Figure 4.6) are the soil sample, fluid inlet, fluid discharge, flow measurement container, attenuation instrument and two manometers. The fluids used were Soltrol and water.

The head or moisture tension can be varied by changing q_{in} or the outlet elevation, which also changes k_r and S when $S < 1.0$. Steady state relationships of S vs. k_r were found. For steady state flow, $q_{in} = q_{out}$. H_1 should be approximately equal to H_2 to
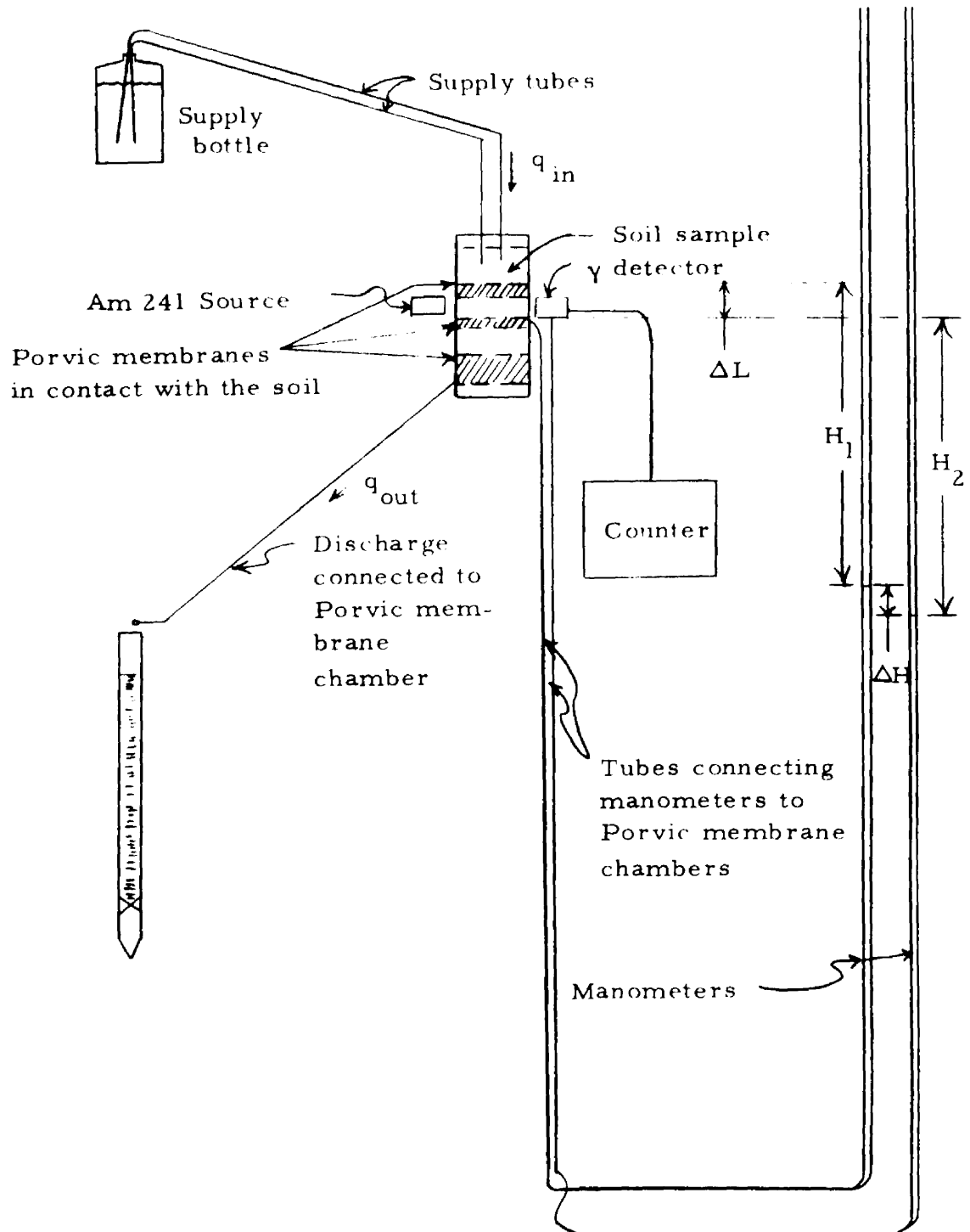
Figure 4.6   Equipment used to obtain ψ-k_r-S relationships for numerical model

make ψ nearly constant throughout the sample. Calculations required to find ψ, k, or S values are:

$$\psi = - \frac{H_1 + H_2}{2} - P_{c_{tube}} / \gamma \qquad (4.13)$$

$$K = \frac{q_{out}}{A} \frac{\Delta L}{\Delta H} \quad \text{for a saturated condition}$$

$$K k_r = \frac{q_{out}}{A} \frac{\Delta L}{\Delta H} \quad \text{for unsaturated conditions}$$

$$S = 1.0 - \frac{C - C_{100}}{C_{100} - C_0}$$

in which

$P_{c_{tube}}$ = capillary pressure rise in manometer tubes,

A = cross sectional area of the soil sample,

C = counter reading ratio $\frac{count\ (sample)}{count\ (standard)}$,

C_{100} = counter reading at $S = 1.0$, and

C_0 = counter reading at $S = 0.0$.

The saturation, S, and counter reading ratio, C, are determined for an air dry sample. A straight line is drawn through C_{100} and $C_{air\ dry}$ on a C vs. S graph. The value of C at $S = 0.0$ is C_0.

Three k vs. ψ curves (Figure 4.7) were obtained for the sandy clay loam, two using Soltrol and one using water. Two k vs.

ψ curves (Figure 4.8) were obtained for the loam, one using Soltrol and one using water.

Soltrol is often used as the infiltrating fluid in this type of test to overcome several problems encountered with water. Water reacts with the soil causing shrinkage or swelling, thereby resulting in considerable data scatter (Figure 4.7). Soil shrinkage and water evaporation at the Porvic barrier causes loss of contact between the soil sample and the Porvic barrier. When loss of contact occurs, the soil sample must be discarded and a new sample prepared.

The saturated permeability values obtained for water and Soltrol are considerably different. This indicates permeability may not be a unique property of the soil for the sandy clay loam and loam tested.

A straight line reasonably fits a plot of log k vs. log ψ at higher values of ψ (Figures 4.7 and 4.8). This straight line fit, on logarithmic coordinates, between capillary pressure and permeability, is discussed by Brooks and Corey (5) and presented as an equation:

$$k_r = \left(\frac{P_b}{P_c} \right)^m \quad \text{for } P_c > P_b \qquad (4.14)$$

in which

k_r = relative permeability

P_b = bubbling pressure - approximately the minimum P_c on the drainage cycle at which a continuous non-wetting phase (e.g. air) exists in a porous medium
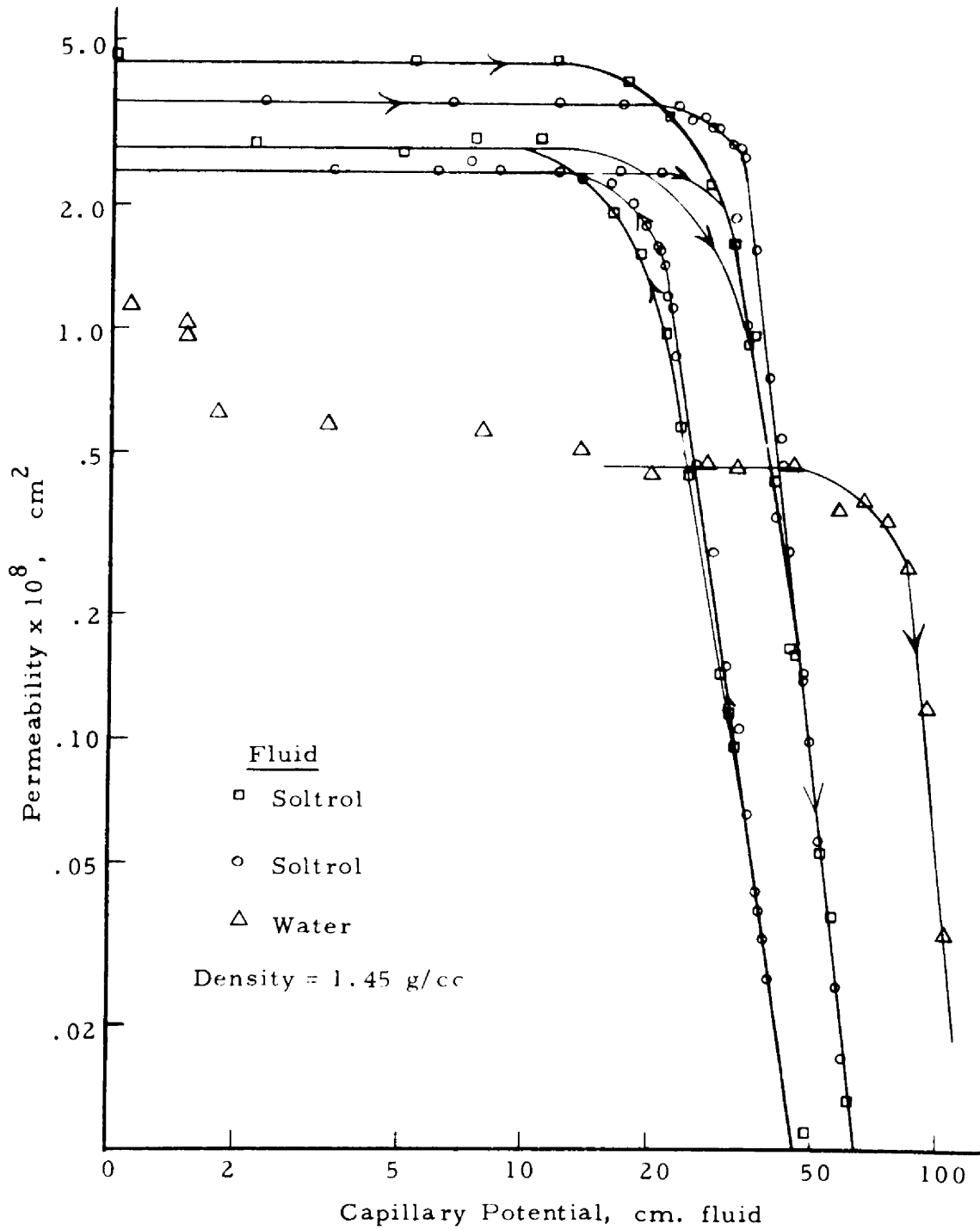
Figure 4.7   Permeability-capillary pressure relationships
for sandy clay loam
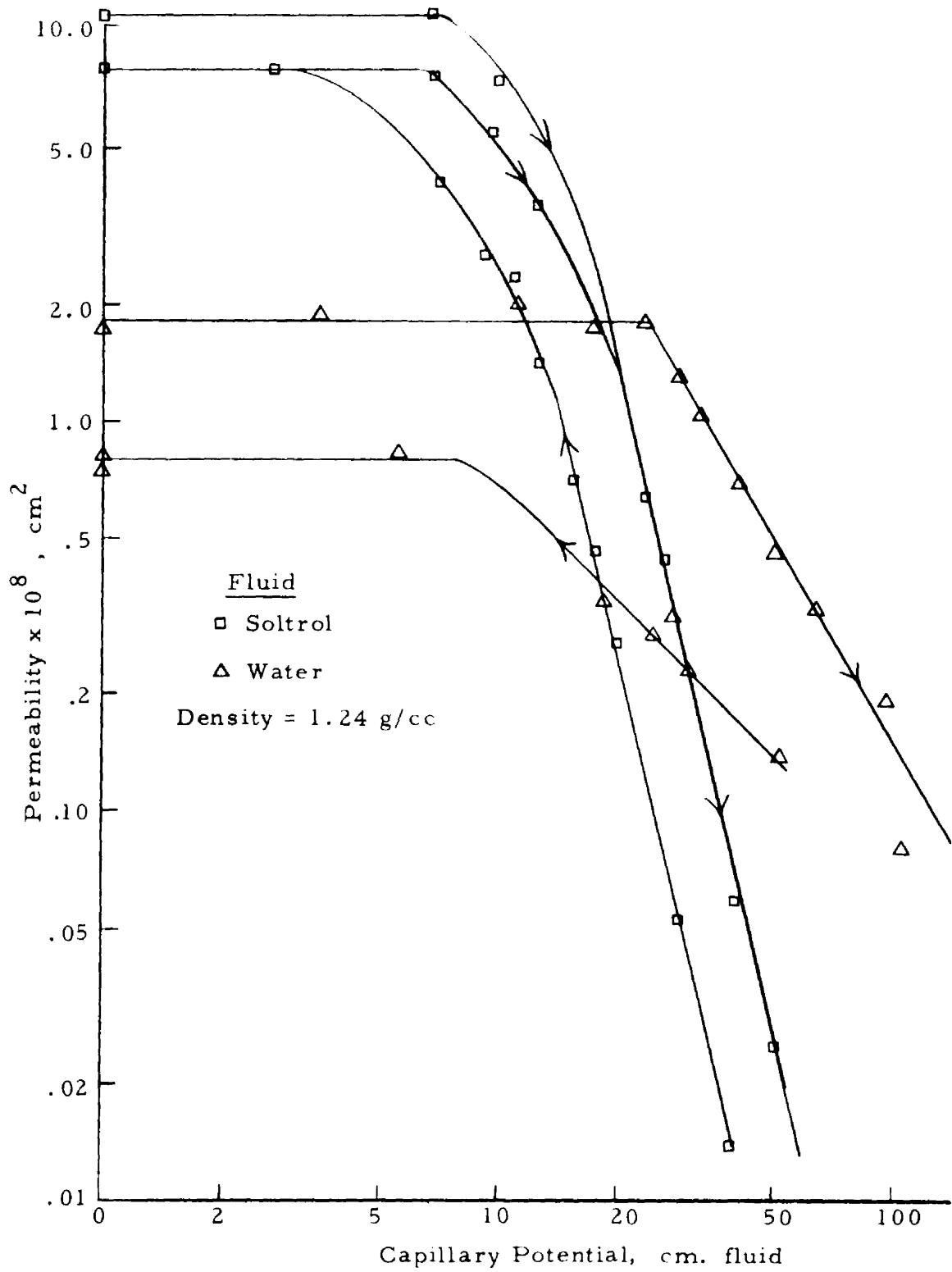
Figure 4.8   Permeability-capillary pressure relationships
for loam

P_c — capillary pressure

m = an exponent.

Values for permeability vs. capillary pressure for

$k < 0.1 \times 10^{-8}$ cm^2 were derived using the relationship expressed

in Equation 4.14.

The upper imbibition curve of Figure 4.7 (Soltrol) was used to

calculate the relationship between relative permeability, k_r, and

capillary potential, ψ, for the sandy clay loam. Also, the imbibition

curve of Figure 4.8 (Soltrol) was used to calculate the k_r vs. ψ

relationships for the loam. The Soltrol curves were used rather than

the water curves because a better defined curve was obtained with

Soltrol.

The relationship between the capillary pressure (expressed in

cm. of fluid) for water and Soltrol was experimentally found to be

$$\left(\frac{P_c}{\gamma}\right)_w = 2.23 \left(\frac{P_c}{\gamma}\right)_{So} \qquad (4.15)$$

where the subscripts w and So designate water and Soltrol,

respectively.

The moisture-tension curves for the two soils are shown in

Figure 4.9. The loam has a more gradual desaturation curve than

the sandy clay loam indicating a more gradual change in pore sizes

for the loam than for the sandy clay loam.
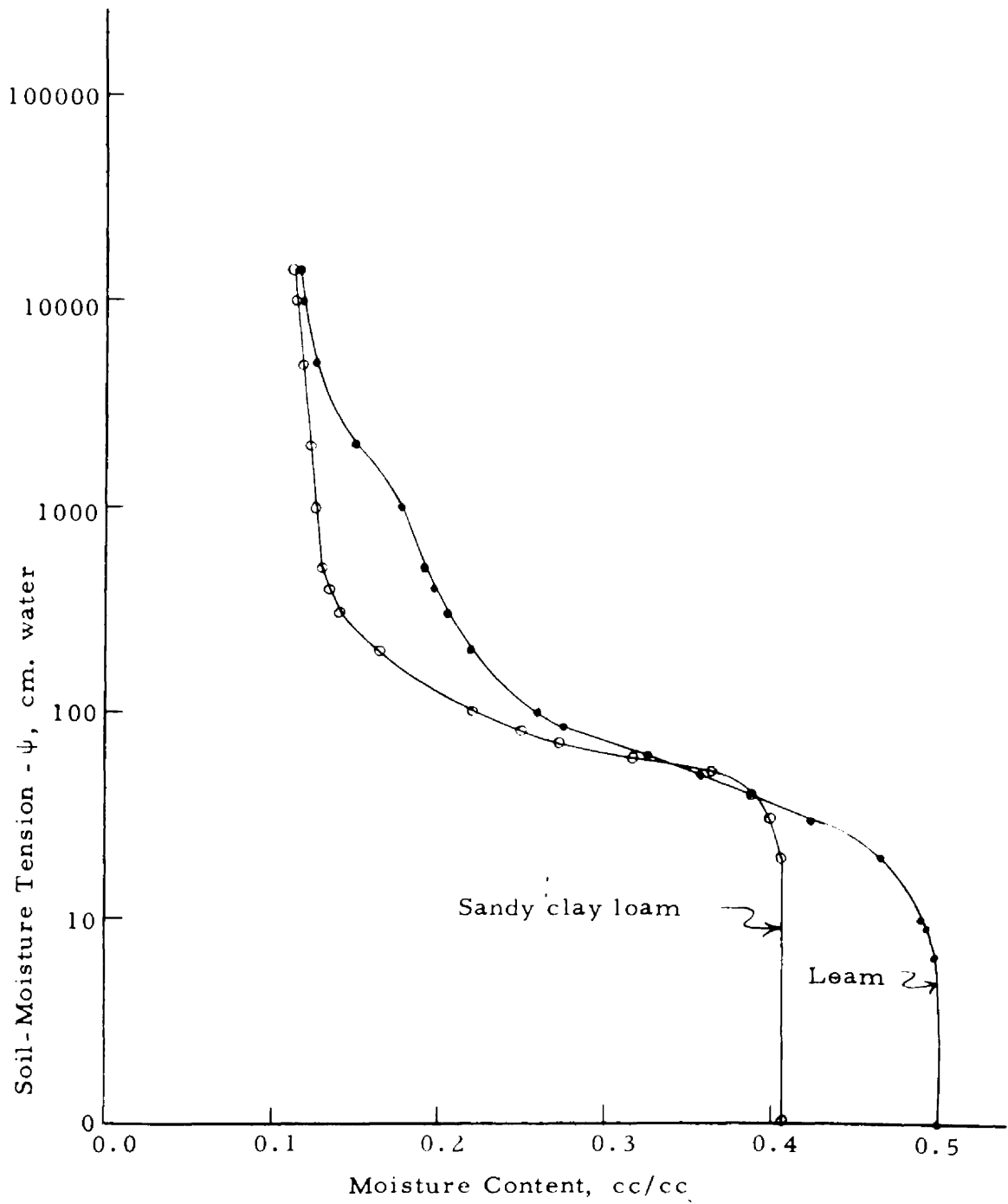
Figure 4.9   Moisture-tension relationships of experimental soils

Iteration

The values of $k_{r_i}^j$, $(STOR)_i^j$, and $(SL)_i^j$ are dependent on the values of ψ_i^j, thereby making Equation 2.28 non-linear. These variables are evaluated by a trial and error solution, where the value of one of the variables is estimated, then knowing the hydraulic properties of the soil the other variables can be calculated. Then, the estimated variable can be calculated and the process repeated until the estimated and calculated value become nearly identical.

The iterative procedure followed in Smith's program is as follows:

1. An initial estimate is made of ψ_i^j, i = 1, N, from which values of $k_{r_i}^j$, $(STOR)_i^j$, and $(SL)_i^j$ are found knowing the soil hydraulic relations.

2. The coefficients a, b, and c are computed and Equation 4.12 is solved.

3. The estimated values of ψ_i^j of step (1) are compared with the computed values of ψ_i^j in step (2). If the estimated and computed values agree within a prescribed limit of the error criteria, Equation 4.12 is considered solved. If the estimated and computed values do not agree within the prescribed limit of the error criteria, and if this was the first or second iteration, the ψ_i^j values obtained in step (2) are used as estimated values of ψ_i^j's.

4. If after three iterations, Equation 4.12 does not meet the
    error criteria, the ψ_i^l values obtained in step (2) are
    "damped" by a weighted average with the last ψ_i^j.

Selection of Depth and Time Increments

The solution of a non-linear finite difference scheme involves a
selection of efficient grid sizes. Selecting very small grid sizes
results in excessive computer time. Selecting grid sizes too large
causes the solution to diverge or to be very inaccurate.

Depth increments, for this model, are chosen very small at the
surface and increase in size downward.

Time increments are changed throughout an event. The criteria
for the time increment size are the change in $\Delta S/\Delta \psi$ over the pre-
vious time step and the local change in curvature $(\Delta^2 S/\Delta \psi^2)_i^j$ of the
soil moisture-tension relation.

Infiltration Calculation

Infiltration can be calculated at the surface when $n = 1$ by use of
Equation 4.11. For $t <$ time of ponding

$$Q = \frac{1}{t} \sum_{i=1}^{N} \Delta Z_i \, \phi_i^l \left[S^j - S^{j-1} \right]_i \qquad (4.16)$$

serves as a continuity test on the performance of the numerical scheme.

Solution Sensitivity

The accuracy of a numerical model, simulating soil moisture flow, depends on the size of the depth increments, time increments and error criteria. The model was tested for sensitivity to change in size of depth increments, time increments and error criteria.

Depth Increment

Changing the depth increment size near the surface had considerable effect on the time that runoff began and on the infiltration curve for the loam (Figure 4.10). A certain depth increment size required a limited time increment size to allow the model to operate. The time increment size limit is analogous to a wave or impulse problem in which the speed of the wave or impulse must be less than the distance increment divided by the time increment.

The depth increments are made smaller near the surface both to accurately define the time runoff begins and to properly define the steeply varying pressures encountered in the upper zone as the moisture begins to disperse into the soil.

The model which was finally used divided the upper three inches into 0.1-inch increments and the lower 25 inches into 0.5-inch increments. Dividing the upper part of the column into smaller increments than 0.1 inches increased the computation time considerably, but caused only minor changes in the infiltration curves resulting from the model. Dividing the lower part of the soil

Saturated Conductivities

Depth, inches	Saturated conductivites, inches per hour
0.0 to 0.2	0.024
0.2 to 25	0.070

Initial Conditions

Depth, inches	Saturation
0.0	0.264
1.5	0.384
3.0	0.406
6.0	0.408

Depth, inches	Depth increment, inches
0.0 to 0.06	0.03
0.06 to 0.16	0.05
0.16 to 3.16	0.10
3.16 to 25.0	0.50
0.0 to 3.0	0.3
3.0 to 25	0.5
0.0 to 3.0	0.2
3.0 to 25	0.5
0.0 to 3.0	0.1
3.0 to 25	0.5
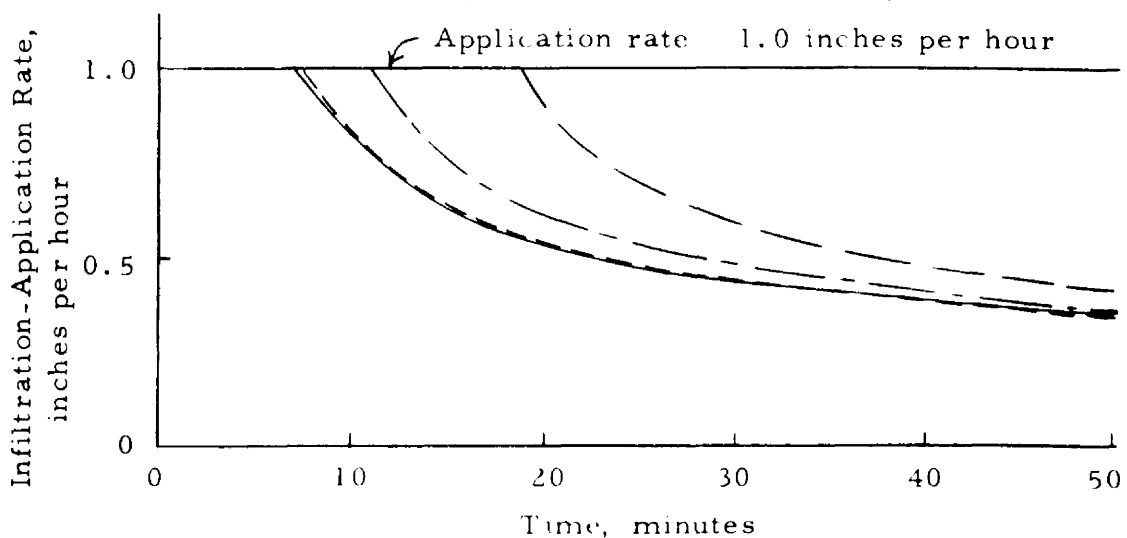
Figure 4.10 Example of the effect of depth increment size on model's infiltration rate curve - loam

column into smaller increments than 0.5 inches only increased computation time.

Time Increment

The computer solution did not prove to be very sensitive to changes in time increment, unless the time increment was too large for the depth increment used, which would cause the model not to run.

No difference occurred with the infiltration curves as t_{max} was reduced from 0.5 to 0.25 minutes and t_{min} was reduced from 0.05 to 0.025 minutes. Therefore, the model used a t_{max} of 0.5 minutes and a t_{min} of 0.05 minutes.

Error Criteria

The allowable error, ϵ, is defined as the maximum difference allowable between the estimated capillary potential, ψ, and the computed capillary potential (step 2 of Iteration). Changing the allowable error, ϵ, from 0.02 to 0.04 inches caused no change in the infiltration curve for the loam. The allowable error was made small enough to nearly eliminate variation in the model infiltration curve. The maximum ϵ value used in the model was 0.05 cm.

Field Infiltrometer Procedures

Equipment

The basic equipment used for these tests was a sprinkler in-filtrometer which was modified to perform the specific functions necessary to produce time varying application rates. Using the infiltrometer, water was supplied to the test plots by a specially constructed sprinkler operating inside a cylindrical shield two feet in diameter. A slot was cut in the shield to permit the application of water to test plots in a 30° arc. While the sprinkler was operating in the remaining 330° inside the shield, water struck the shield, fell to the bottom and was pumped back to the holding tank. The inside of the shield was lined with three spaced layers of brass screen to prevent splashing by dissipating the energy of the water.

Water under pressure was supplied to the sprinklers through a high pressure hose from the pump which was driven by an air-cooled gasoline engine. By varying the pump speed and by adjusting the discharge and bypass valves, it was possible to obtain any desired discharge up to 110 gallons per minute at any desired pressure up to 100 pounds per square inch. Water was supplied to the pump from a 325-gallon holding tank which was refilled as necessary from convenient water sources. A low pressure pump was used to return the unused water caught in the sprinkler shield to the holding tank. The entire unit was trailer mounted for transport between tests areas.

The sprinkler head used in these tests was specially constructed with provision for ten sprinkler nozzles oriented in one direction. All of the nozzles could be used or some outlets blocked to get any desired discharge and pattern shape. Specially designed slotted nozzles,

80 psi operating pressure and fine meshed screens in front of nozzles were used to reduce drop size in an effort to prevent effects due to drop size variations. A special combination of nozzles was selected to obtain a nearly linear decrease from peak application rates near the sprinkler head to a zero application rate at the end of the wetted area. This permitted simultaneous observation of a family of application rate curves for each pattern of variation in application rates with time.

Variations in application rates with time were obtained by controlling the frequency with which the sprinkler head passed the slot in the shield. A solenoid operated plunger retained the sprinkler head as it approached the slot. When the sprinkler had been retained for the length of time necessary, the solenoid was temporarily activited to release the sprinkler head. After the sprinkler head had passed across the slotted shield at a rate of approximately one revolution per minute, a rotating drive was engaged and the sprinkler head was rapidly rotated around the back of the shield to near the point were it was retained by the solenoid operated plunger. Application rates were proportional to the frequency with which the plunger was released.

The control was operated by a variable speed drive which was regulated by a follower arm riding on a cam. The shape of the cam and the time interval for the follower to complete the cam cycle determined the pattern of variation in application rates with time. The cam shapes used produced patterns typical of present center-pivot sprinkler irrigation systems and patterns selected especially to provide observations over a wide range for all variables involved.

Preliminary Tests

To check out the equipment and procedures, preliminary field tests were run in the summer of 1969 at the CSU Horticulture Farm. These tests were run under the assumption that (1) most water applied above the rate of infiltration capacity will run off and (2) when water is applied at a rate below the infiltration capacity, very little runoff will occur. On the basis of these two assumptions (later found to be invalid), no runoff was collected from the tests. Only puddling times and runoff times were recorded. Puddling was considered to be the time when the water applied during one pass of the sprinkler still appeared on the surface of the soil when the sprinkler passed again. Runoff was considered to be the time when the water first ran more than two feet on the surface of the soil.

Two parallel rows of catch cans, two feet apart, were set at three-foot intervals in front of the slot opening in the infiltrometer shield. Puddling times and runoff times were recorded as observed around the individual catch cans. Tests were run during periods of very low wind conditions and a snow fence was set up around these plots to reduce variability caused by wind. Because many of the sprinkler drops were extremely small, these precautions did not prove to be adequate, for it could be observed while the tests were in progress that the wind was still having some effect on the sprinkler application pattern. The resulting changes in application rates at different times during the test, was considered to be a major factor in data variability.

Soil samples were taken immediately prior to each test to obtain antecendent moisture at the surface of the soil and at a depth of six

to eight inches below the surface. These samples were taken at two different locations within each plot to check the variability of the antecendent moisture within the plot. They also made it possible to make comparisons between plots, since a different pattern was used on each plot and possible varability of antecendent moisture between plots needed to be known in interpretating results.

Application rate and applied depth at any time during a given test run were determined by calculations based on the shape of each pattern and the time in which the total applied depth was accumulated.

There was a surprisingly large amount of variability which was apparently caused by differences in drop size. This appeared to occur because the linear decrease in application rate with distance in front of the sprinkler was obtained by using screens in front of some of the nozzles to get a high application rate near the sprinkler. The water which struck the soil farther from the sprinkler did not pass through the screen. It was observed from the data that considerable reductions in puddling time were caused by larger drops that occurred in these areas. These differences occurred even though small nozzles and high pressures produced much smaller drops then occur under conventional sprinklers.

The results of these tests as well as observations made during other uses of this infiltrometer appear to be important for three reasons. The first is that it shows that there is great importance in achieving small drop size on center-pivot systems in order to maximize infiltration rates. The second is that the usually recommended operating pressures for sprinklers produce considerably reduced infiltration

rates on all but sandy soils. It is commonly assumed that pressures considerably lower than the 80 psi that was used in these tests produce adequate drop breakup for nozzles which are larger than the test nozzles. The third reason is that great care needs to be taken in running and interpreting sprinkler infiltrometer tests. It was found that the larger drops which fell at about 75% of the sprinkler radius caused puddling at much lower application rates than did the smaller drops which fell closer to the sprinkler.

Modified Procedures

Field sprinkler infiltrometer tests were run in the summer of 1970 at the CSU Agronomy Farm on a clay loam soil. Refinements in the test procedures and equipment were accomplished prior to these tests. The field where the tests were conducted had been disked lightly approximately three weeks before the tests. Small amounts of rainfall had helped to maintain soil moisture, but the surface was loose and dry. Each plot site was sprinkled with approximately 1/2 inch of water in the form of a very fine spray about 48 hours before each test was run.

Intake observations were made in nine 20-inch diameter rings. These rings were constructed by rolling 3-inch strips of steel into a circular shape and welding the ends together. One edge of each ring was sharpened to facilitate driving the rings into the ground. A small spout was attached to each ring to direct water into a hose which carried it into runoff measuring cans. The rings were driven into the ground in a row extending from 8 feet to about 23 feet in front
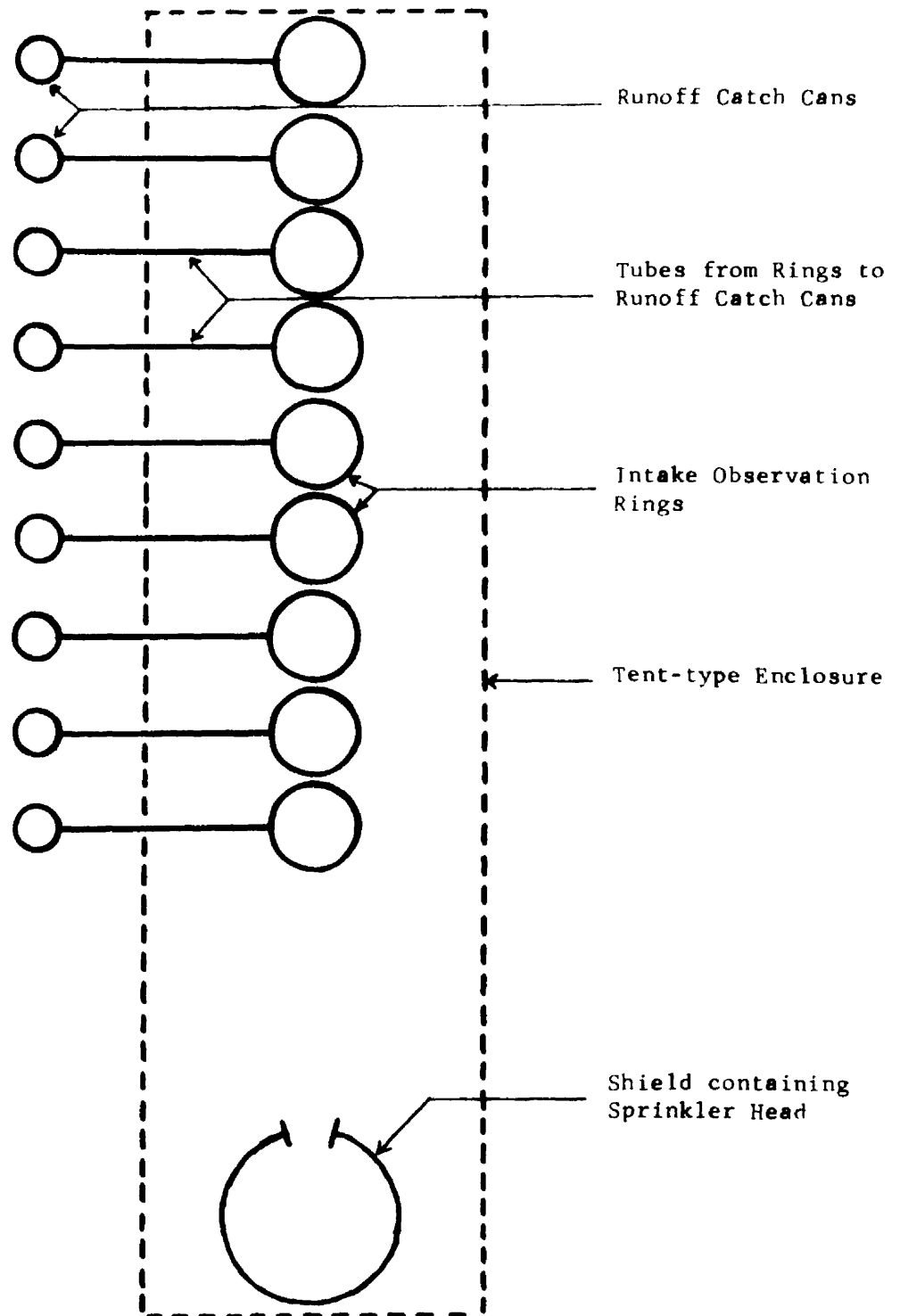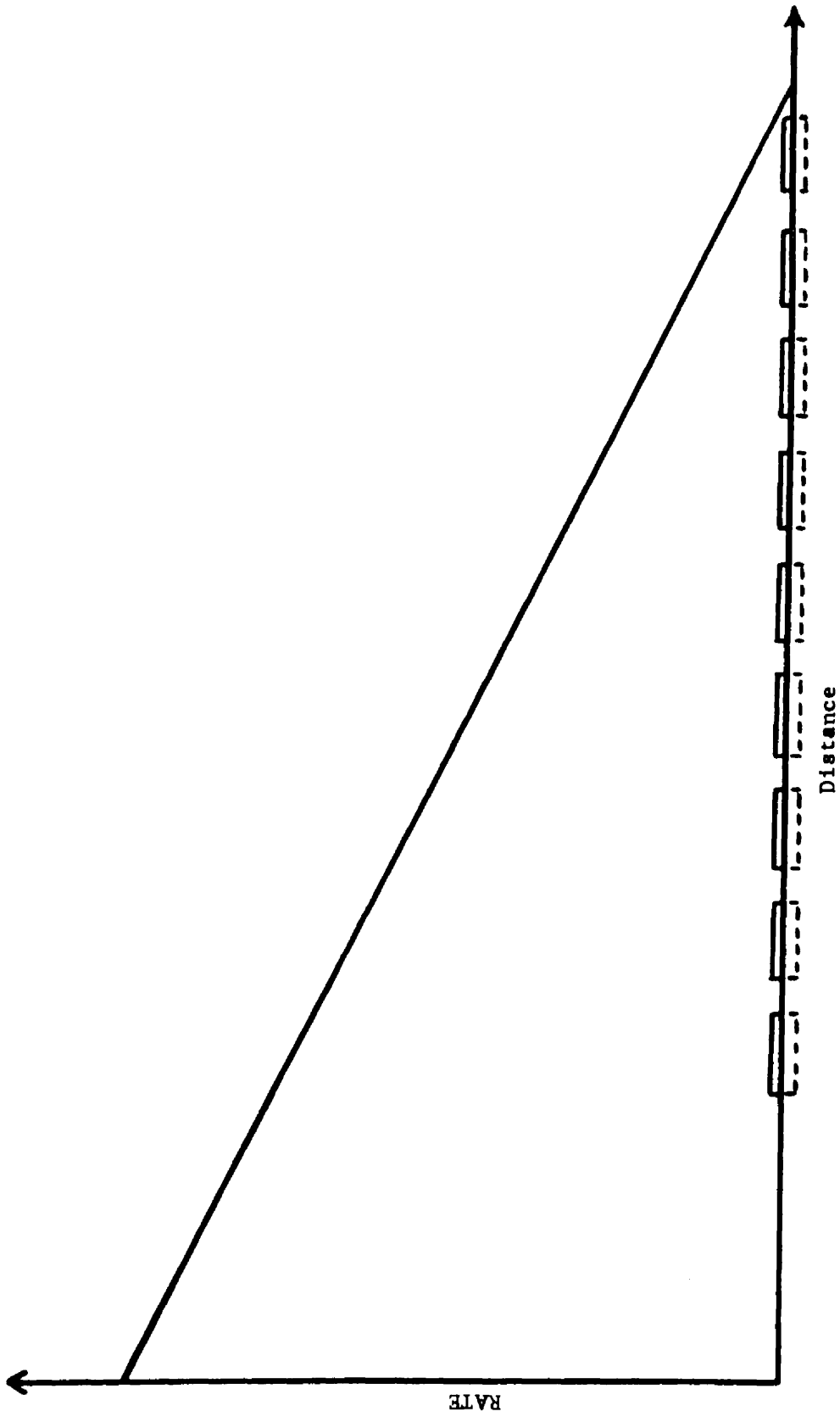
Figure 4.11. Field Plot Layout

Figure 4.12. Linearly decreasing sprinkler application pattern with schematic inset of intake observation rings.

of the sprinkler. Catch cans were placed in a square pattern around each ring to measure total depth of water applied (Figure 4.11). This total depth for each ring was calculated as the average depth of the four observations around that ring.

During each test run the entire area including the sprinkler shield and all the intake observation rings was enclosed in a tent-type structure to prevent any variation in application rates being caused by wind. Because of variation in drop sizes found in the preliminary tests, the entire slot in the sprinkler shield was covered with a fine mesh screen to try to make all drops small enough to eliminate variability in intake rates caused by large drops destroying the surface structure of the soil in the test plots. Also the width of slot in the slotted nozzles was limited to a maximum of 0.03 inch to reduce drop sizes.

Through nozzle orientation and the use of deflectors, a linearly decreasing sprinkler application pattern was approximated. The highest application rate was near the sprinkler with the rate decreasing with distance from the sprinkler out to zero application rate at a distance of about 23 feet from the sprinkler (Figure 4.12).

Runoff depth from each ring was collected in cans (Figure 4.11) and measured at small time intervals to determine the intake depth and rates for each ring at any given time. The frequency at which the sprinkler passed across the opening slot in the cylindrical shield was recorded on an event marker as a check of the actual number of sprinkler passes against the control system designed frequency for any given pattern.

These tests were conducted using two time varying application rate patterns, as shown in Figures 4.13 and 4.14, and a constant rate pattern with two replications for each. The constant rate pattern is identified as Pattern 1, Figure 4.13 as Pattern 2, and Figure 4.14 as Pattern 3. Patterns 2 and 3 were run with a one-hour time base for each pattern. The constant rate tests were run for only one-half hour because of the limit on water available at the test plot location.

Before each test was run, soil moisture samples were taken at about four foot intervals along the row of infiltration observation rings. Samples were taken from the surface two inches and six to eight inches below the surface.

Applied depths, infiltrated depths, application rates, runoff rates and infiltration rates were calculated for each ring. For Pattern 1 (constant rates) the total depth applied to each ring was calculated by taking the average of the four depths measured around the ring. The time for each run, and therefore for each of the nine rings within each run, was 30 minutes. Runoff from each ring was measured and re-corded along with time of measurement at intervals during the test run. Cumulative runoff depths were plotted and the curve smoothed to eliminate the effects of the time of reading in relation to sprinkler passes. The runoff depth for any time during the one-half hour run could then be determined. Using the total depth found as explained previously, the application rate for each ring was determined by divid-ing the total depth by the one-half hour interval during which the depth was accumulated. It was assumed that the equipment maintained a con-stant rate throughout the run so this average was considered to be the
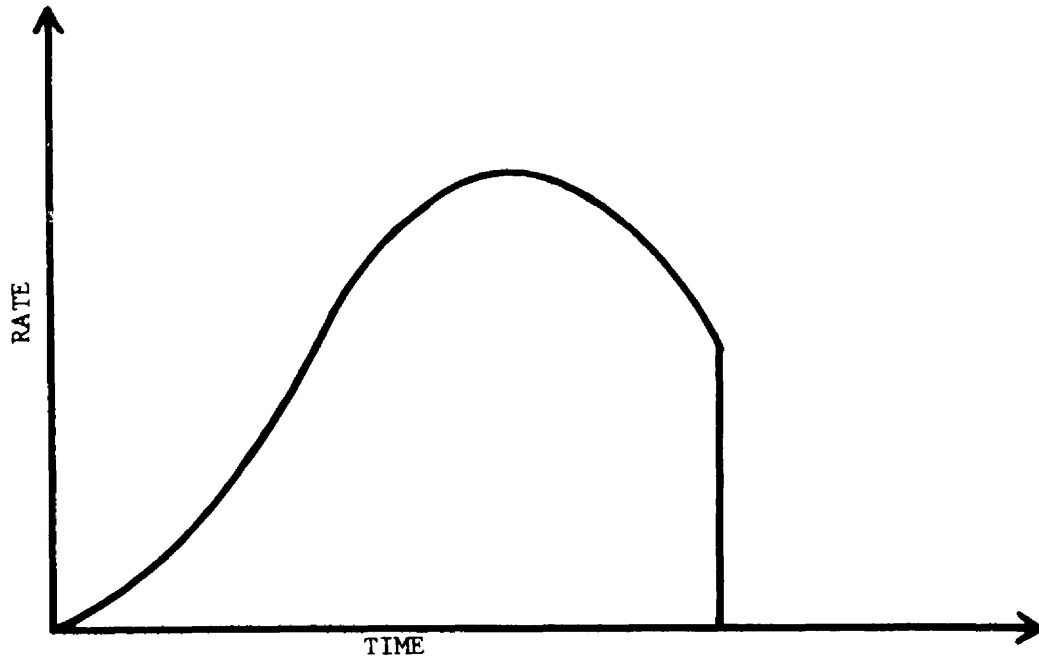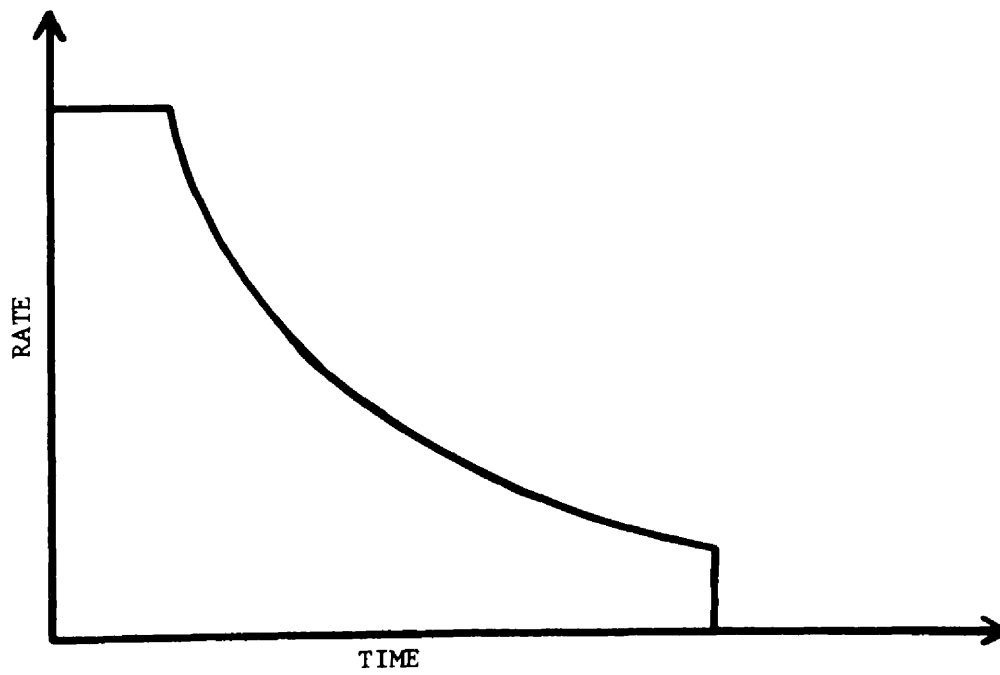
Figure 4.13. Pattern 2.

Figure 4.14. Pattern 3.

constant application rate. Runoff depth-time relationships were taken

from cumulative runoff depth curves. Infiltrated depths were determined

by subtracting the runoff depth from the applied depths at correspond-

ing times.

Pattern 2 (Figure 4.13) simulates how most center-pivot type

sprinkler systems apply water. The end of the pattern was cut off

for these tests because lack of importance in the runoff problem.

Two test runs were made, each over a one hour time period.

Total depths applied were found in the same manner as was done

with the constant rate runs. Runoff from each ring was also measured

and recorded in a similar manner.

The maximum rate applied to each ring was determined by the

dividing the total applied depth for a given ring by the fraction of

the total area that the unit control curve for the pattern enclosed.

This was done assuming that the equipment used maintained a consistent

and true pattern throughout the runs, an assumption that was verified

by the event recorder. Runoff depth-time relationships were again taken

from the smooth cumulative runoff depth curves. Infiltrated depths were

determined by subtracting the runoff depths from the applied depths by

corresponding times. Runoff rates and infiltration rates were deter-

mined as in the constant rate runs by determining the slopes of cumula-

tive depth curves.

Pattern 3 (Figure 4.14) starts at a peak maximum application rate

and continues at a constant rate for approximately 0.1 hour. Then the

application rate pattern decreases on some kt^{-n} curve based on an

estimate of the infiltration curve for the soil. All calculations were

performed as for Pattern 2.

Tillage and Planting Methods

Practices Studied

Six types of row crop tillage and planting methods were tested for their ability to prevent runoff. They were: (1) Clean till and flat plant; (2) surface mulch and flat plant; (3) disk mulch and flat plant; (4) clean till and bed plant; (5) clean till, bed plant and chisel between beds; and (6) bed plant with crop residue partially incorporated between beds. Methods 1, 3 and 4 are commonly used. Method 2 was included to determine the value of the surface mulch in protecting soil surface structure. The purpose of method 5 was to see if chiseling between beds would keep the soil open during irrigation. Although treatment 6 was rather hard to accomplish, it was included because of the apparent great potential for creating high infiltration rates in low areas where water would accumulate. Individual plots were 60 feet long and 20 feet wide to allow buffer areas on the edges for working. A randomized block design was used to facilitate statistical analysis. The tests were replicated four times. All plots sloped approximately one percent in the direction of their longest dimension. Runoff from each plot was caught in a ditch to prevent it from getting onto other plots.

Equipment

The sprinkler infiltrometer described previously was used to make these tests. The sprinkler was located at the lower end of the plot being tested. Applied water was measured in rain gauges which were located at three foot intervals along a line extending from the

sprinkler toward the upper end of the plots. Constant application rates were used.

Data Recorded

As in the sprinkler infiltrometer tests previously described, the highest application rates were close to the sprinkler with the lowest being farthest away. Runoff began first in the high application rate areas with the water running toward the sprinkler because of the slope. Whenever surface water movement began, the water would run on to an area of higher application rates where the runoff had begun previously.

Whenever water from the previous pass of the sprinkler head first remained on the soil surface adjacent to a rain gauge at the time the sprinkler passed again, puddling was considered to have occurred. The amount of water in that rain gauge and the time since the beginning of the test were recorded. This was done at each of the rain gauges at which puddling occurred during the tests. From this data, application rates and the length of time required for puddling to take place at that application rate were determined.

Similarly when water movement began adjacent to a rain gauge, the time and amount of water in the gauge were recorded. From this data application rates and the times required for runoff to occur at these application rates were determined.

CHAPTER V

RESULTS AND DISCUSSION

Constant and Two Step Application Rate Patterns

Constant and two-step application rate pattern tests were run in the laboratory to determine relationships between infiltration rate with time and infiltration rate with depth of intake for the two soils and to calibrate the model.

Initial moisture contents of the tests are shown in Table 5.1. The soil bulk density for the sandy clay loam was 1.45 g./cc, except near the surface. The soil bulk density for the loam was 1.24 g./cc except near the surface.

Table 5.1 Initial moisture contents

Depth, inches	Percent Moisture by Volume	
	Sandy Clay Loam	Loam
0	13.6	13.2
1	20.3	15.3
2	22.1	19.4
6	23.4	20.4

Infiltration curves are shown in Figures 5.1, 5.2, and 5.3 for nine tests of each soil using three patterns: 8-5, 2-5 and 5. The application rates associated with the patterns are:

8-5   12 minutes of 1.6 iph (inches per hour) followed

        by 32 minutes of 1.0 iph,

2-5   12 minutes of 0.4 iph followed by 40 minutes of

        1.0 iph, and

5   48 minutes of 1.0 iph.

Each plotted point represents the average infiltration rate of six soil compartments over a two- or four-minute time interval.

The nine sandy clay loam tests were run in the following order: 5, 8-5, 2-5, 2-5, 8-5, 5, 2-5, 5, and 8-5. The nine loam tests were run in the following order: 5, 2-5, 8-5, 8-5, 2-5, 5, 8-5, 5, 2-5.

Data from only six of the eight soil compartments is used because compartments 1 and 8 gave quite variable results. Large cracks developed because heated air flowed on one side of each of these two compartments.

The laboratory infiltration data points of Figures 5.1, 5.2, and 5.3 are averaged and the resulting smoothed curves are drawn on Figures 5.4 and 5.5. The infiltration curves of patterns 8-5 and 5 nearly coincide, but the infiltration curve of pattern 2-5 is completely separated from the other two curves. Therefore, representing infiltration rate only as a function of time is questionable for different types of application rate patterns.
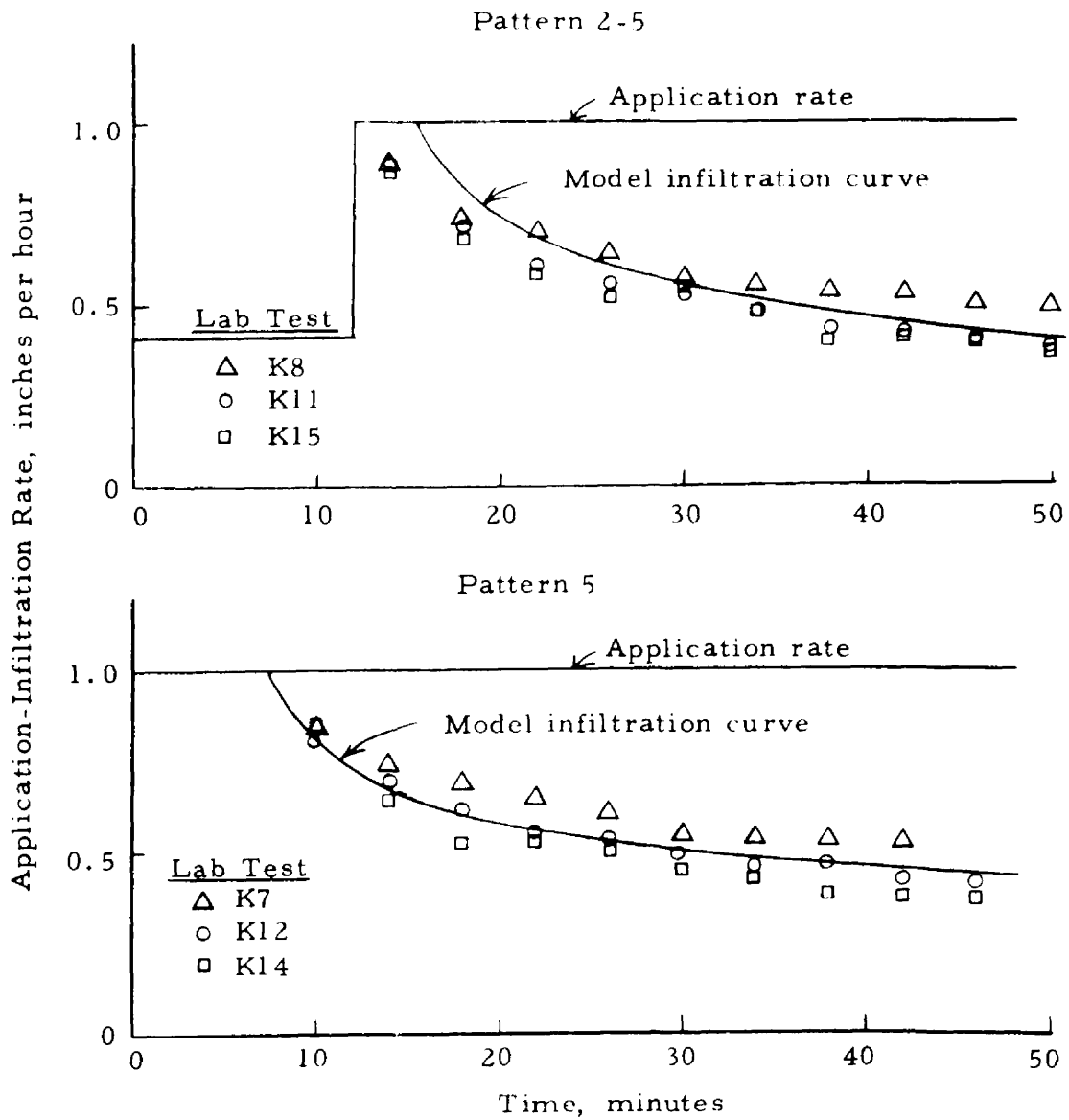
Figure 5.1   Infiltration rate curves for constant and two-step application rate patterns - loam
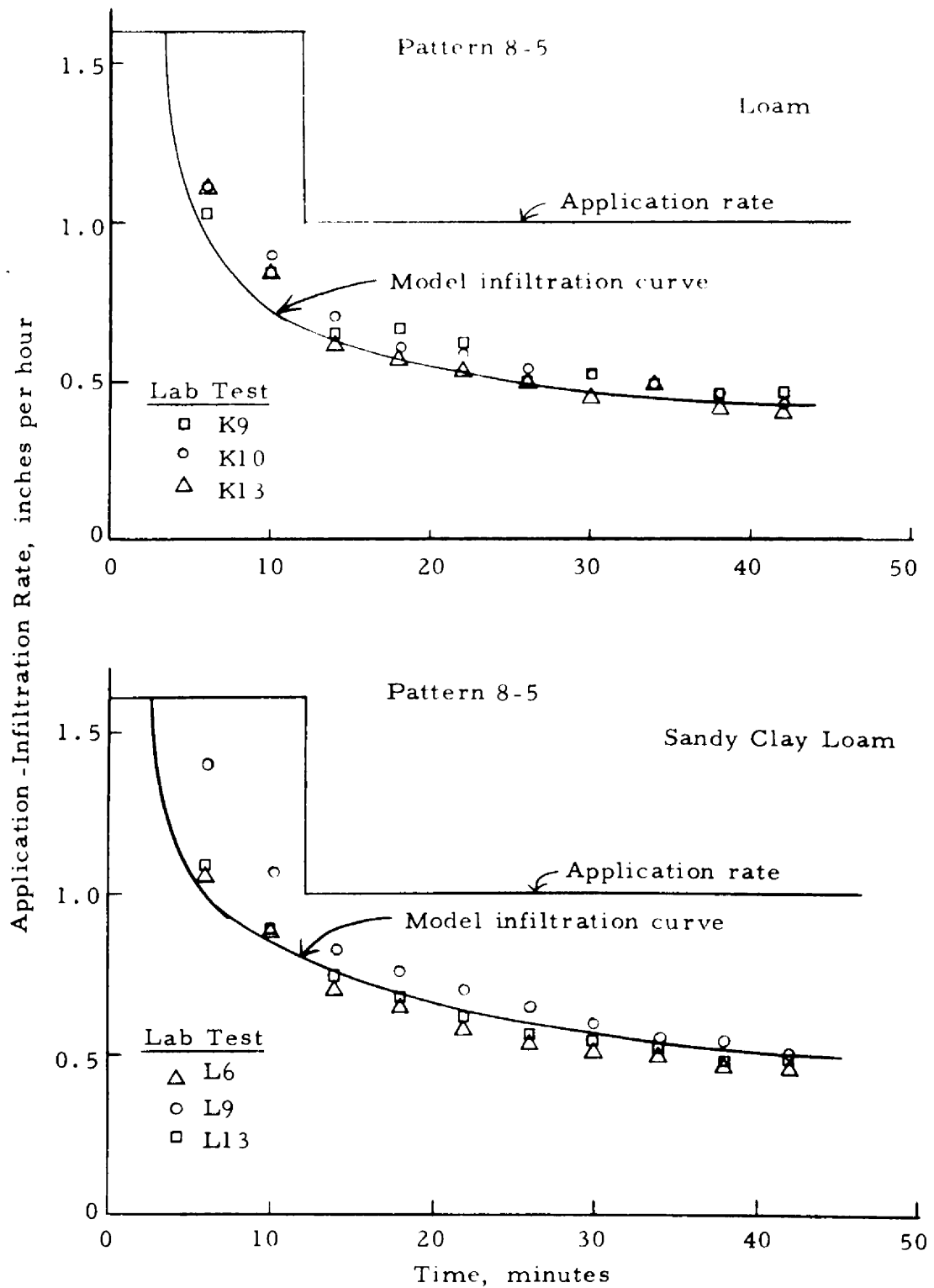
Figure 5.2 Infiltration rate curves for two-step application rate patterns
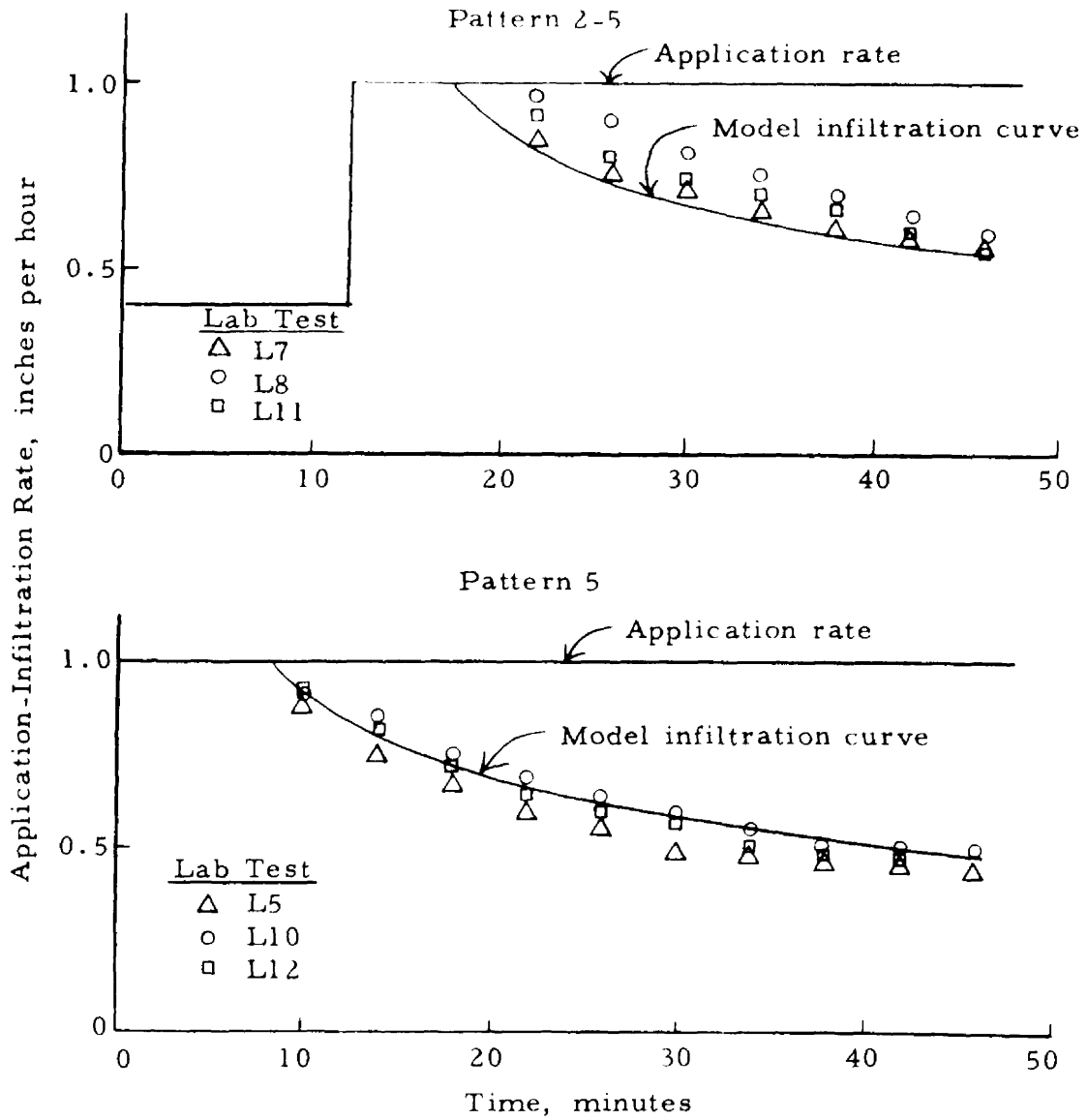
Figure 5.3   Infiltration rate curves for constant and two-step application rate patterns - sandy clay loam
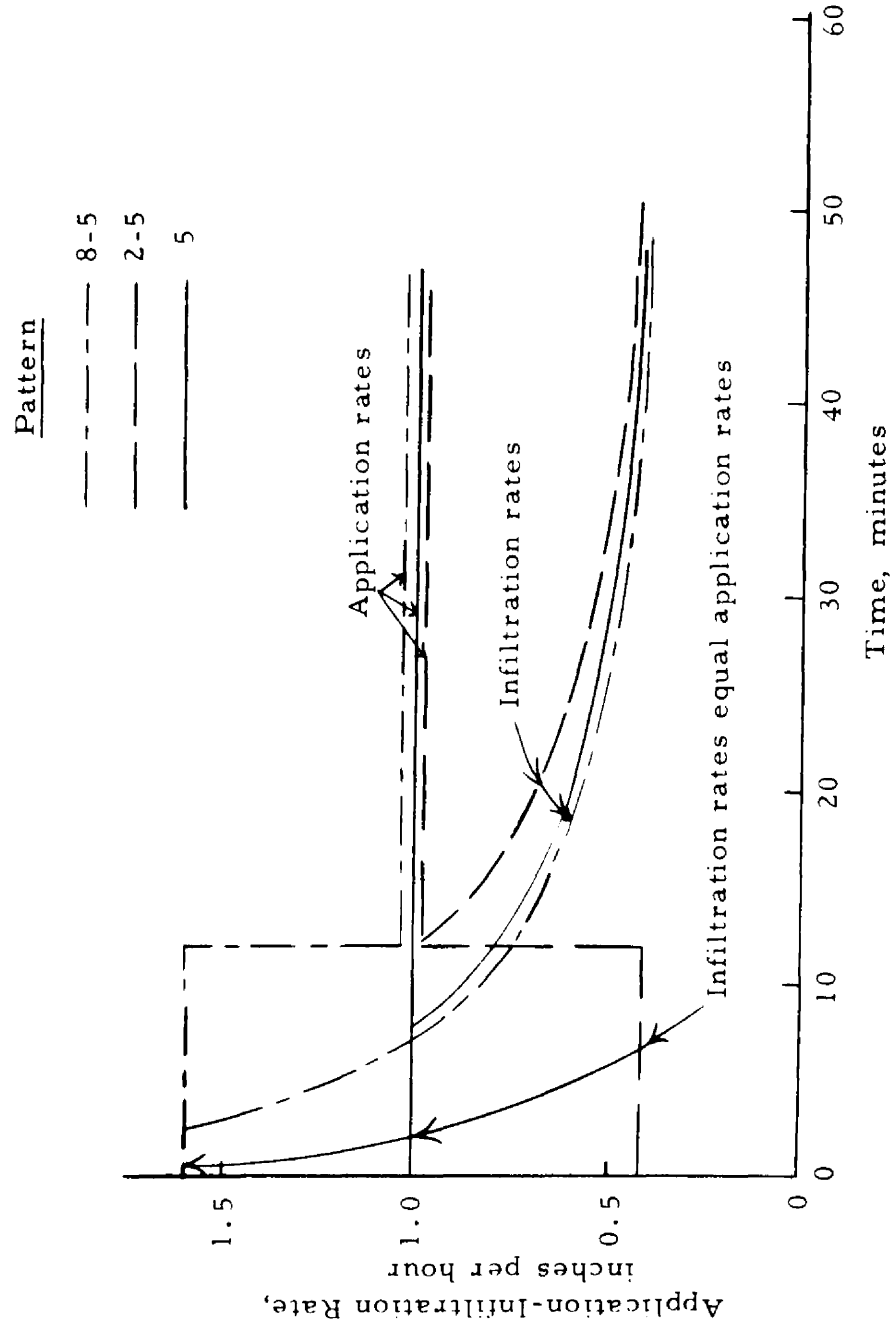
Figure 5.4   Average infiltration rate and time for a loam from laboratory tests
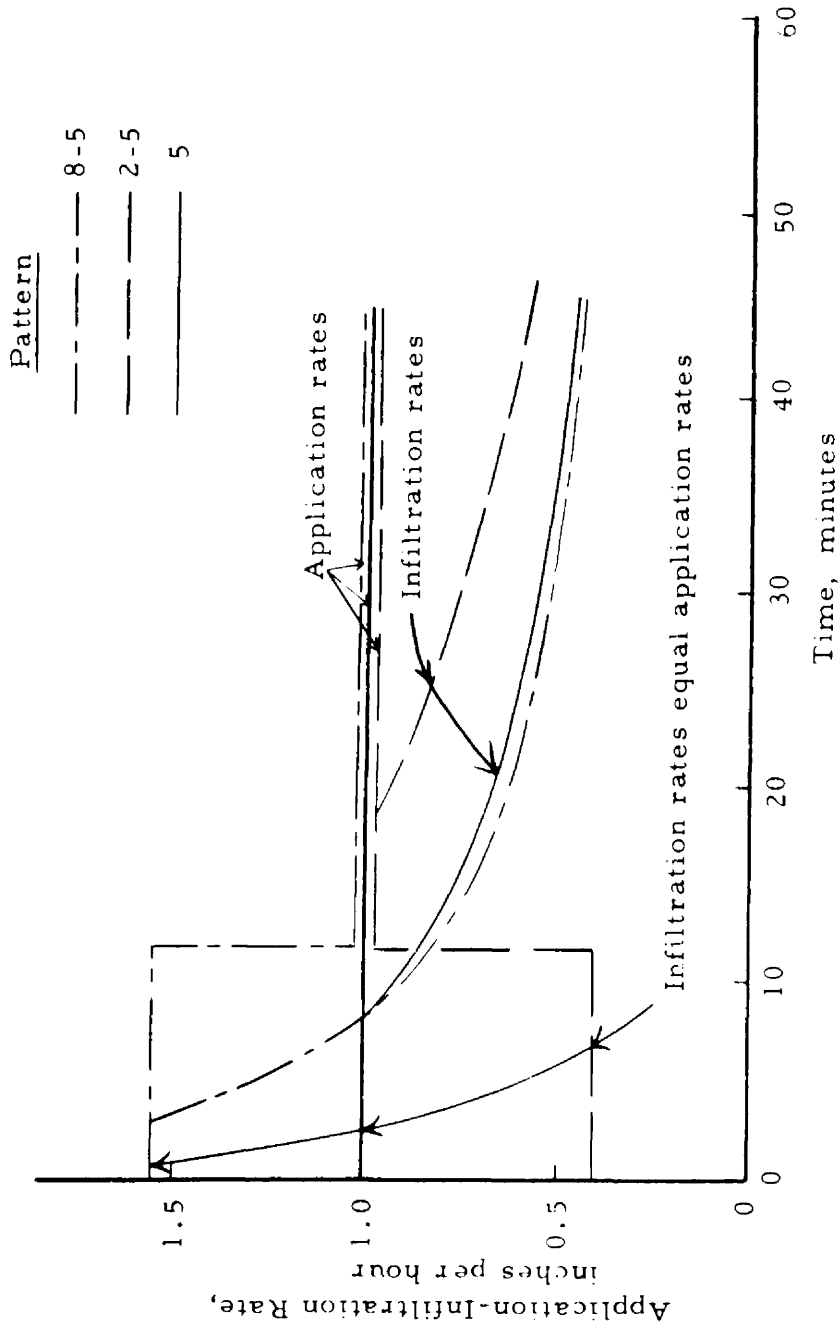
Figure 5.5 Average infiltration rate and time for a sandy clay loam from laboratory tests

Next, the relationship between infiltration rate and depth of intake was determined. The laboratory data of Figures 5.1, 5.2, and 5.3 were averaged to establish relationships between infiltration rate and depth of intake (Figures 5.6 and 5.7). For the loam (Figure 5.6), the infiltration curves for patterns 5 and 2-5 are nearly identical, but the infiltration curve for pattern 8-5 is substantially different. However, for the sandy clay loam (Figure 5.7), the infiltration curves for patterns nearly coincide. Therefore, representing infiltration rate only as a function of intake depth may be valid for one soil but questionable for another, since the type of application rate pattern affects this relationship.

Calibration of Model to Fit Laboratory Tests

The model was calibrated to achieve a reasonable simulation of the laboratory data. Three possibilities were considered for ensuring that the model would simulate the laboratory tests. The possibilities tested consisted of using a homogeneous soil, using a stratified soil, and choosing saturated conductivity, K, values other than those obtained in the permeability tests for the homogeneous and stratified soil. Before discussing the three possibilities, some important aspects of the model will be discussed that pertain to verifying the simulation.

The model utilizes a numerical solution to two basic moisture flow equations -- Darcy's law and continuity. Moisture-tension-
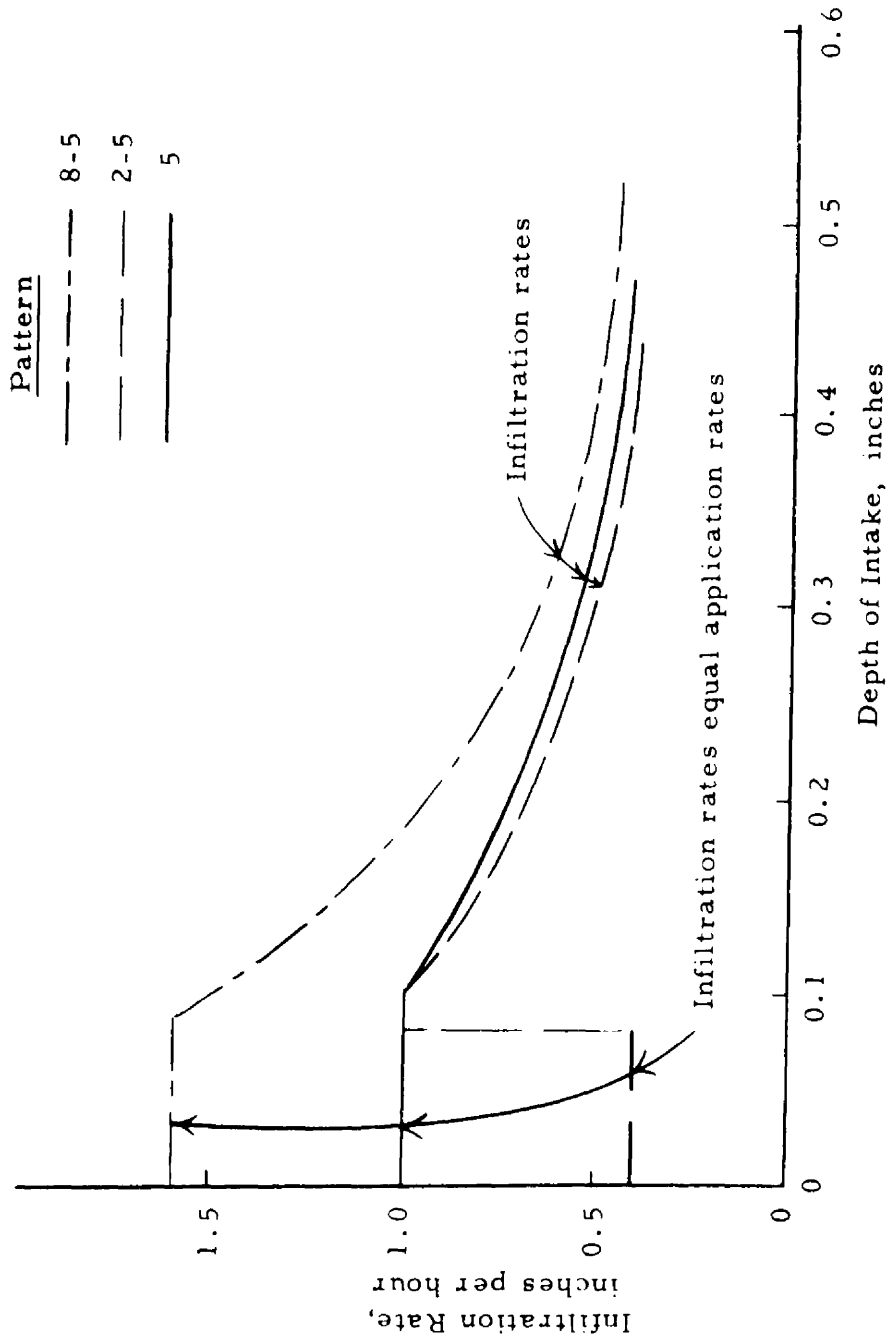
Figure 5.6 Average infiltration rate and depth of intake for a loam from
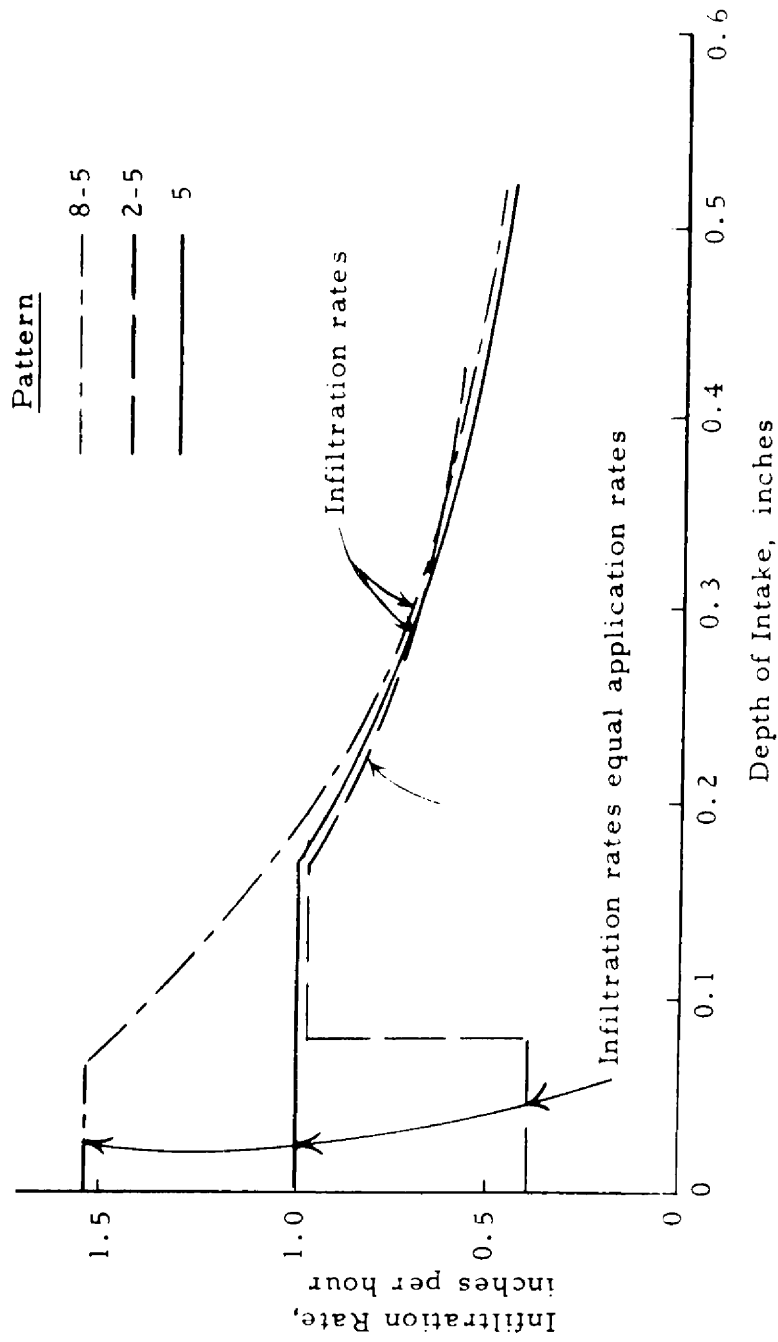laboratory tests

Figure 5.7   Average infiltration rate and depth of intake for a sandy clay loam from laboratory tests

permeability relationships for a particular soil were employed as model inputs. Initial moisture contents (Table 5.1) were used as the initial conditions for the model.

A semi-infinite column (25 inches) was assumed for the lower boundary condition of the model by prescribing a constant potential at 25 inches. Static equilibrium is assumed below the lowest depth specified (six inches) for the initial moisture contents (Table 5.1).

The upper boundary conditions are the application rate, until runoff begins, and a saturated upper boundary - zero potential - after runoff begins.

Homogeneous Soil Model

Several saturated conductivity, K, values and a homogeneous soil were input to the model to simulate the laboratory infiltration tests of patterns 8-5, 5, and 2-5. The fitting of the model to the infiltration curve of pattern 5 for the sandy clay loam is described here.

The model indicated no runoff using a K value of 0.415 inches per hour estimated from the water permeability test (Figure 4.7). The model did not produce a good fit using other K values for a homogeneous soil. A K value of 0.04 inches per hour produced the closest approximate average fit (Figure 5.8); however, the infiltration curve was too steep and was not well fitted to the data. A K value lower than 0.04 inches per hour would be required to make the computed curve fit the
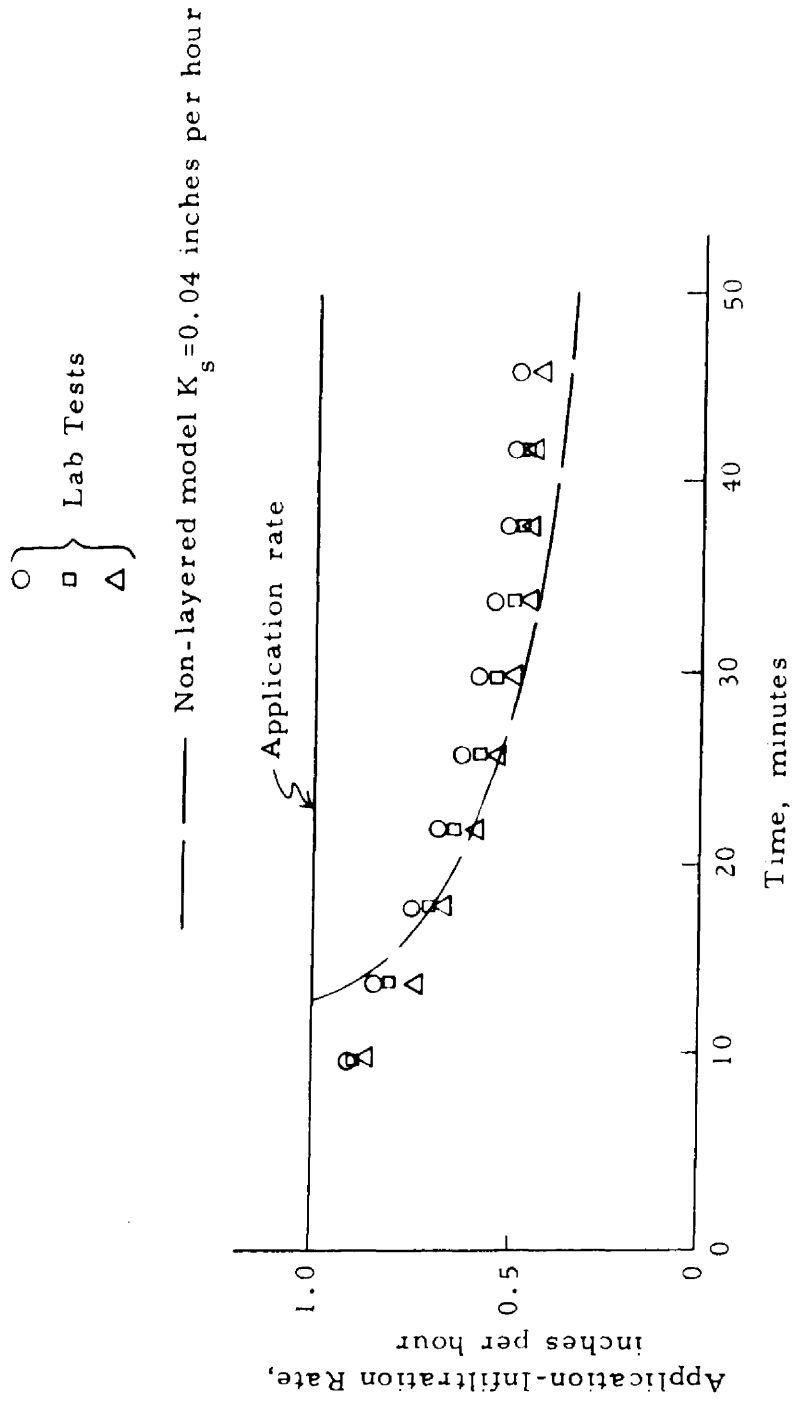
Figure 5.8 Infiltration rate comparison between a non-layered model and laboratory test data - sandy clay loam

data in the initial runoff stage. A K value higher than 0.04 inches per hour would be required to make the computed curve fit the data in the final part of the tests. Therefore, no single value of saturated conductivity would yield a curve whose shape was reasonably matched by the laboratory data.

Stratified Soil Model

The soil surface appeared to be puddled in the laboratory tests; therefore, simulating a stratified soil should give a better approximation to laboratory conditions (and very likely field conditions) than simulating a homogeneous soil.

Several combinations of K values and layer thicknesses were tested. First, a low K value was used for the upper 0.2 inches and the K value of 0.415 inches per hour estimated from the water permeability test (Figure 4.7) was used for the lower layer. An example of using a low K value (0.007 inches per hour) at the surface is shown in Figure 5.9. Using 0.415 inches per hour for the K value in the sublayer required a low K value for the surface layer to approximate the final laboratory infiltration rate. The low K value for the surface layer caused runoff to begin too soon and resulted in an infiltration curve which was too steep at the start of runoff.

Secondly, increasing the K value at the surface to 0.017 inches per hour and increasing the surface layer thickness to 0.5 inches, while the K value for the lower layer remained 0.415 inches per hour, caused an infiltration curve which was also too steep at the time of

Layered Model

Depth, inches	Saturated Conductivity, inches per hour
0.0 to 0.2	0.007
0.2 to 25	0.415
0.0 to 0.5	0.017
0.5 to 25	0.415
0.0 to 0.2	0.013
0.2 to 25	0.10

$\circ$
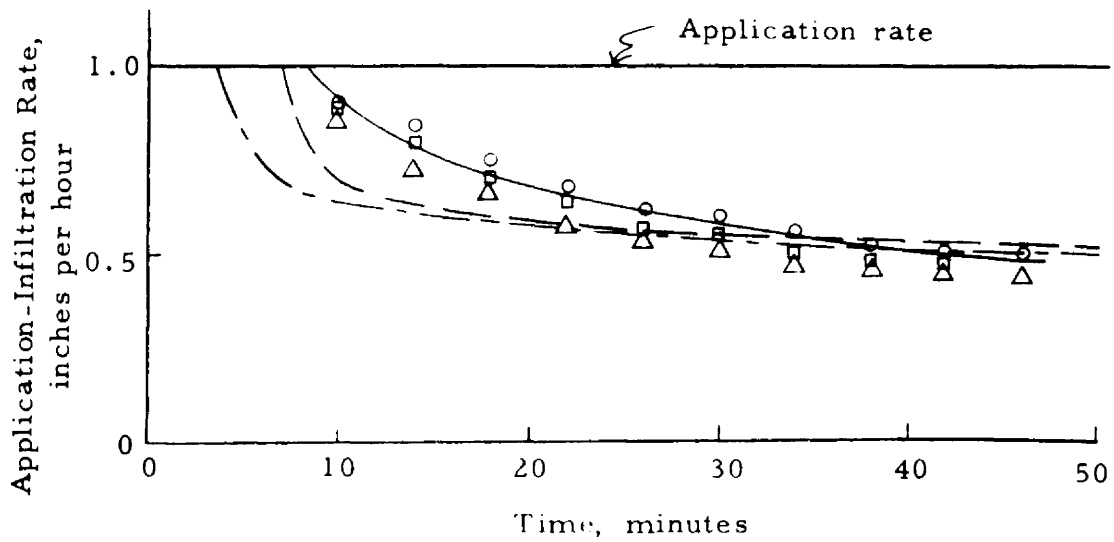$\square$ } Laboratory test data
$\triangle$

Figure 5.9   Infiltration rate comparison between a layered model with a high K value in the lower layer and laboratory test data - sandy clay loam

runoff. After reasoning that the puddled layer should not be over 0.5 inches thick, the conclusion was that the K value in the lower layer had to be reduced below 0.415 inches per hour.

Third, K values and layer thicknesses were chosen to obtain a reasonable fit of the model simulation to the laboratory infiltration curves. After numerous trials, a K value of 0.013 inches per hour was chosen for a surface layer thickness of 0.2 inches, while a K value of 0.10 inches per hour was chosen for the lower layer (Figure 5.9) for the sandy clay loam.

Three combinations of K values and surface layer thickness described for the sandy clay loam were also used for the loam. The K values which produced the best model-experiment agreement for the two soils are listed in Table 5.2.

Table 5.2 Saturated conductivity values chosen for the model

Soil	Saturated Conductivity, inches per hour	
	0.2 Inches of Surface Soil	Soil Below 0.2 Inches
Sandy Clay Loam	0.013	0.10
Loam	0.020	0.10

The K values could have been higher in the permeability tests than in the laboratory infiltration tests for several reasons, such as small errors in density measurement and differences in microbiological activity. A small increase in density can decrease conductivity

considerably as described in the literature review (Equations 2.1 and 2.2). An increase in microbiological activity can result in slime coating the pores and decreasing conductivity.

At this point, the following data are required for the model:

1. Relationships between moisture content or saturation and capillary pressure (Figure 4.9);

2. Relationships between relative permeability and capillary pressure (e.g., the upper Soltrol imbibition curve shown in Figure 5.2 and the Soltrol imbibition curve shown in Figure 5.3 are used to calculate the $k_r - \psi$ relationships for the sandy clay loam and loam, respectively);

3. Initial moisture contents of laboratory infiltration tests (Table 5.1); and

4. Saturated conductivity values (Table 5.2), which were chosen to attain good agreement between laboratory tests and an assumed stratified soil model.

Model Verification

Computed infiltration curves, using the model, are presented in Figures 5.1, 5.2 and 5.3, along with the laboratory data. A reasonable fit was obtained between laboratory and model tests for the constant and two-step application rate patterns.

Simulated Center-Pivot Application Rate Patterns

The next steps were to use center-pivot application rate patterns in laboratory infiltration tests, simulate the laboratory tests with the model using the same center-pivot patterns, and check the fit of the model infiltration curves with the laboratory infiltration curves.

One symmetrical and two non-symmetrical application rate patterns were selected for study (Figures 5.10 to 5.14). The symmetrical pattern is similar to a pattern existing near the outer end of many center-pivot systems in the field. The non-symmetrical patterns, humped toward the front, are possibilities for proposed patterns.

Because of laboratory equipment limitations, laboratory patterns are stair-stepped rather than smooth curves as encountered with field center-pivot patterns.

Peak application rates, time lengths and applied depths considered practical in the field were chosen for the patterns; however, the peak rates, time lengths and applied depth can vary considerably in the field. Each pattern applied the same total depth of water.

Infiltration rates for the tests simulating center-pivot patterns are shown in Figures 5.10 to 5.14. Each plotted point represents the average infiltration rate of six soil compartments over a two- or four-minute time interval.

Figure 5.10 Application and infiltration rates for center-pivot
pattern B

Figure 5.11 Application and infiltration rates for center-pivot pattern C - loam

Figure 5.12 Application and infiltration rates for center-pivot pattern C - sandy clay loam
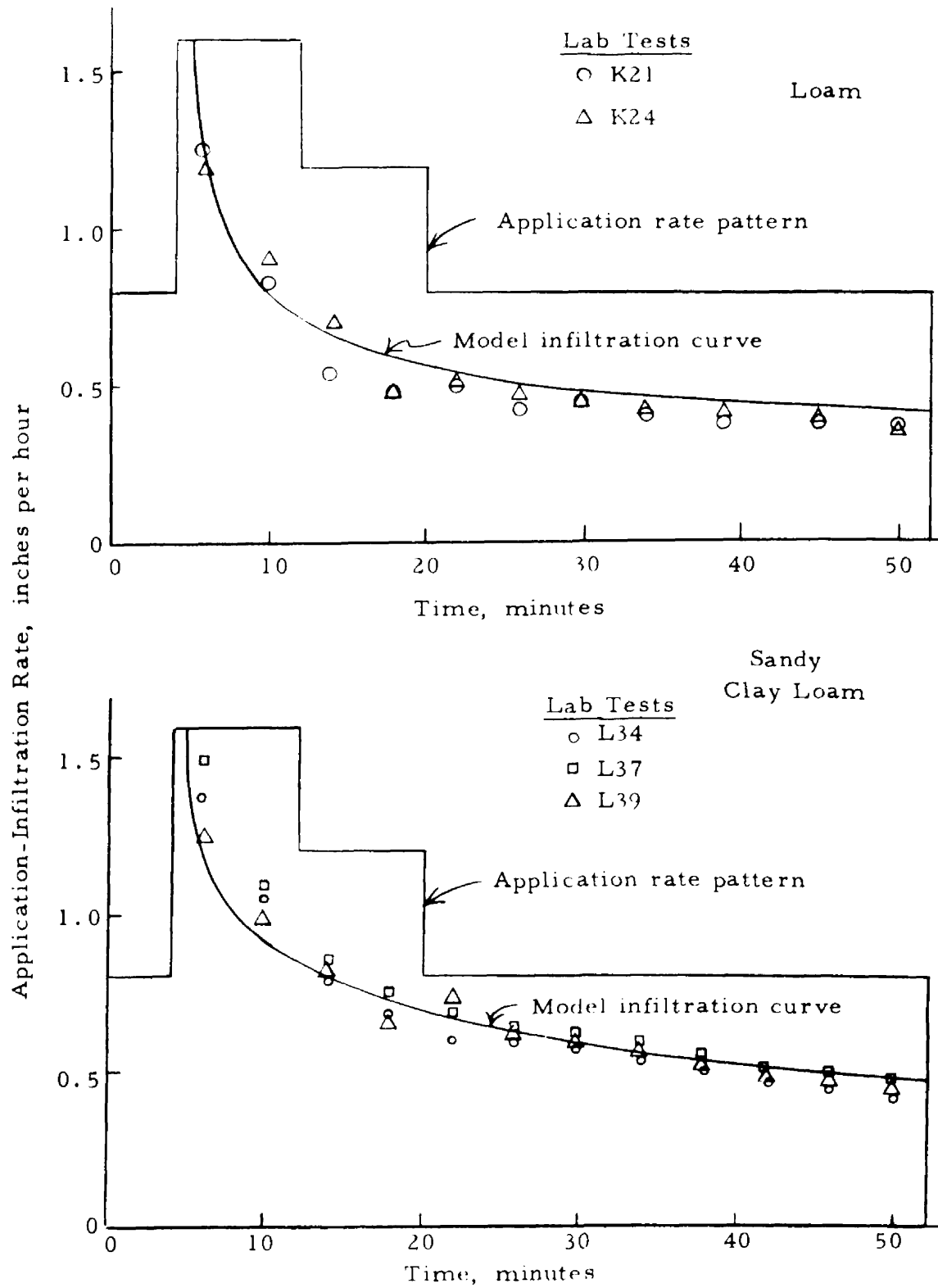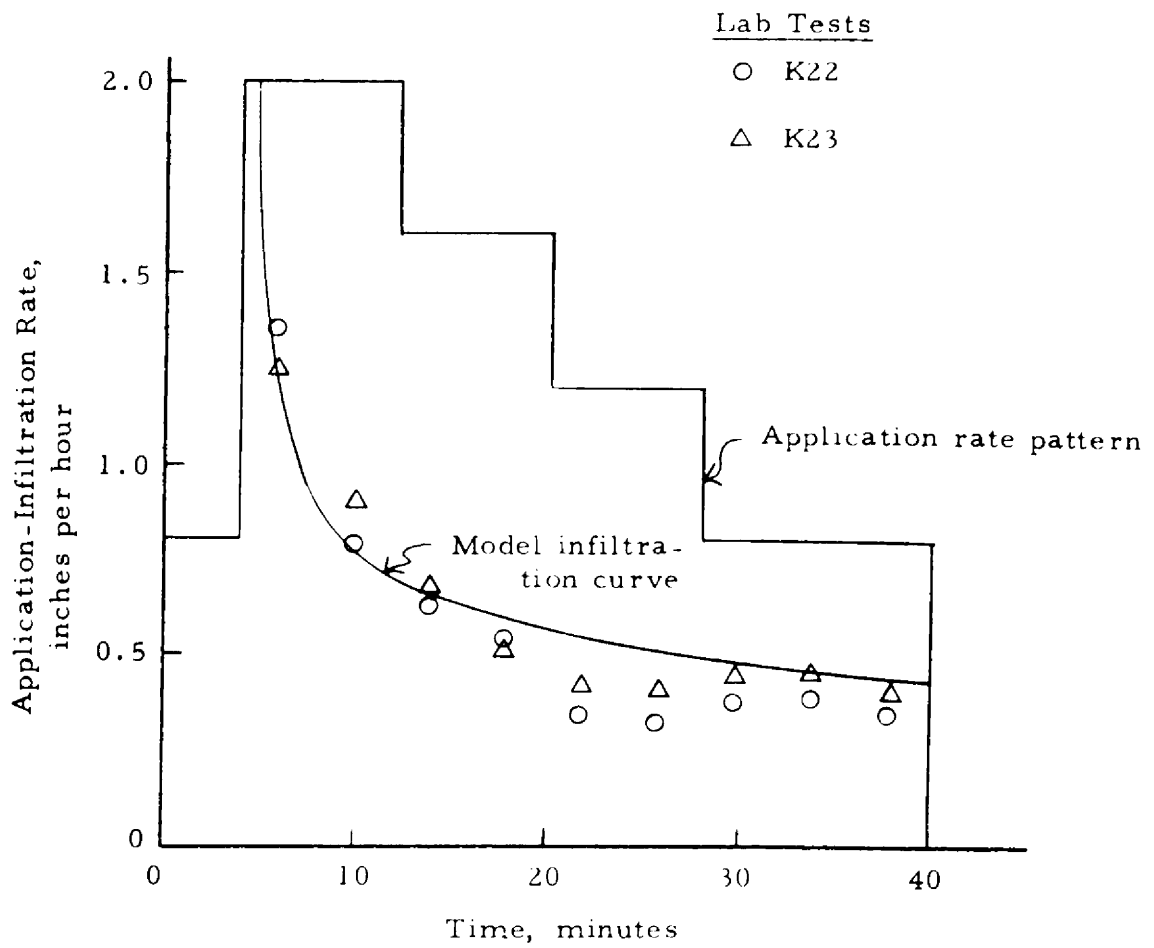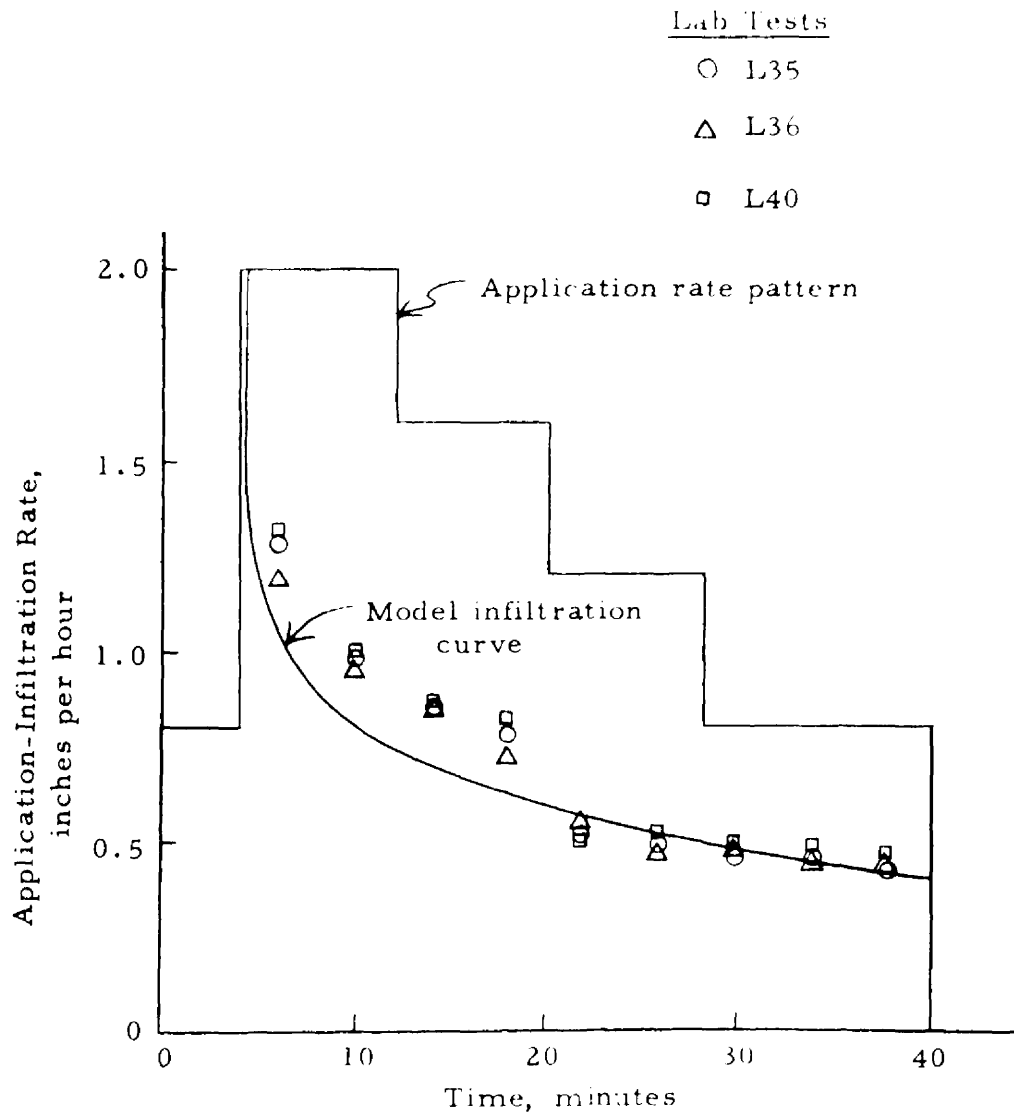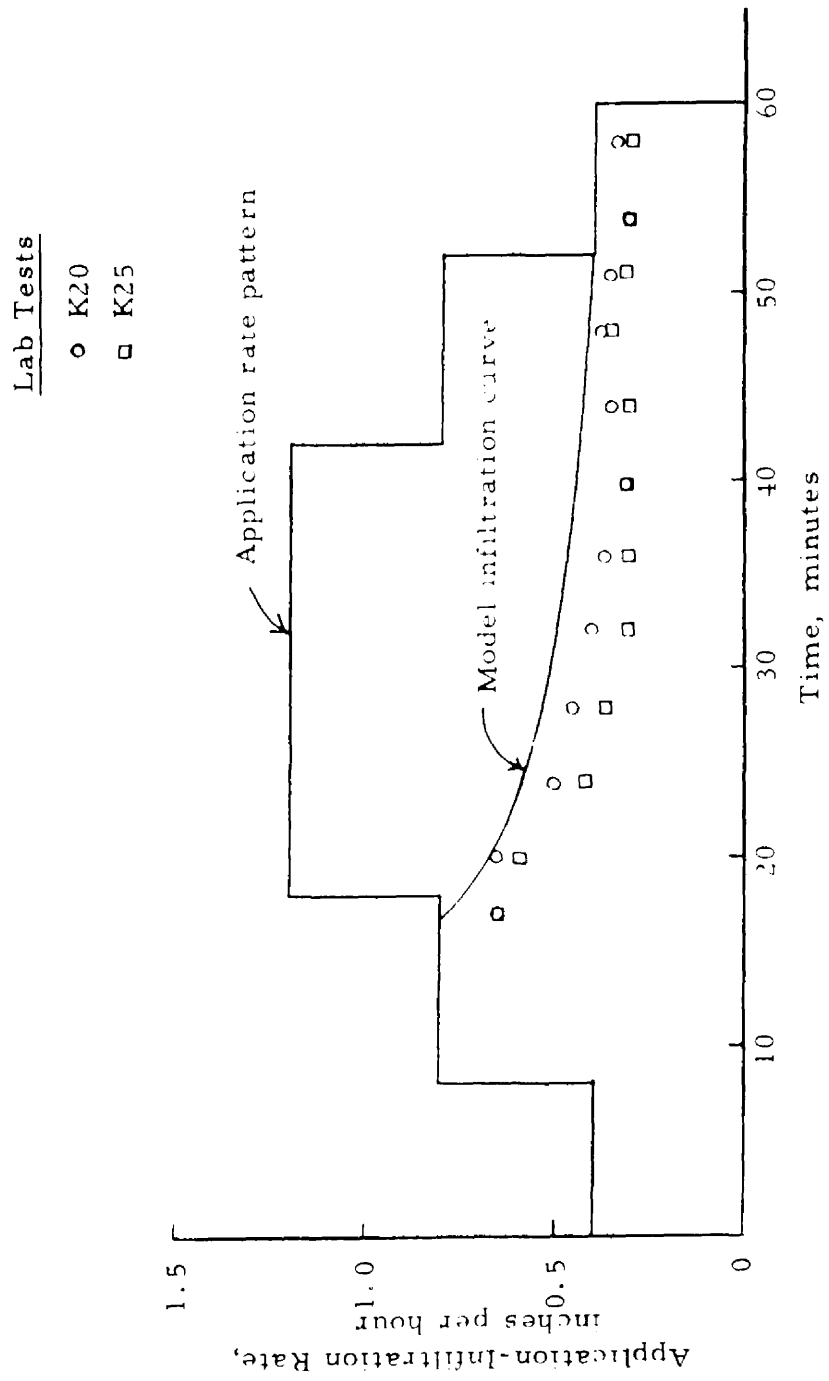
Figure 5.13 Application and infiltration rates for center-pivot pattern A - loam
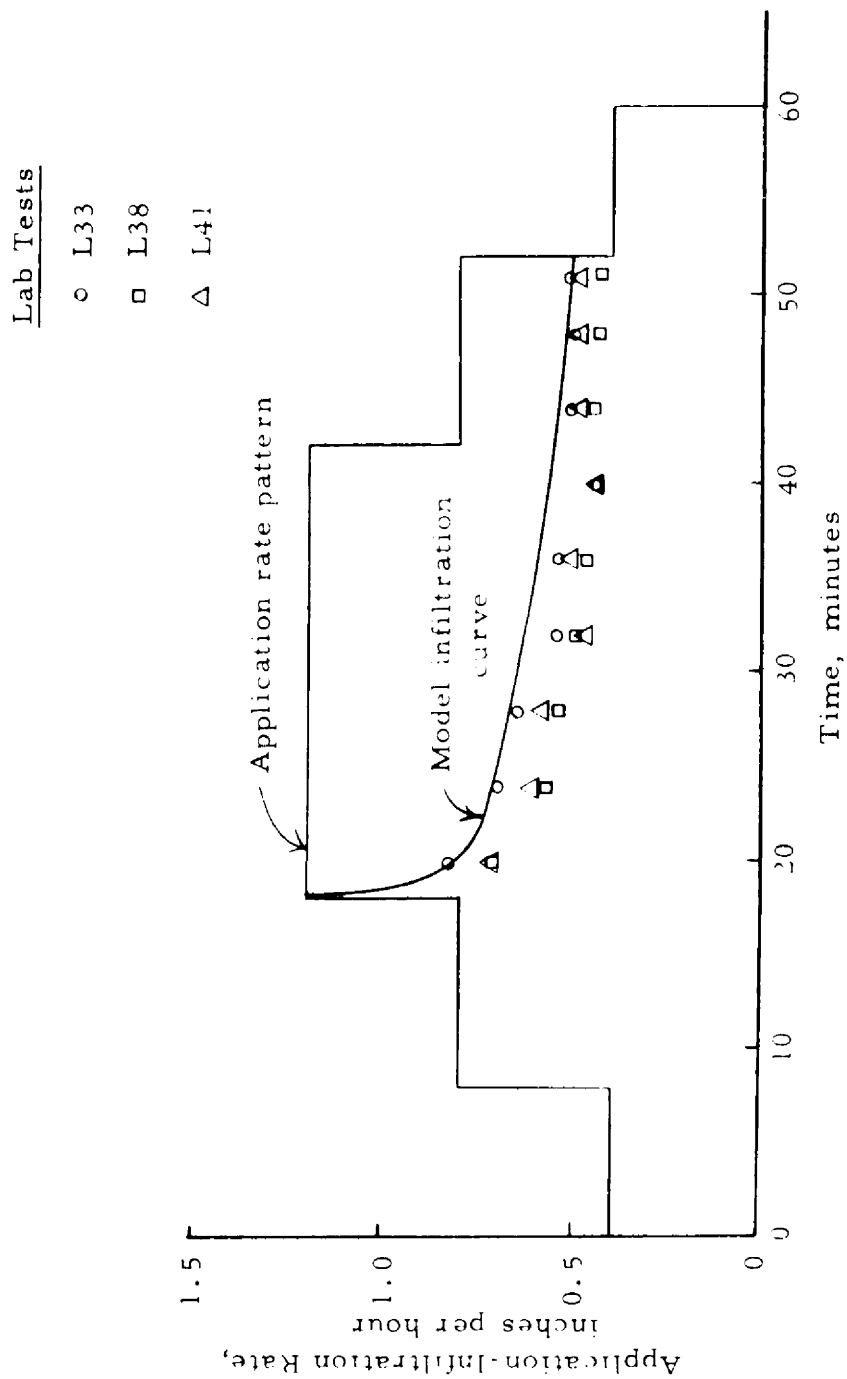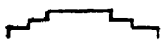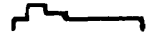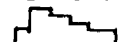
Figure 5.14 Application and infiltration rates for center-pivot pattern A - sandy clay loam

The six tests on the loam were run in the following order: A, B, C, C, B, and A. The nine tests on the sandy clay loam were run in the following order: A, B, C, C, B, A, B, C, and A.

Average intake depth for each pattern for the sandy clay loam is presented in Table 5.3. For the laboratory results, pattern B had a significantly higher intake depth than A or C at the 95% confidence level, as tested with a paired t statistic and described by Dixon and Massey (12) (Appendix A). There is no significant difference in intake depth between patterns A and C. The laboratory intake depth of pattern C is approximately the same as for pattern A; however, the pattern C's time length is two thirds the time length of A.

Table 5.3 Intake depth for center-pivot patterns on a sandy clay loam soil - applied depth of 0.85 inches
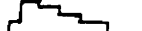
Pattern [2]	Time Length Minutes	σ_D [1]	Intake Depth, inches Laboratory	Model
A 2 4 6 4 2	60		0.55	0.59
		0.058		
B 4 8 6 4	52		0.61	0.59
		0.078		
C 4 10 8 6 4	40		0.54	0.49
		0.106		

[1] σ_D is the standard deviation of the differences from a paired t statistic, e.g. 0.058 is the standard deviation of paired differences of patterns A's and B's intake depth (Appendix A).

[2] The numbers behind the pattern letter indicate number of nozzles operating. Each nozzle applied 0.2 inches per hour.

Average intake depth for each pattern for the loam is presented

in Table 5.4. For the laboratory tests, there are significant differences,

at the 95% confidence level, between the intake depths of all three

patterns for the loam.

Table 5.4 Intake depths for center-pivot patterns on a loam - applied
depth of 0.85 inches

Pattern	Time Length		Intake Depth, inches	
	Minutes	$\sigma_D{}^1$	Laboratory	Model
A 2 4 6 4 2	60	0.047	0.44	0.53
B 4 8 6 4	52	0.031	0.49	0.52
C 4 10 8 6 4	40	0.051	0.41	0.44

[1] σ_D is the standard deviation of the differences from a paired t statistic
e.g. 0.058 is the standard deviation of paired differences of patterns A and Bs'
intake depth (Appendix A).

The laboratory tests indicate a definite advantage for front-humped

non-symmetrical application rate patterns. For both soils, the

laboratory tests show approximately an 11 percent increase in intake

depth of humped pattern B over symmetrical pattern A even though the

time length was reduced approximately 13 percent (Tables 5.3 and 5.4).

The laboratory tests also indicate a disadvantage for front-

humped patterns if the time length is shortened considerably. Humped

pattern C had approximately two percent and seven percent less intake

depth than symmetrical pattern A for the silty clay loam and loam, respectively; however, the time length of pattern C is 33 percent less than A.

The next question was, how well does the model simulate the laboratory infiltration tests using the center-pivot patterns.
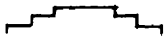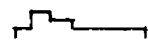
Model Simulation of Infiltration Under Center-Pivot Application Rate Patterns

The initial moisture contents of the laboratory tests using the center-pivot patterns were approximately the same as the tests with the constant and two-step patterns. Therefore, the only change in the model is the upper boundary with the center-pivot application rate patterns.

A reasonable fit of the model to the laboratory tests was achieved as illustrated in Figures 5.10 to 5.14. The main differences between the model and laboratory tests occurred in the model's overestimating the infiltration rate for symmetrical pattern A on both soils (Figures 5.13 and 5.14).

The ratios between model and laboratory intake depths for three center-pivot patterns (Table 5.5) show that the model overestimated intake depth for pattern A more than for the other two patterns.

Table 5.5 Ratios of model and laboratory intake depths taken from Tables 5.4 and 5.5

Pattern	Ratio - $\dfrac{\text{Model Intake Depth}}{\text{Laboratory Intake Depth}}$	
	Sandy Clay Loam	Loam
A 2 4 6 4 2	1.07	1.20
B 4 8 6 4	0.97	1.06
C 4 10 8 6 4	0.91	1.07

If K were allowed to decrease with time from the start of a test, a better estimate of intake depth should have resulted. A reduction of K with time should have reduced the computed intake depth for pattern A more than for patterns B and C because A's time length is longest and A's peak application rate occurs later in time than B's or C's.

A reduction of K with time can possibly be explained by swelling. As the soil dries, shrinking occurs causing cracks and increasing K. When water is added, swelling occurs which decreases K. As shown in Figure 2.2, time has considerable effect on the amount of swelling. The conclusion drawn was that noticeable errors are introduced in the model by assuming the porous media (soil) is stable.

Extension of Model to Situations
Beyond Laboratory Tests

The model was next applied to situations beyond the laboratory tests. The laboratory tests were somewhat limited in range of initial moisture content values and conductivity values. Several other application rate patterns appear frequently on center-pivot systems. The time length was shortened as the peak application rate of the pattern increased. Perhaps the time length for a humped pattern could be the same as the time length for a symmetrical pattern. Also, the time step was quite large in the laboratory tests and the effect of this large time step was checked. The effect of changing initial moisture content, conductivity, application rate patterns, time length, and time step size were studied using the model.

Effect of Initial Moisture Content

The drying method used in the laboratory tests dried the surface soil but left the soil at the two-inch depth near field capacity. In the field, the moisture content might be in a dry range to a depth of one foot or more.

The model indicates that lowering the initial moisture content in the lower layers increases the intake depths as expected (Tables 5.6 and 5.7), but the increase is not large.

Table 5.6 Intake depths for two moisture levels - sandy clay loam - applied depth of 0.85 inches
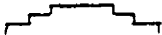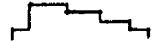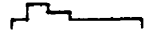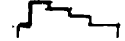
Pattern	Time Length Minutes	Computed Intake Depth, inches	
		Initial Moisture Contents @ Table 4.1	Initial Moisture Content 0.136 cc/cc
A 2 4 6 4 2	60	0.59	0.61
B 4 8 6 4	52	0.59	0.63
C 4 10 8 6 4	40	0.49	0.52

Table 5.7 Intake depths for two moisture levels - loam - applied depth of 0.85 inches

Pattern	Time Length Minutes	Computed Intake Depth, inches	
		Initial Moisture Contents @ Table 4.1	Initial Moisture Content 0.132 cc/cc
A 2 4 6 4 2	60	0.53	0.54
B 4 8 6 4	52	0.52	0.53
C 4 10 8 6 4	40	0.44	0.46

The humped pattern B now shows a greater intake depth than symmetrical pattern A for the lower initial moisture content on the sandy clay loam (Table 5.6).

Lowering the initial moisture content would increase shrinking and crack sizes on the sandy clay loam and loam in actual tests. An increase in shrinking should produce a greater advantage in intake depth for humped non-symmetrical patterns B and C than for symmetrical pattern A.

Effect of Conductivity

Low conductivity values for the two soils in the model have been used to approximate the laboratory infiltration curves. The soils were sieved in the laboratory tests, thereby reducing the conductivity. Very likely the soils would have had higher conductivity values in the field because the soils would have had more structure if they were not sieved.

Increasing the conductivity values used in the model by 30 percent increased the intake depths 12 percent to 18 percent for the sandy clay loam (Table 5.8) and 10 percent to 14 percent for the loam (Table 5.9). After increasing the conductivity values, the model shows greater intake depths for both soils for the humped pattern B than for the symmetrical pattern A.

Table 5.8 Intake depth for two conductivity levels - sandy clay loam - applied depth of 0.85 inches

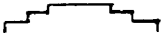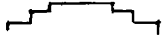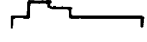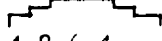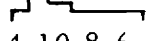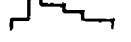| | Time Length | Computed Intake Depth, inches | |
Pattern	Minutes	K = 0.013 iph K = 0.100 iph	K = 0.0169 iph K = 0.130 iph
A 2 4 6 4 2	60	0.59	0.67
B 4 8 6 4	52	0.59	0.70
C 4 10 8 6 4	40	0.49	0.55

Table 5.9 Intake depths for two conductivity levels - loam - applied depth of 0.85 inches

| | Time Length | Computed Intake Depth, inches | |
Pattern	Minutes	K = 0.020 iph K = 0.100 iph	K = 0.026 iph K = 0.130 iph
A 2 4 6 4 2	60	0.53	0.59
B 4 8 6 4	52	0.52	0.60
C 4 10 8 6 4	40	0.44	0.51

If shrinking and swelling were considered in the tests shown in Tables 5.8 and 5.9, pattern B should have an 11 percent or greater intake depth than A. The 11 percent is the percentage difference of the intake depths between patterns B and A given in the laboratory tests (Tables 5.3 and 5.4).

Effect of Distance From Pivot and Sprinkler Spacing

The application rate pattern varies at different points along a center-pivot system. At the pivot, the peak application rate is lower and the time length is longer than near the outer end of the system. Pattern A (Figure 5.13) would occur (as a smooth curve without the steps) near the outer end of many center-pivots. Pattern D (Figure 5.15) would be approximated near the center of many center-pivots. The computed intake depths of pattern D are considerably greater than the computed intake depths of pattern A for both soils (Table 5.10).

Some systems use smaller sprinklers spaced closer together than a typical system with 30- to 33-foot sprinkler spacings. At the outer end, the sprinkler spacing may be only seven feet. The application rate pattern resulting from this close spacing is shown in Figure 5.15 as pattern E. Pattern E shows a considerably smaller computed intake depth for both soils than pattern A (Table 5.10).
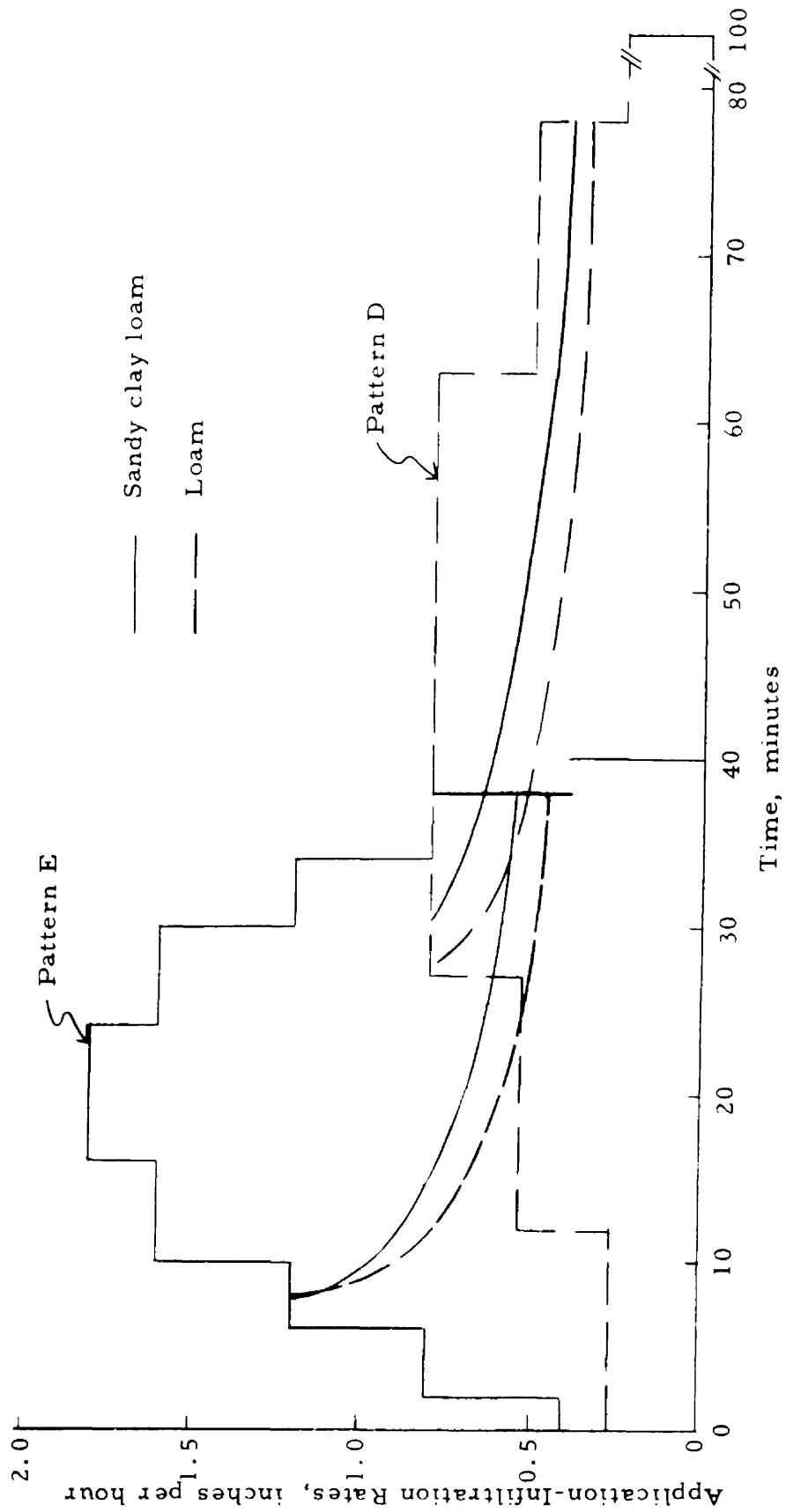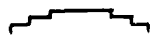
Figure 5.15 Application rates and computed infiltration curves - Patterns D and E

Table 5.10 Intake depths for three symmetrical patterns with different peak rates and different time lengths - applied depth of 0.85 inches

Pattern	Time Length Minutes	Computed Intake Depth, inches Sandy Clay Loam	Loam
E 2 4 6 8 9 8 6 4 2	40	0.48	0.43
A 2 4 6 4 2	60	0.59	0.53
D 1.3 2.6 4 2.6 1.3	90	0.73	0.63
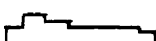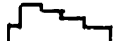
If shrinking and swelling were considered, the short symmetrical pattern E should have more increase in intake depth than the longer symmetrical pattern D especially for fine textured soils which were allowed to get drier between irrigations. However, the intake depth would still be lower for pattern E under the conditions of the laboratory tests.

Effect of Time Length

A humped non-symmetrical pattern would most likely require a shorter time length than a symmetrical pattern.

The ideal pattern is a humped pattern having the same time length as a symmetrical pattern, applying an equal depth. Extending pattern B to 60 minutes, with the model, increases the intake depth approximately seven to ten percent (Table 5.11). Extending pattern C

Table 5.11 Intake depths for different time lengths using patterns A,
B and C - applied depth of 0.85 inches

| | | Intake Depths, inches | |
| | | Computed Laboratory | |
Pattern	Time Length Minutes	Sandy Clay Loam	Loam
A 2 4 6 4 2	60	$\dfrac{0.59}{0.55}$	$\dfrac{0.53}{0.46}$
B 4 8 6 4	52	$\dfrac{0.59}{0.61}$	$\dfrac{0.52}{0.49}$
B_m 4 8 6 4 2^2	60	$\dfrac{0.63}{0.65}^1$	$\dfrac{0.57}{0.54}^1$
C 4 10 8 6 4	40	$\dfrac{0.49}{0.54}$	$\dfrac{0.44}{0.41}$
C_m 4 10 8 6 4 2^3	60	$\dfrac{0.61}{0.67}^1$	$\dfrac{0.57}{0.53}^1$

[1] Lower number is potential intake depth assuming laboratory
tests had gone 60 minutes; e.g. for sandy clay loam - B_m -

$$\dfrac{\left[\left(\dfrac{0.63 - 0.59}{0.59}\right) 0.61 + 0.61\right] - 0.55}{0.55} = 0.65$$

[2] Pattern B_m consists of 4 minutes of .08 iph, 4 minutes of 2.0 iph,
4 minutes of 1.5 iph, 8 minutes of 1.2 iph, 20 minutes of 0.8 iph, and
20 minutes of 0.4 iph.

[3] Pattern C_m consists of 4 minutes of 0.8 iph, 6 minutes of
1.6 iph, 6 minutes of 1.2 iph, 34 minutes of 0.8 iph, and 10 minutes of
0.4 iph.

to 60 minutes increases the intake depth approximately 25 to 30 percent (Table 5.11). The model now shows a greater intake depth for humped patterns B_m and C_m than for symmetrical pattern A.

Extending the time length of the humped patterns with the laboratory tests to 60 minutes would also increase the humped patterns' intake depths. Assuming the same percentage increase in intake depth would occur in the laboratory tests, as occurred with the model simulation, because of extending the tests to 60 minutes (Table 5.11), the potential results would be as follows:

loam - 60-minute humped pattern B_m would have a 23 percent

greater intake depth than symmetrical pattern A;

- 60-minute humped pattern C_m would have a 20 percent

greater intake depth than symmetrical pattern A;

sandy clay loam - 60-minute humped pattern B_m would have an

18 percent greater intake depth than symmetrical pattern

A:

- 60-minute humped pattern C_m would have a 22 percent

greater intake depth than symmetrical pattern A.

Effect of Time Step Size

The effect of size of time increment was described under solution sensitivity. In this section, the effect of size of the time step used in the application rate pattern will be examined.

A center-pivot system produces a smooth application rate pattern and no steps such as are used in this study. A model comparison using sandy clay loam soil was made between pattern A and a smoother pattern, but with the same general shape as A. The results (Figure 5.16) show the same intake depth for both patterns.

The upper pattern of Figure 5.16 is slightly steeper than the lower pattern which may have had a small effect on intake depth; however, the conclusion is reached that the size of time step has little effect on intake depth as long as the general shape of the pattern is maintained.
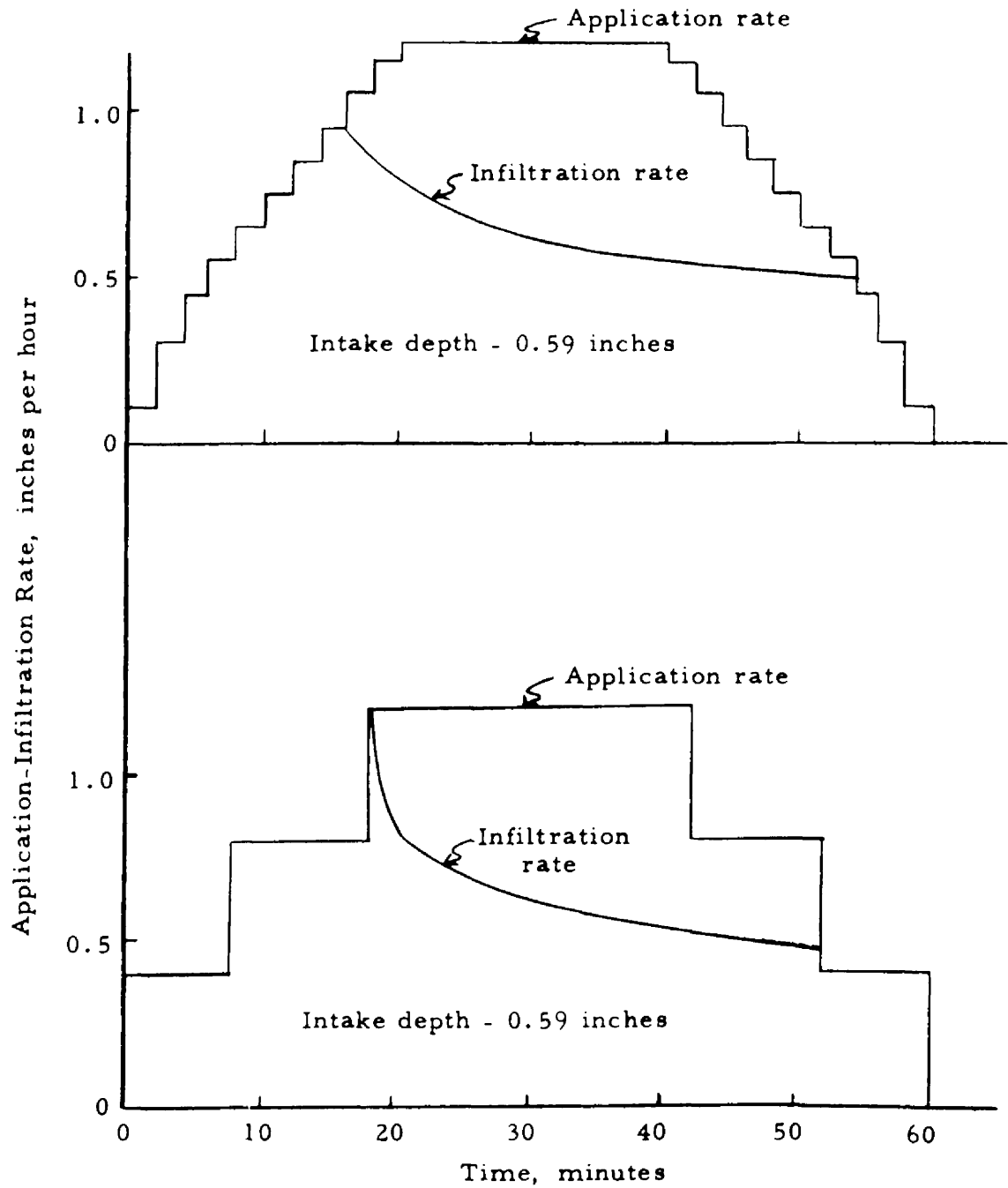
Figure 5.16 Infiltration curves for two patterns with different time-step sizes using the model - sandy clay loam - applied depth of 0.85 inches

Field Infiltrometer Studies

Preliminary Tests

The preliminary tests which compared six different time varying application rates and a constant rate were run without collecting any runoff data. These tests were run assuming that the time of puddling was when the application rate approached the infiltration capacity for the soil on which the tests were being run, an assumption which was later found to be invalid. These tests also had excessive variability due to differences in drop sizes and wind. They were not used for drawing final conclusions but rather to provide indications for better design of both field and laboratory tests.

Most of the application patterns which started at a high rate resulted in infiltration of about 1/2 inch more water before puddling than those that started low. It appeared that time from the beginning of water application had more influence on infiltration rate than the total amount of water infiltrated. Because no runoff data was collected from these tests, no infiltration information after puddling was available. The question remained regarding the degree to which the greater infiltration depths at puddling for the patterns which started at a high application rate were compensated for by reduced infiltration rates later in the tests. Also for the time-varying application rate patterns in these tests, the initial application rates were not high enough to take full advantage of the high initial infiltration capacity of the soil.

One of the results of these tests was found to be the great effect of difference in drop sizes even though the drops were small compared with the drop sizes from most commercial sprinkler nozzles. An effort had been made to avoid drop size effects by constructing special slotted nozzles. Each nozzle had a slotted opening of 0.06 inch or less and the sprinkler was operated at 80 psi pressure so it was assumed that the drop size effects would be negligible. The lower six nozzles were operated through screens to shorten their range, thereby producing the desired sprinkler distribution pattern. When an attempt was made to analyze the data, it was found that the soil at the outer end of the pattern puddled too soon for the amount of water being applied. This was a result of receiving water from the sprinkler's upper two nozzles which was not run through screens. It was necessary to discard the data from the outer rings which received water from the two upper nozzles.

To avoid these drop size problems in the 1970 field tests the slotted nozzle openings were reduced to about 0.03 inch and all the water was directed through screens. Since drop size and energy from the falling drops was now quite uniform, it was necessary to use deflectors on some of the nozzles and change the orientation of other nozzles to achieve the desired pattern. Very small, fairly uniform drop sizes resulted and the variation in infiltration rates caused by drop size effect appeared to be eliminated.

Modified Field Infiltrometer Tests

The 1970 tests included three patterns as described previously. Pattern 1 was a constant rate pattern. Pattern 2 was similar to rates

applied by center-pivot sprinklers as shown in Figure 4.13. Pattern
3 was a special experimental pattern as shown in Figure 4.14.

The experimental procedures resulted in a family of curves of
each of these application rate patterns and permitted the determination
of a family of curves of corresponding infiltration rates. Typical
examples of application and infiltration rate curves for Pattern 1
are shown in Figure 5.17. Those rings receiving water at the higher
application rates had total infiltrated depths at the end of the tests
which were greater than those which received water at the lower rates.
The tests were concluded at the end of one-half hour because of the
limited water supply so it was not known if the infiltration rates for
high application rates would eventually drop below those for the lower
application rates.

Typical examples of application and infiltration rate curves for
Pattern 2 are shown in Figure 5.18. Those rings receiving water at
higher application rates also maintained higher infiltration rates
throughout these tests, although as with the constant rate tests, the
percentage of runoff was much smaller for the lower rates.

Similar results were obtained with Pattern 3. Typical examples
of application and infiltration rate curves for this pattern are shown
in Figure 5.19. Because of the shape of this pattern, the percentage
runoff was much lower for all application rates than for the constant
rate application. It appeared that the high initial application rates
resulted in considerable increase in intake rates during the first part
of the tests. Higher rates appeared to contribute mostly to increased
runoff rather than increased infiltration during later times. It was
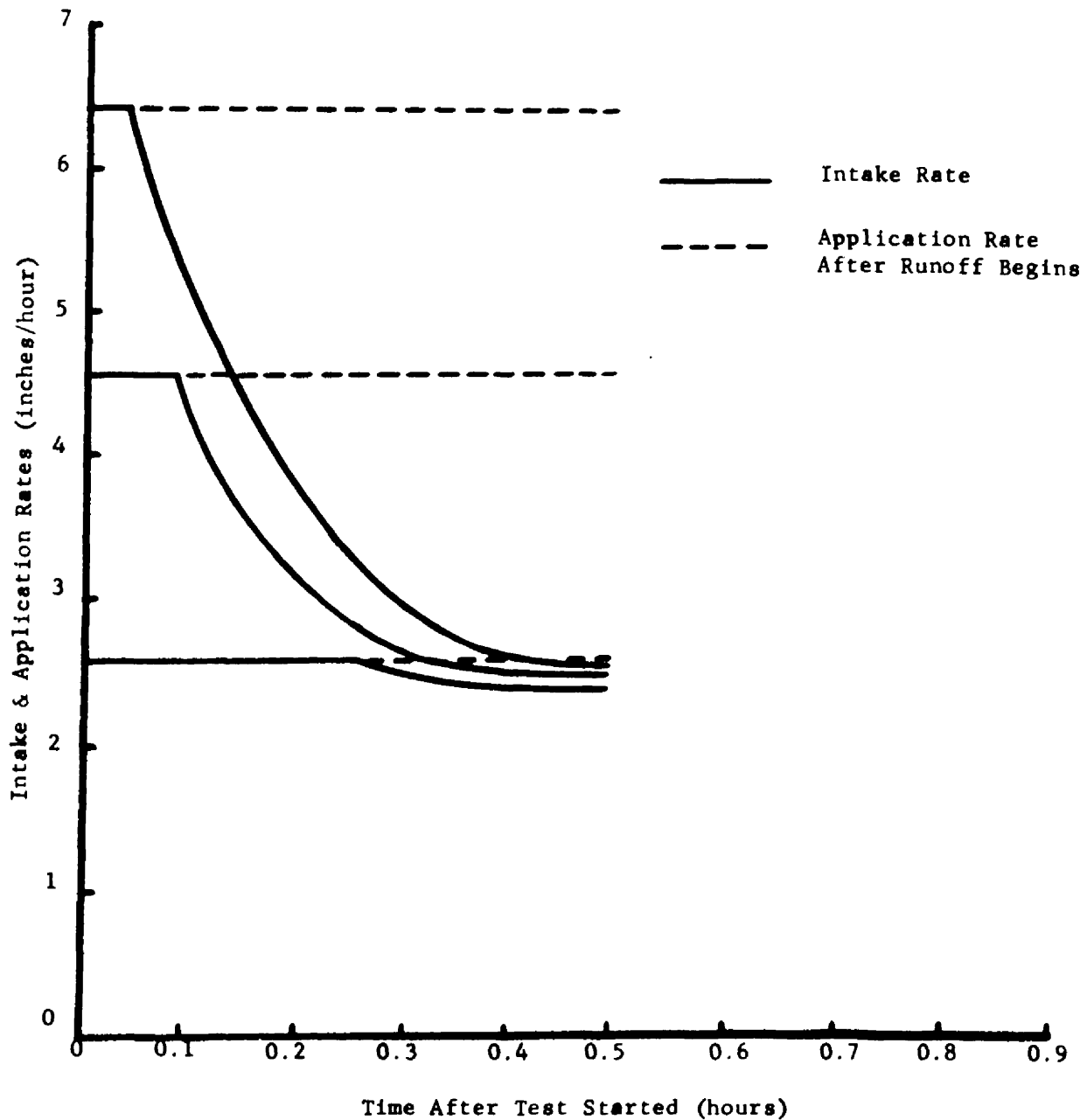
Figure 5.17. Typical examples of application and infiltration rate
curves for pattern 1.
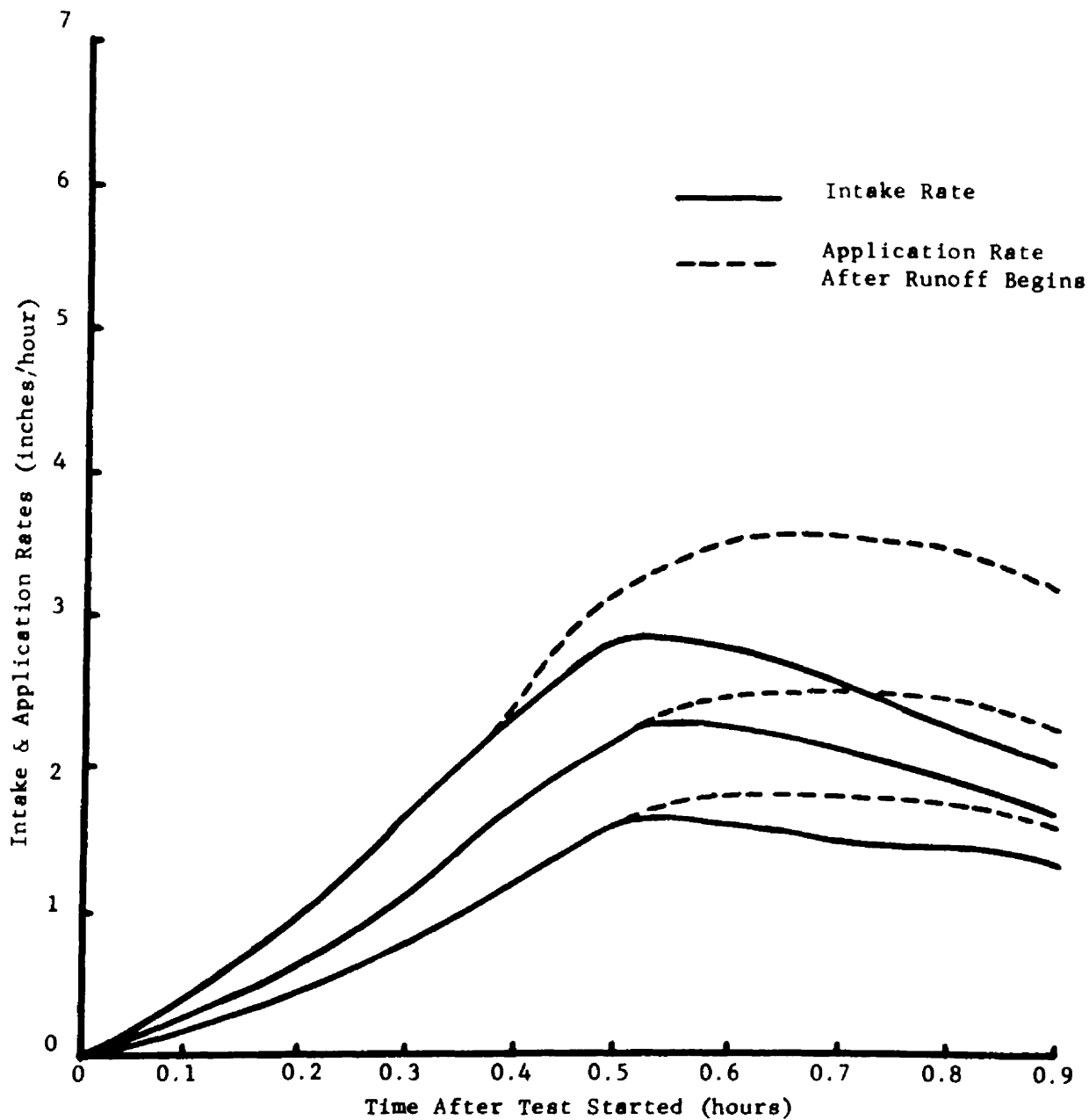
Figure 5.18. Typical examples of application and infiltration rate curves for pattern 2.
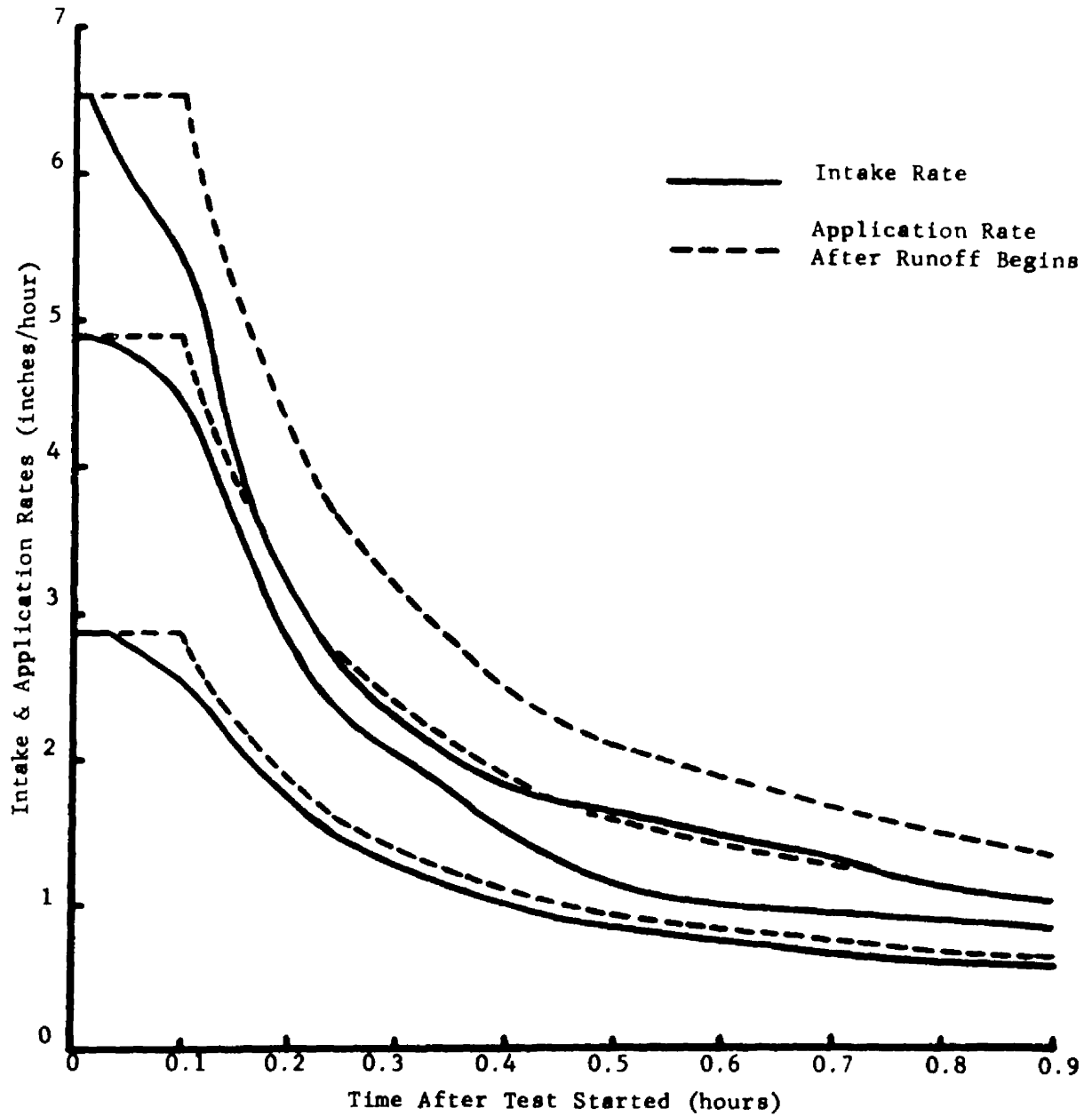
Figure 5.19. Typical examples of application and infiltration rate curves for pattern 3.

also noted that infiltration increased greatly as runoff rates increased from zero to about six percent. Application rates which resulted in runoff rates of more than six percent had little effect on infiltration rates.

Tillage and Planting Practices

Figure 5.20 shows the effect of tillage and planting treatments on the application rates which were possible before runoff began. These were not best fit curves for the data, but rather minimum value curves. For example, on treatment 3, for nearly all instances in which runoff began during the first 40 minutes the application rate exceeded 2 inches per hour.

Treatment 2 is not included in Figure 5.20 because one of the four replications had to be eliminated as a result of weedy conditions and another was ruined because of equipment failure on one of the tests. Data from the remaining replications appeared to be quite similar to that for treatment 1. Little significance should be attached to those results because of the incomplete data and because of the small drop sizes used in the tests. It is likely that surface mulch such as treatment 2 would result in considerable improvement over clean tillage under typical center-pivot sprinkler systems because of the larger drop sizes involved.

Treatment 5 (clean till bed planting with chiseling between the beds) is also omitted from Figure 5.20 because is showed no advantage over treatment 4. Initial irrigation apparently closed all chisel marks and resulted in the condition being essentially the same as treatment 4.

TREATMENT EFFECT ON INTAKE BEFORE RUNOFF BEGINS

(not to be confused with intake rate curves)

1 - Clean tillage -- flat planted
3 - Disked -- flat planted
4 - Clean tillage -- bed planted
6 - Bed planted -- residue between beds
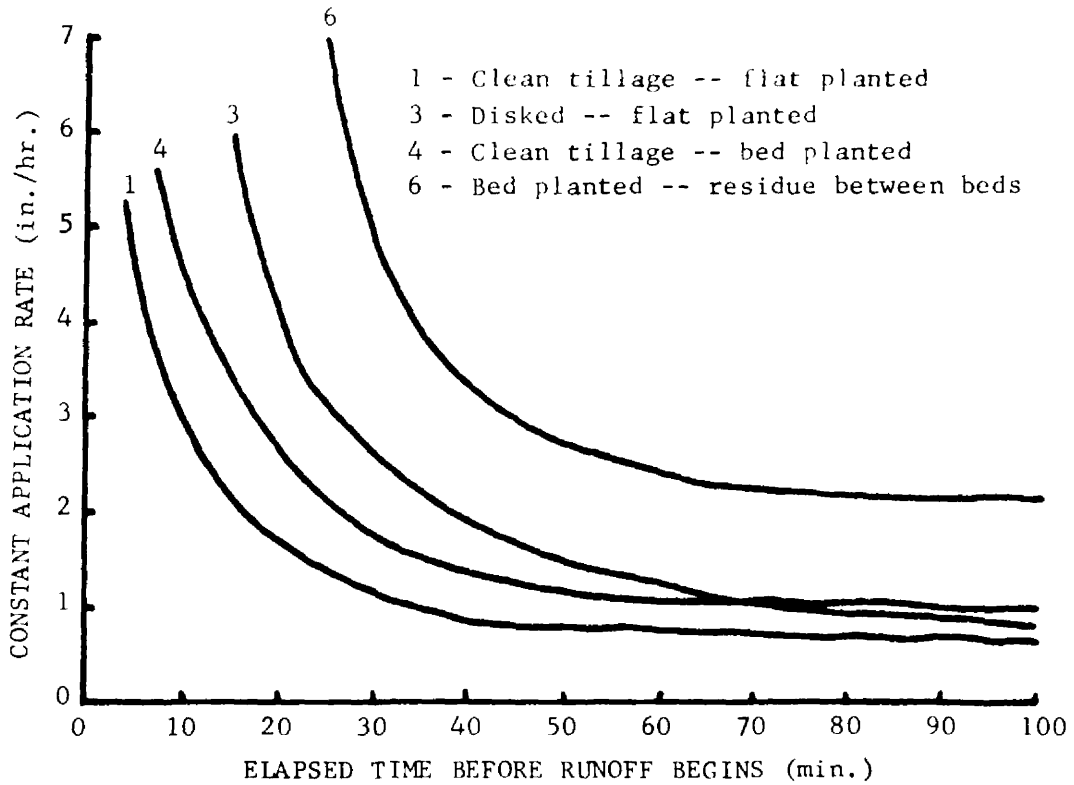
Figure 5.20. Effect of tillage and planting treatments on water application rates which can infiltrate without runoff.

Statistically significant differences were found between treat-
ments 1, 3 and 4 during the first 40 minutes. The differences after
this time were not statistically significant. There appears to be con-
siderable advantage for partially incorporating crop residue with a
disk if the sprinkler pattern is such that it will apply water initially
at high rates. For a typical center-pivot system high rates occur
later so it does not seem likely that this practice would eliminate
runoff. However, it should be noted that only the time when runoff
began was recorded and that there was no measurement of the amount of
runoff. Visual observation during the tests indicated that the total
amount of runoff from treatment 3 was considerably less than for treat-
ments 1 and 4.

The difference in performance of treatment 6 over all other treat-
ments was statistically highly significant in all instances. The suc-
cess of this treatment in preventing runoff under essentially all kinds
of conditions which are encountered under center-pivot systems seemed
too good to be true. There appeared to be no way of making these
results seem reasonable in comparison with those obtained from the other
treatments. However, findings of the field sprinkler infiltrometer
tests and the laboratory tests indicated that infiltration rates in-
creased as application rates were increased above the rates which would
initially cause runoff. As discussed later in this report, these
findings make the performance of treatment 6 seem reasonable.

CHAPTER VI

CONCLUSIONS AND RECOMMENDATIONS

General Conclusions

Numerical Model

This study indicated that a numerical moisture-flow model can be a helpful research tool in infiltration studies. A reasonable fit of laboratory infiltration data was obtained through model prediction.

It was found that laboratory measurements of saturated conductivity could not be made with sufficient accuracy for direct use in the model. Adjustments of saturated conductivity values were necessary to calibrate the model. Also a good fit could be obtained only when the soil was treated as two layers with the surface layer having a greatly reduced saturated conductivity.

Noticeable errors occurred because of ignoring shrinking and swelling in the model. These errors were of major importance only during the first few minutes of the irrigation.

Time-Varying Application Rates

The manner in which center-pivot sprinkler application rates vary with time increases potential runoff by causing high maximum application rates and by causing maximum application rates to occur after soil infiltration rates have declined from their high initial values.

Laboratory tests using loam and sandy clay loam soils indicated only a minor advantage in infiltration for front-humped application rate patterns. This advantage could be increased if the total application time could be as great for these patterns as for symmetrical patterns, but known methods of creating front-humped patterns reduce the pattern length. Field infiltrometer tests on a clay loam soil indicated a considerable advantage if the water application pattern could be begun abruptly. Swelling and shrinking plays an important role in this effect on soils which have high clay contents.

Ponded Infiltration Rates

Field measurements of ponded infiltration rates made in ring infiltrometers could not be satisfactorily correlated with sprinkler infiltration. There appeared to be a much closer relationship for soils which have high sand contents than for other soils. This is probably because porosity of an extremely sandy surface soil is not greatly disturbed by sprinkler drop impact. It appears likely that disturbance of the surface soil by sprinkler drops is responsible for much of the frequently observed depression of sprinkler infiltration rates over those for ponded conditions.

Another likely reason for the difference between sprinkler infiltration and ponded infiltration is that during sprinkler application surface soils frequently become saturated after a pass of the sprinkler and drain before the next pass. During the time the surface is nearly saturated, soil particles are partially buoyed by the water in the pores.

Upon draining this buoyance effect is removed and the particles tend to shift to a close packed position, thereby reducing permeability. This fluctating moisture condition does not exist under ponded infiltration.

Soil Moisture Content

Soil moisture potential is greatly affected by soil moisture content and the distribution thereof. This is the basis for the modified potential infiltration rate proposed by Kincaid et al. (28). Such a shift in the potential infiltration rate curve is likely to take place to a much greater extent in a soil which is high in sand content than in one which has a considerable amount of clay because swelling is highly time related.

High antecendent moisture not only reduces soil moisture tension but also prevents shrinking between irrigations. Drying near the soil surface is necessary for most soils to regain infiltration rates.

Sprinkler Frequency

One of the greatest problems in evaluating the data from the field sprinkler infiltrometer tests resulted from the frequency of sprinkler passes. On this clay loam soil it was found that infiltration rates decreased rapidly with increasing time between sprinkler passes for times greater than 30 seconds. It appeared to be probable that some of this effect was also present during more frequent sprinkler passes, especially when very little runoff was occurring.

Likely causes for this phenomenon are believed to be that less water is available to infiltrate at lower frequencies and more soil

settling is likely to occur. As the period of time between sprinkler passes increases, water runs off a larger portion of the area. Therefore, water is available for infiltration on less of the surface. Where free water is not present at the soil surface, soil moisture tension develops immediately below the surface and the soil moisture gradient is reduced. This would directly reduce the infiltration rate and may also contribute to soil settling in that the higher soil moisture tension would tend to pull the soil particles into a close packed position.

Water Drop Energy

Levine (32), Duley (14), Ellison and Slater (17), Laws (31), Bisal (2) and others have reported substantial reductions in infiltration rates resulting from water drop energy. Infiltrometer work in this study indicated that, for heavier soils, drop energy effects may be greater than commonly thought. Substantial reductions in infiltration rates occurred when using very small nozzles at high operating pressures to produce drops which are much smaller than those resulting from the use of conventional sprinklers at normally recommended pressures.

The extremely great effect of drop size on infiltration rates indicates that this factor should be given consideration in the design of sprinkler irrigation systems. However, precautions to protect the soil surface structure by the use of extremely small sprinkler drops may be made useless by the destruction done by high intensity rainfall.

Although sprinkler system designs cannot do anything about rainfall effects, protection of the surface by a mulch or crop canopy can. This can be very important on heavier textured soils.

Water drop energy is responsible for much of the crust formation in the field. However in the laboratory infiltration tests, sufficient crust developed that the mathematical model had to be treated as a stratified soil with the saturated conductivity below the surface layer of 0.2 inch being from five to eight times as great as for the surface soil.

Infiltration Rate - Application Rate Relationships

Research by Mantell and Goldberg (34), Moldenhauer and Long (36), and Sor and Bertrand (45) indicates that considerable reduction and infiltration rates can be caused by excessive application rates. However, these investigators found infiltration rate reductions from application rates which greatly exceeded the infiltration rates. In both our laboratory and field studies it was found that infiltration rates were considerably higher when runoff rates equal about 6% of the applied water than when runoff rates were less than 1%. Visual observations during these tests indicated that when the amount of runoff was very small it was usually occurring from only part of the surface area. This was probably due in part to variations in infiltration rate over the surface. Also, water ran off higher spots quickly. Therefore, the infiltration potential was being achieved on only part of the area. As the application rate was increased, water became available for infiltration over more of the area and the infiltration rate appeared to increase until water was available for infiltration on all of the area at all times.

On steeper slopes there is tendency for easy surface water movement. Therefore, the infiltration rate which is possible without movement on the surface is reduced as the slope increases. Local slope is also very important in that water infiltration will be reduced in local high spots. Therefore, to maximize infiltration rate the slope should be minimized and the surface smooth.

Design Recommendations

System Capacity

Early center-pivot systems were designed with quite excessive system capacity. This increased the application rate. Therefore, a higher percentage of the applied water ran off local high spots and slopes to collect in low areas causing very nonuniform irrigation. Reducing the system capacities reduced the application rates, resulting in the water being applied to the surface of the soil for a longer period of time. More infiltration took place on the high spots and slopes. Irrigation uniformity was increased.

Initial recommendations from Colorado State University in 1965 resulted in renozzling many systems to these lower rates. Also, most newer systems have been equipped with sprinklers of the lower capacity. However, there has been a recent trend to go much farther in reducing system capacities. The result is improved irrigation uniformity, but in many cases the total amount of water applied is not adequate to keep up with the crop water requirements.

Deep rooted crops on heavier soils can make use of stored soil moisture to meet the evapo-transpiration needs during peak water use

periods. This permits use of a lower system capacity. On the other extreme, a shallow rooted crop on loamy sand can draw very little stored soil moisture. Therefore, the system has to be designed with a capacity which is capable of providing for the peak daily crop water requirements.

Sprinkler Selection

An important factor in determining sprinkler selection is whether a sprinkler system will be used on bare or protected soils. Much more attention needs to be paid to drop size if bare soils are involved. Drop size can be reduced by reducing sprinkler nozzle diameters and increasing operating pressure. A reduction in nozzle sizes means that a closer sprinkler spacing has to be used to provide the same capacity and that the area on each side of the sprinkler lateral be irrigated at any one time is reduced. Therefore, the application rates are higher than for larger nozzles. On bare soils, especially of heavier textures, resulting increases in infiltration rates may more than offset the increase in application rate. The opposite is probably true for protected loamy sand soils. Much question remains about intermediate conditions. However, field observations have generally indicated better results for close sprinkler spacing if operating pressures are adequate.

Three types of application rates are involved in design of center-pivots. The average application rate for any given time period is the applied depth divided by the time during which it was applied. It must be recognized, however, that a common impact sprinkler actually applies water for only a small portion of this time. The rate at which the water is applied during that period is the instantaneous application

rate and is many times as great as the average rate. The average application rate is probably the most important in infiltration if the sprinklers pass frequently so that a very small amount of water is applied during each sprinkler pass. However, lower sprinkler frequencies result in higher instantaneous application rates and more water being applied per pass so that more is likely to run off the surface before it gets a chance to infiltrate. Also, there will be longer periods of time when no water is available on the surface for infiltration.

Small sprinklers operated under high pressures result in very small drops which tend to float to the ground more slowly, producing lower instantaneous application rates. Because of the closer sprinkler spacing, there is more overlap between sprinklers; therefore, more frequent sprinkler passes. As a result, water application tends to be fairly constant which may account for the greater success of close sprinkler spacing under some conditions where it would not be expected on the basis of just drop size and average application rates.

It would be desirable to have time-varying application rates which begin at high rates and taper off gradually, much as in experimental Pattern 3 in Figure 4.14. However, two difficulties are encountered in using impact type sprinklers to try to produce this result. The first is that the total length of the pattern is usually reduced and may be reduced enough to more than compensate for the advantage. The second is that conventional impact heads cannot create a pattern which starts abruptly at a high rate.

The greatest possibility for taking advantage of the extremely high initial infiltration rates on heavy soils is probably the use of

spray nozzles which start very abruptly. These nozzles would have greatest application to soil with a high clay content. In one field of corn on a clay loam soil, nearly three inches of water was infiltrated during the first six minutes of application. After ten minutes, the infiltration rate for this soil was less than 0.1 inch per hour. However, when water was applied with a conventional sprinkler at 0.3 inch per hour, runoff began in nine minutes with only 0.05 inch of total infiltration. This field had not been irrigated for two weeks, but there was adequate soil moisture in the lower portion of the root zone so the crop had not suffered for lack of moisture and the three inch irrigation was adequate to refill the root zone.

End-Guns

Center-pivots irrigate a circle out of a square field. End-guns are used to try to irrigate a portion of the land in the corners. However, they almost always lose money for their owners because of doing a poor job of irrigating. The combination of the end-gun and of the smaller sprinklers located immediately inward from it results in very non-uniform irrigation of about 1/4 of the field. Application rates under the end-guns are also very excessive.

Although end-guns are spectacular and there is a psychological factor involved in irrigating the corners, proper elimination of them can result in higher total production on 10 fewer acres for the typical system. Farming costs are lower and the total amount of water used is less.

Smaller sprinklers are used immediately inward from the end-gun
to avoid excessive overlap with the high application rates which result
in the area served by the end-gun. Therefore, the area where the smaller
sprinklers are located, is usually under-irrigated. Also the fringe
area outward from the end-gun is under-irrigated, while an excessive
amount of water is applied near the end-gun. For the typical 132-
acre system, there is about 100 acres of highly uniform water application
located inward from where the uneven distribution begins. By elimina-
tion of the end-gun the same pattern of sprinkler sizing can be con-
tinued to the end of the lateral. At this point a part circle sprinkler
having approximately the same capacity as nearby full circle sprinklers
should be operated 180° inward. This produces uniform distribution of
water over the entire area.

At first thought it might seem that the half-circle sprinkler
should have only half the capacity of a full circle sprinkler located
at this point. However, this sprinkler needs to have about 70% of the
capacity of the full circle sprinkler which would be located at this
point on a longer lateral to make up the lack of overlap from the
sprinklers which would normally be located beyond this sprinkler. The
reason for recommending that the capacity of this final sprinkler be
equal to that of a full circle sprinkler rather than 70% as great is
because there is a high evapo-transpiration rate at the outer edge of
the field.

Using the typical 132-acre system as an example, the elimina-
tion of the end-gun will reduce irrigated acreage to 122 acres. How-
ever, the uniformity of irrigation will usually result in more total

yield from the 122 acres without having to till, plant, fertilize, irrigate and harvest the additional 10 acres. Water conservation advantages should also be considered.

Field Preparation

Only part of the solution of infiltration problems under center-pivot systems can be found in improvements in applying the water. The inherent principles of operation of center-pivot sprinkler systems makes it impossible to apply water in a manner which will match the infiltration characteristics of most soils. Whatever improvements that are possible in design should be made, but they should work hand-in-hand with field preparation methods which will increase the ability of the soil to infiltrate the water where it falls.

Circular Planting

Square pegs don't fit round holes. Traditional farming methods don't fit center-pivot irrigation much better.

Preparations for the conditions which exist under center-pivot sprinklers do not involve any startling new concepts. Rather they are just a matter of applying old solutions to a new problem. For example, farmers don't keep water off a road by building diversion ditches to convey the water into the area they want to keep dry. Instead they divert it away. The same concept applies to center-pivot wheel tracks. Most traction problems result from water which runs into ruts, not that which fall in them. When farming is done across these ruts, water runs down the rows until it is intercepted by the track. Runoff water from

all the rows accumulates in the rut and runs to the low points. This process allows the water much longer to wet the soil in the track, making it easier for the machine to bog down. It also results in more infiltration of water immediately upslope from the wheel tracks than on the downslope side.

When farming is done in a circle, the wheel tracks don't cross the rows. Instead of collecting in the tracks, most of the water moves down the rows until it infiltrates resulting in more uniform irrigation. Although circular farming is only part of the answer, it greatly reduces traction problems and helps improve the uniformity of irrigation by causing surface water movement to take place over a greater distance allowing more uniform infiltration.

Circular planting is only part of the answer in preventing traction problems. Some water can collect in local surface depressions. Also, in fields of alfalfa and pasture, water runs into the tracks readily because of the lack of rows to guide it.

Gravel, posts, old tires, concrete and all types of material have been placed in the ruts in an attempt to solve these traction problems. Extensions have been made in the pipe laterals to relocate the ruts so in some fields a series of deep ruts have been the result. None of these actions taken after the problem develops are satisfactory.

The answer is found in one simple principle. Water runs downhill. Under most conditions the wheel track is low so the water runs into it. A simple solution is to run the wheel on a slight ridge so the water will run away from it. If possible, the ridges should be constructed before the first crop is planted. The procedure for building ridges

begins with installing the center-pivot system well in advance of planting time. The system should be run around the field once to determine the wheel track locations. Then using a moldboard plow or a one-way disk plow, the soil is moved toward the track using the track as if it were a dead furrow from a previous pass of the plow. The plow is then operated on the opposite side of the track still treating the wheel track location as a dead furrow. A slight ridge will result. The rest of the field should then be plowed parallel to the ridge, leaving the dead furrows midway between the towers.

Land Smoothing

Too often, center-pivot owners have assumed that by purchasing these systems they are avoiding any need for land forming operations. This definitely is not so. Land smoothing is needed although not to the extent which is required for surface irrigation.

Small undulations from general slopes cause local steep slopes. Much more water movement occurs on steep than on flat slopes. When undulations exist, water runs from both directions and collects in low spots. Uneven water penetration is the result.

This situation can be greatly relieved by planing parallel to the wheel tracks to eliminate excessive slope undulation. If following the formation of ridges for the wheels to run on, the entire field is plowed with dead furrows being left between the towers, planing becomes easy. Precisely uniform slopes are not necessary, but the slopes should be made continuous when practical.

There are two important reasons for this land smoothing. First, the general slope is much less steep than local slopes; therefore, less

water moves on the surface. The second reason is that the planing opera-
tion produces slopes which are continuous for a much greater distance.
Therefore any surface water movement continues along the slope until
the water infiltrates or reaches a major low point. Infiltration is
then much more uniform than in the case where water is trapped in local
depressions.

Tillage and Planting

Circular farming with elimination of the end-guns, running wheels
on ridges and smoothing the surface are procedures which will help to
eliminate infiltration problems and increase the profit potential of
center-pivot irrigation farming. Special tillage and planting practices
can also help considerably. Study of tillage and planting practices as
a part of this project have indicated that partial incorporation of
crop residue is very helpful in reducing surface runoff. However, by
far the greatest improvement resulted from the practice of planting row
crop on beds with the crop residue being partially incorporated in the
furrow between the beds. It seems probable that other approaches would
be equally successful providing partially incorporated crop residue
was located so as to intercept runoff within a foot or two of where the
water falls.

The experimental work done in this project indicated that by
partially incorporating the crop residue in the furrows, essentially
all runoff from sprinkler irrigation and rainfall could be prevented.
These results seemed unreasonable when compared with the clean-till
bed planting practice and the disking and flat planting practice.

However, bed planting with the trash in the furrows results in a greater concentration of residue in the low area which collects the runoff water from the ridges. In both the laboratory and field infiltrometer tests it was found that infiltration rates increased very considerably when water was applied rapidly enough to cause more than 6% runoff. Therefore, it appears that the superior performance of this treatment can be explained by substantially increasing infiltration rates on the beds with the excess water from the beds running into the furrow where the infiltration rates are increased to a great degree by the concentration of partially incorporated crop residue.

It also would appear that infiltration rates could be increased considerably by continued use such planting and tillage practices. Repeated partial incorporation of crop residue would result in higher organic matter content of the surface soil. Because the surface provides most of the resistance to infiltration, the increase in permability resulting from higher organic matter content would be quite important.

System Operation

Pre-irrigation

Irrigation management practices also contribute greatly to elimination or reduction of infiltration problems. One of the most important practices is the use of pre-irrigation. On most soils it is nearly impossible to apply all of the water which is needed by the crop during the growing season without causing excessive water movement on the surface. By pre-irrigating to the full depth of the root zone, resulting

crusts can be broken up at the time of planting, leaving the soil in a condition to accept irrigation water more readily. This avoids the destruction of surface soil structure which would result from refilling the root zone early in the season. In the case of row crops it is desirable to apply only a light germination irrigation and then not irrigate until crop cover is obtained. At this time it is usually a good practice to cultivate once to destroy weeds and volunteer crop. The cultivation also serves a very useful function in increasing the infiltration rate of the soil if heavy rains have destroyed some of the soil surface structure. This cultivation will often double the rate at which the soil will take water, particularly on heavy soils. Once complete crop cover has been obtained, the impact of sprinkler drops has less effect on the future intake rate of the soil.

Speed of Operation

A common misconception exists regarding the effects of changing the speed of rotation. It is often assumed that the application rate can be decreased by speeding up the system. When the rotation speed is changed it affects only the application depth. The application rate remains the same; only the period of application is reduced. Increasing the speed of rotation and decreasing the application depth per revolution decreases the amount of water applied per revolution, but more revolutions are needed to apply an equal amount of water. The more frequent irrigation probably increases evaporation losses.

Higher speed of operations, and therefore increased irrigation frequency, reduces the infiltration rates of many soils. The surface

soil tends to stay wetter. Very little shrinkage takes place between irrigations in soils which tend to swell and shrink considerably. By deferring irrigation on these soils, surface cracking results and the macro-pores become larger. The soil can then take water very rapidly if applied at a higher application rate by spray nozzles. When using common impact sprinklers the infiltration rate remains considerably higher than for more frequent irrigations. For deep rooted crops on heavy soils in eastern Colorado, field tests have shown major runoff reductions by irrigating at 14 to 18 day intervals. This practice has been successful on soils which were high in clay content, but only limited success has been obtained on soils containg large amounts of silt.

BIBLIOGRAPHY

1   Baver, L. D. and H. F. Winterkorn, Sorption of Liquids by
    Soil Colloids, II. Surface Behavior in the Hydration of Clays.
    Soil Science, Vol.40, p. 403, 1935.

2   Bisal, F., Infiltration Rate as Related to Rainfall Energy.
    Canadian Journal of Soil Science, Vol. 47, pp. 33-37, 1967.

3   Bityukov, K. K., Preservation of Soil Structure During Over-
    head Irrigation. Trans. Jour. Agr. Engr. Res., Vol. 2,
    No. 4, pp. 313-320, 1951.

4   Borst, H. L. and R. Woodburn, The Effect of Mulching and
    Methods of Cultivation on Runoff and Erosion from Muskingums
    Silt Loam. Agr. Engr., Vol. 23, pp. 19-22, 1942.

5   Brooks, R. H. and A. T. Corey, Hydraulic Properties of
    Porous Media. Hydrology Paper No. 3, Colorado State
    University, March, 1964.

6   Carmen, P. C., Fluid Flow through Granular Beds. Trans-
    actions, Institute of Chemical Engineering (London). Vol. 15,
    1937.

7   Childs, E. C. and N. Collis-George, Soil Geometry and Soil-
    Water Equilibria. Discussion Faraday Society, Vol. 3, pp.
    78-85, 1948.

8   Childs, E. C. and N. Collis-George, The Permeability of
    Porous Materials. Proc. Royal Society, Vol. 201A, pp. 394-
    405, London, 1950.

9   Corey, A. T., Flow in Porous Media. A. E. 728 and 730 Class
    Notes, Colorado State University, Agricultural Engr. Dept.,
    Fort Collins, Colorado, 1969.

10   Darcy, H., Les Fontaines Publiques de la Ville de Dijon. Victor Dalmont, Paris, 1856. as quoted in Hubbert, L. J., Darcy's Law and the Field Equations of the Flow of Underground Fluids. Jour. of Petr. Tech., October, pp. 24-59, 1956.

11   Day, P. R. and G. G. Holmgren, Microscopic Changes in Soil Structure During Compression. Soil Science Soc. of Amer. Pro., Vol. 16, pp. 73-77, 1952.

12   Dixon, W. J. and F. J. Massey, Introduction to Statistical Analysis. McGraw Hill Book Co., Inc., New York, 1957.

13   Dubose, L. A., Discussion of Engineering Properties of Expansive Clays. Trans. ASCE, Vol.121, pp. 674-676, 1956.

14   Duley, F. I., Surface Factors Affecting the Rate of Intake of Water by Soils. Soil Science Soc. Amer. Proc., Vol. 4, pp. 60-64, 1940.

15   Edwards, W. M. and W. E. Larson, Infiltration of Water Into Soils as Influenced by Surface Seal Development. ASAE Paper 68-212, 1968.

16   El-Shafei, Y. Z., A Study of Flooded and Rain Infiltration Relations with Surface Ponding. PhD Thesis, Utah State University, Logan, Utah, 1970.

17   Ellison, W. D. and C. S. Slater, Factors That Affect Surface Sealing and Infiltration of Exposed Soil Surfaces. Agr. Engr., VoL26, pp. 156-157, 1945.

18   Fair, G. M. and L. P. Hatch, Factors Governing the Streamline Flow of Water Through Sand. Amer. Water Works Ass. Jour., Vol. 25, pp. 1551-1563, 1933.

19   Fletcher, J. E. and Y. Z. El-Shafei, A Theoretical Study of Infiltration into Range and Forest Soils. PRWG60-1, Utah Water Research Laboratory, Utah State University, Logan, Utah, July, 1970.

20   Freeze, R. A., The Mechanism of Natural Ground-water Recharge 1. One-dimensional, Vertical, Unsteady, Unsaturated Flow above a Recharging or Discharging Ground-water Flow System. Water Resources Res., Vol. 5, No. 1, pp. 153-179, 1969.

21   Frost, K. R. and H. C. Schwalen, Sprinkler Evaporation Losses. Agr. Engr., Vol. 36, pp. 328-328, 1955.

22   Green, W. H. and G. A. Ampt, Studies on Soil Physics, Part 1, The Flow of Air and Water Through Soils. Jour. of Agr. Science, Vol. 4, Part 1, pp. 1-24, 1911.

23   Hanks, R. J. and S. A. Bowers, Numerical Solution of the Moisture Flow Equation for Infiltration Into Layered Soils. Soil Science Soc. Amer. Proc., Vol. 26, pp. 530-534, 1962.

24   Holtan, H. N., A concept for Infiltration Estimates in Watershed Engineering. Agr. Res. Service 41-51 1961.

25   Holtan, H. N., C. B. England and V. O. Slanholtz, Concepts in Hydrologic Soil Grouping. Trans. ASAE, Vol. 10, pp. 407-409, 1967.

26   Horton, R. E., An Approach Toward a Physical Interpretation of Infiltration Capacity. Soil Science Soc. Amer. Proc., Vol. 5, pp. 399-417, 1940.

27   Keller, J., The Effect of Application Rate on Moisture Content and Settlement of a Loam Soil During Watering. PhD Thesis, Utah State University, 1967.

28   Kincaid, D. C., D. F. Heermann and E. G. Kruse, Application Rates and Runoff in Center-Pivot Sprinkler Irrigation. Trans. ASAE, Vol. 12, No. 6, pp. 790-794, 1969.

29   Klute, A., A. Numerical Method for Solving the Flow Equation for Water in Unsaturated Materials. Soil Science, Vol. 73, No. 2, pp. 105-116, 1952.

30   Kostiakov, A. N., Cn the Dynamics of the Coefficient of Water Percolation in Soils and on the Necessity for Studying it From a Dynamic Point of View for Purposes of Amelioration. Trans. 6th Comm. Intern Soil Science, (Russian), Part A, pp. 17-21, 1932. quoted from Childs, E. C., The Physical Basis of Soil Water Phenomena, John Wiley and Sons, Ltd., 1969.

31   Laws, J. O., Recent Studies in Raindrops and Erosion. Agr. Engr., Vol. 21, No. 11, pp. 431-433, 1940.

32   Levine, G., Effects of Irrigation Droplet Size on Infiltration and Aggregate Breakdown. Agr. Engr., Vol. 33, pp. 559-560, 1952.

33   Mannering, J. V., The Relationships of Some Physical and Chemical Properties of Soils to Surface Sealing. PhD Thesis, Purdue Univ., 1967.

34   Mantell, A. and D. Goldberg, The Effect of Water Application Rate on Soil Structure. Jour. of Agr. Engr. Res., Vol. 11, No. 2, pp. 76-79, 1966.

35   McIntyre, D. S., Soil Splash and the Formation of Surface Crusts by Raindrop Impact. Soil Science, Vol. 85, pp. 261-266, 1958.

36   Moldenhauer, W. C. and D. C. Long, Influence of Rainfall Energy on Soil Loss and Infiltration Rates, I. Effects Over a Range of Texture. Soil Science Soc. Amer. Proc., Vol. 28, pp. 813-814, 1964.

37   National Technical Advisory Committee, FWPCA, Water Quality Criteria. U. S. Gov. Printing Office, Wash., D. C., 1968.

38   Palmer, R. L., Waterdrop Impact Forces. Trans. ASAE, Vol. 8, pp. 69-70, 1965.

39   Peele, T. C. and O. W. Beale, Laboratory Determination of Infiltration Rates of Disturbed Soil Samples. Soil Science Society Amer. Proc., Vol. 19, p. 429-432, 1955.

40   Philip, J. R., The Theory of Infiltration: 1. The Infiltration Equation and its Solution. Soil Science, Vol. 83, No. 5, pp. 345-357, 1957.

41   Philip, J. R., The Theory of Infiltration: 4. Sorptivity and Algebraic Infiltration Equations. Soil Science, Vol. 84, No. 3, pp. 257-264, 1957.

42   Philip, J. R., Hydrostatics and Hydrodynamics of Swelling Soils, Water Resources Research, Vol. 5, No. 5, October, 1969, pp. 1070-1077.

43   Richards, L. A., Capillary Conduction of Liquids Through Porous Mediums. Physics, Vol. 1, p. 318-333, 1931.

44   Rubin, J., Theory of Rainfall Uptake by Soils Initially Drier than Their Field capacities and its Application. Water Resources Res., Vol. 2, No. 4, pp. 739-749, 1966.

45   Sor, K. and A. R. Bertrand, Effects of Rainfall Energy on the Permeability of Soils. Soil Science Soc. Amer. Proc., Vol. 26, pp. 293-297, 1962.

46   Smith, R. E., Mathematical Simulation of Infiltrating Watersheds. PhD Thesis, Colorado State University, 1970.

47   Smith, R. E. and D. A. Woolhiser, Overland Flow on an Infiltrating Surface. Water Resources Res., Vol. 7, No. 4, pp. 899-913, 1971.

48   Swartzendruber, D., R. W. Skaggs and D. Wiersma, Characterization of the Rate of Water Infiltration into Soil. Purdue Univ., Water Resources Research Center, Lafayette, Indiana, Technical Report 5, December, 1968.

49   Tressler, R. E., and W. O. Williamson, Particle Arrangements and Differential Imbibitional Swelling in Deformed on Deposited Kaolinite-Illite Clay, Clays and Clay Minerals: Proc. of 13th Nat. Conf., pp. 399-410, 1964.

50   U. S. D. I., FWPCA, Southeast Water Laboratory, Role of Soils and Sediment in Water Pollution Control, Part 1, 1968.

51   Varga, R. S., Matrix Iterative Analysis. Prentice-Hall, Englewood Cliffs, N. Y., 1962.

52   Whisler, F. D. and A. Klute, The Numerical Analysis of Infiltration, Considering Hysteresis, into a Vertical Soil Column at Equilibrium under Gravity. Soil Science Soc. Amer. Proc., Vol. 29, No. 5, pp. 489-494, 1965.

53   Winterkorn, H. F. and L. D. Baver, Sorption of Liquids by Soil Colloids, I. Liquid Intake and Swelling by Soil Colloidal Materials. Soil Science, Vol. 39, pp. 291-298, 1934.